Republic of Iraq
Ministry of Higher Education
and Scientific Research
University of Babylon
College of Science
Department of Physics

A Theoretical and Practical Study to Assess Alpha Emitters in Water Samples of Dhi-Qar Governorate

A Thesis
Submitted to the Council of College of Science, University of Babylon in Partial Fulfillment of the Requirements of the Degree of Doctorate of Philosophy in Physics.

By

Awsam Abdulsattar Marza Ali Ghulam
B.Sc. in Physics /2010
M.Sc. in Physics /2017

Supervised by

Prof. Dr.
Mohammed A. Al-Shareefi

Prof. Dr.
Ali Abid Abojassim

2021 A.D.

1443 A.H.

بِسْمِ اللَّهِ الرَّحْمَٰنِ الرَّحِيمِ

﴿ وَاللَّهُ أَنزَلَ مِنَ السَّمَاءِ مَاءً فَأَحْيَا بِهِ
الْأَرْضَ بَعْدَ مَوْتِهَا إِنَّ فِي ذَٰلِكَ لَآيَةً
لِّقَوْمٍ يَسْمَعُونَ ﴾

صَدَقَ اللهُ العَلِيُّ العَظِيم

سورة النحل : الآية (٦٥)

Supervisor's Certification

We certify that this thesis titled **(A Theoretical and Practical Study to Assess Alpha Emitters in Water Samples of Dhi-Qar Governorate)** was prepared by **(Awsam Abdulsattar Marza Ali Ghulam)** under our supervision at Department of Physics, College of Science, University of Babylon, as a partial fulfillment of the requirements for the degree of doctor of philosophy science in physics.

Signature:
Advisor: Dr. Mohammed A. Al-Shareefi
Title: Professor
Address: Department of Physics,
College of Science, University of Babylon
Date : / / 2021

Signature:
Advisor : Dr. Ali Abid Abojassim
Title : Professor
Address : Department of Physics,
College of Science, University of Kufa
Date : / / 2021

Certification of the Head of the Department

In view of the available recommendation, I forward this thesis for debate by the examination committee.

Signature:
Name: Dr. Abdulazeez O. Mousa Al-Ogaili
Title: Professor
Address: Head of Physics Department,
College of Science, University of Babylon.
Date: / / 2021

Examining Committee Certification

We certify that we have read this thesis entitled **(A Theoretical and Practical Study to Assess Alpha Emitters in Water Samples of Dhi-Qar Governorate)** and in our opinion as an examining committee examined the Ph.D. student **" Awsam Abdulsattar Marza Ali Ghulam "** in the contents, it is adequate with **(Excellent)** as a thesis meets the standard for the degree of Doctor of Philosophy in physics.

Signature:
Name: **Dr. Khalid Hussain Hatif**
Title: Professor
Address: University of Babylon-College of Science-Department of Physics.
Date: / /2021
(Chairman)

Signature:
Name: **Dr. Hussien Abid Ali Bakir Mraity**
Title: Professor
Address: University of Kufa-College of Science-Department of Physics.
Date: / /2021
(Member)

Signature:
Name: **Dr. Abdalsattar Kareem Hashim**
Title: Professor
Address: University of Kerbala -College of Science-Department of Physics.
Date: / /2021
(**Member)**

Signature:
Name: **Dr. Musa Kadhim Mohsin**
Title: Assistant Professor
Address: University of Babylon-College of Science-Department of Physics.
Date: / /2021
(Member)

Signature:
Name: **Dr. Rawaa Mezher Obaid**
Title: Assistant Professor
Address: University of Babylon-College of Science-Department of Physics.
Date: / /2021
(**Member)**

Signature:
Supervisor: **Dr. Mohammed A. Al-Shareefi**
Title: Professor
Address: University of Babylon-College of Science-Department of Physics.
Date: / /2021
(Member and Supervisor)

Signature:
Supervisor: **Dr. Ali Abid Abojassim**
Title: Professor
Address: University of Kufa -College of Science-Department of Physics.
Date: / /2021
(Member and Supervisor)

Approved by the College of Science Committee on Graduate Studies.

Signature:
Name: **Dr. Enas M. Al-Robayi**
Title: Professor
Address: Dean of the College of Science-University of Babylon.
Date: / /2021

Dedication

To... Who left us with her body but her spirit still flutters in the sky of my life:

﴿My mother God's mercy﴾

To… I humiliated the difficulty and endured hardship throughout the duration of my studies and helped me in all stages:

﴿My dear wife﴾

To… Those who support and encouraged me to continue my scientific career dear uncles:

﴿Hekmat & Sahib﴾

To.. The soul of my dearest friend who passed early

﴿Hassan Abd-Ulzahra Mohammed﴾

To… The most beautiful in life and hope for the future:

My sons

﴿Ali & Mahdi﴾

To… Support of my life:

﴿My family & friends﴾

Awsam 

Acknowledgments

First, I would like to express my deep thanks to the Almighty ALLAH, JALA JALALAH, for what I have been, prayer and peace be upon the best of his creation Mohammed and his progeny and companions.

I would like to express my deep gratitude and appreciation to my supervisors ***Prof. Dr. Mohammed Abdul Ammer Al-Shareafi*** and ***Prof. Dr. Ali Abid Abojassim*** for suggesting the topic of the thesis, continuous advice and their guidance through out this work.

I would like also to thanks express for the head of the Department of Physics ***Prof. Dr. Abdulazeez O. Mousa Al-Ogaili*** for support and cooperation.

Special thanks are due to Prof. Dr. Hayder Hamza Hussain for providing the necessary facilities and help. I want to take the opportunity to thank all the working people in the Physics department laboratories at University of Babylon and University of Kufa , and many people who have contributed to this thesis in one way or another.

I am grateful to water directorate of Dhi-Qar, center for restoration of Iraqi marshes and wetlands and Dhi-Qar health department for help.

Finally, my great thanks and respect to all who help me.

Awsam

Summary

Water indispensible for life therefore monitoring water quality is of high importance. This research focuses on measuring alpha emitters such as radon and uranium concentrations in 125 water samples of six types (30 samples of tap water, 20 samples of marshes water, 20 samples of stations water, 15 samples of surface water, 20 samples of groundwater, and 20 samples of RO water) that collected from different sites of Dhi-Qar governorate. The experimental study is done by CR-39 detectors that produced by TASTRAK Analysis System. Also, some radiological factors with chemical of toxicity risk due to uranium concentrations and it is isotopes, as well as ^{226}Ra concentrations, ^{238}U concentrations and radiological parameters due to radon concentrations were calculated using different theoretical equations. ^{222}Rn in groundwater were measurement using RAD-7 detector. Also, pH, EC, and TDS in marshes water for same study area were measured using different techniques. Then, the Geographic Information System (GIS) technique was used for the mapping of uranium concentrations, radon concentrations and some radiological hazard for all samples under study.

Also, this research aims at investigating theoretical properties (structural and optical) of the polymeric nuclear track detectors (CR-39) using the theory of functional density (DFT). The average value of uranium concentrations in μg/L for six types of water were 0.89±0.021, 1.23±0.05, 0.84±0.016, 0.87±0.04, 0.87±0.02, and 0.93±0.04, respectively, while the results of the average value of radon concentrations in unit Bq/m^3 for same six types of water were 441.61±77.02, 288.92±34.10, 285.54±56.87, 324.91±71.19, 224.35±23.85, and 389.47±68.60, respectively. Also, it was found that there was a good correlation between measuring uranium and radon concentrations using three counts methods, which were TASLIMAGE dosimetry system, microscopic system, and the developed Matlab (CR-39-D2) program. Good correlation between

uranium concentrations and physicochemical properties for marshes water were found, as well as good correlation for determined radon concentrations in groundwater using CR-39 and RAD-7 detectors.

The DFT investigation demonstrated that there was an increase in the number of transitions between HOMO and LUMO in addition to a decrease in the excitation energy with the increase in the emitted wavelengths because of increase in the interaction between the alpha particles emitted from radon gas. As a result, this leads to a distortion of the polymer material that the CR-39 detector is made of and to obtain the tracks that are related to the intensity of the radiation (alpha particles emitted). Accordingly, the results of uranium and radon concentrations, as well as radiological hazard indices from water for six types of Dhi-Qar governorate, were within the world levels limit that recommend by several organizations and commissions, including the EPA, WHO, UNSCEAR, and ICRP. Finally one may conclude that there is no danger from radiological hazard due to alpha emitter in most water samples of the present study on human health.

CONTENS

LIST OF FIGURES

LIST OF TABLES

LIST OF SYMBOLS AND ABBREVIATIONS

Symbol	*Description*
α	Alpha Particle
AED	Annual Effective Dose
B3LYP	Becke three term, Lee, Yang and Parr
Bq	Becquerel
Bq/m^3	Becquerel per cubic meter
Bq/L	Becquerel per Liter
^{14}C	Carbon -14
^{137}Cs	Cesium-137
^{60}Co	Cobalt-60
DFT	Density Functional Theory
DNA	Deoxyribonucleic acid
EC	Electrical Conductivity
E_A	Electron Affinity
eV	Electron Volt
w	Electrophilicity Index
ESP	Electrostatic Potential
E_g	Energy Gap
EPA	Environmental Protection Agency
ECR	Excess Cancer Risk
GTOs	Gaussian Type Orbitals
GGA	Generalized Gradient Approximation
GIS	Geographic Information System
H	Global Hardness
GPS	Global Positioning System
S	Global Softness
HQ	Hazard Quotient
HOMO	Highest Occupied Molecular Orbital
ICRP	International Commission on Radiological Protection
I_E	Ionization Potential
kBq/m^3	kilo Becquerel per cubic meter
^{206}Pb	Lead-206
^{207}Pb	Lead-207
^{208}Pb	Lead-208
LADD	Lifetime Daily Average Dose
L/day	Liter per day
LDA	Local Density Approximation
LUMO	Lowest unoccupied Molecular Orbital
µg/L	Micro gram per Liter

µS/cm	Micro Siemens per centimeter
mSv	Mille Sievert
mSv/y	Mille Sievert per year
ppm	Part Per million
^{210}Po	Polonium-210
CR-39	Polyallyl Diglycol Carbonate Detector
pH	Potential of Hydrogen
$C_{Ra}^{s,a}$	Radium activity concentration inside the sample
^{226}Ra	Radium-226
$C_{Rn}^{s,a}$	Radon activity concentration inside the sample
RAD-7	Radon Activity Detector-7
C_{Rn}^{a}	Radon concentration in the air of the tube
C_{Rn}^{s}	Radon concentration in the sample
^{222}Rn	Radon-222
STOs	Slater Type Orbitals
NaOH	Sodium Hydroxide
SSNTD	Solid State Nuclear Track Detectors
S.E	Standard Error
^{232}Th	Thorium-232
TD-DFT	Time Dependent Density Functional Theory
E_T	Total Annual Effective Dose
TDS	Total Dissolved Solids
TASL	Track Analysis Systems Ltd
U_3O_8	Triuranium octoxide
$C_{U}^{s,a}$	Uranium activity concentration inside the sample
UC	Uranium concentration
UO_2	Uranium dioxide
UO_3	Uranium trioxide
^{234}U	Uranium-234
^{235}U	Uranium-235
^{238}U	Uranium-238
λ	Wavelength
WHO	World Health Organization

CHAPTER ONE

GENERAL INTRODUCTION

Chapter One
General Introduction

1.1 Introduction

Radiation is emitted from the floor and walls of our homes, the food and drink we consume, and the air we breathe. Alpha particles, beta particles, and gamma rays are the most frequent types of ionizing radiation. Radiation can come from a variety of sources, including natural radionuclides as well as man-made ones. The water immense benefits cannot be counted, but it reception of pollutants in the environment and then get pollution, which is described as any change in the characteristics or the basic components of the environmental component and causes for many of the health problems [1]. Incorporating radioactive materials, whether liquid, solid, or gas, with the environmental elements of water, air, and soil leads to the rapid spread of intrusive materials in the air, with more of them becoming liquid or solid, resulting in air pollution and soil and water contamination [2]. As a result of rainfall, leaks of radioactive materials in liquid form entered the soil and spilled into rivers and groundwater. The geological and topographical features of the location determine the ordinary radioactive isotopes in rivers' water. The amount of uranium in water is hundreds of times lower than that found in soil and rocks. The concentration of uranium in some natural water (save in specified regions) can be exceedingly high, and the isotope of radon must also be considered (^{222}Rn). Radon levels in surface waters are lower than those in groundwater [3]. The other source of radioactivity in the water is radium (^{226}Ra) as one of the most important radioactive isotopes due to its lengthy half-life, it can be detected in water, especially drinking water. Radium behaves in the body similarly to calcium, with a ratable proportion deposited in the bone, which can lead to bone and head-sinus cancer [4].Various health agencies pay close attention to the quantities of

dangerous radioactive elements in drinking water, including uranium. The World Health Organization (WHO) is an international organization that promotes (WHO) as acceptable limit for uranium in water was previously advised to be 0.015 mg/l; however, following extensive research, the (WHO) now advises that the acceptable level in water valid for drinking to be 0.03 mg/l. The ICRP recommends an acceptable limit level of 0.019 mg/l for uranium exists in water, but "India's Atomic Energy Regulatory Board" has set a maximum acceptable level of 0.06 mg/L for uranium in water [5].

1.2 Radioactivity

The term "radioactivity" is used to represent the time rate of disintegration of elements. For any element there exist a certain number of neutrons to proton ratios for it to remain stable, As a result, any deviation from this value will result in an atom that is unstable. By producing energy in the form of radiation, an unstable atom can become stable. Such atoms are said to be radioactive and the process is called radioactivity. Therefore, natural radioactivity is defined as the spontaneous transformation of unstable nuclei that results in the formation of new elements with the emission of particles and radiations [6].The most prevalent types of emitted radiation have traditionally been classed as alpha, beta and gamma. Other types of nuclear radiation include the emission of protons or neutrons, or the spontaneous fission of a large nucleus [7]**.** Alpha and beta particles are ionizing radiation that can only be produced by charged particles. Ionizing radiation is produced indirectly by photons or uncharged particles such as neutrons. In this situation, ionization happens following the formation of one or more energetic charged particles. By disrupting the DNA in the cell nucleus, all

ionizing radiation can have a biological effect [8],[9]. There are two sources of radioactivity (background radiation) as following :

1.3 Natural Source of Radiation

1.3.1 Cosmic Radiation

A radiation stream is created when charged light and star beams contact with the earth's atmosphere and magnetic field. Because of the differences in height and the effects of the world's magnetic field, the amount of cosmic radiation reaches different places of the globe [10]. Cosmic radiation is made out of an incredibly high energy particles (up to 10^{18} eV), and are for the most part protons (87%), with some bigger particles (alpha radiation 13%). A vast level of it originates from the outside of our solar system and is saved all through space. A portion of the essential enormous radiation evolves from our sun which is created amid sun based flares [11]**.**

1.3.2 Terrestrial Radiation

Terrestrial radiation sources include naturally happening radioactive materials that exist in rocks, soil, water, and vegetation. The uranium series, thorium series, and a single potassium series are the principal isotopes of concern for terrestrial radiation. In different parts of the planet, the amount of radiation from earthly sources varies. Higher portion levels are found in areas with high uranium and thorium concentrations in their soil [10]. With half-lives spanning hundreds of millions of years, they appear to be eternal. Radionuclides with half-lives longer than 30 years are not detectable. This section also includes the progeny or rot consequences of long-lived radionuclides [6]. The series decay can be classified naturally in three types; including, uranium series (^{238}U), actinium series (^{235}U) and thorium series (^{232}Th) see (Figure 1.1). Uranium happens normally as the radioisotopes ^{238}U and ^{235}U which

offers rise to decay series that is terminated in the steady isotopes (^{206}Pb and ^{207}Pb), individually. The half-lives of (^{238}U and ^{235}U) are ($4.46x10^{9}$ and $7.13x10^{8}$) years, individually. Thorium happens normally as the radioisotope (Th) which offers rise to decay series that is terminated in the steady isotope ^{208}Pb (Figure 1.1). The half-lives of (^{232}Th) is ($1.39x10^{10}$) years. Not one or the other (^{238}U, nor ^{232}Th) discharge gamma-rays, and gamma-emissions from their radioactive daughter items are utilized to evaluate their focuses [12].

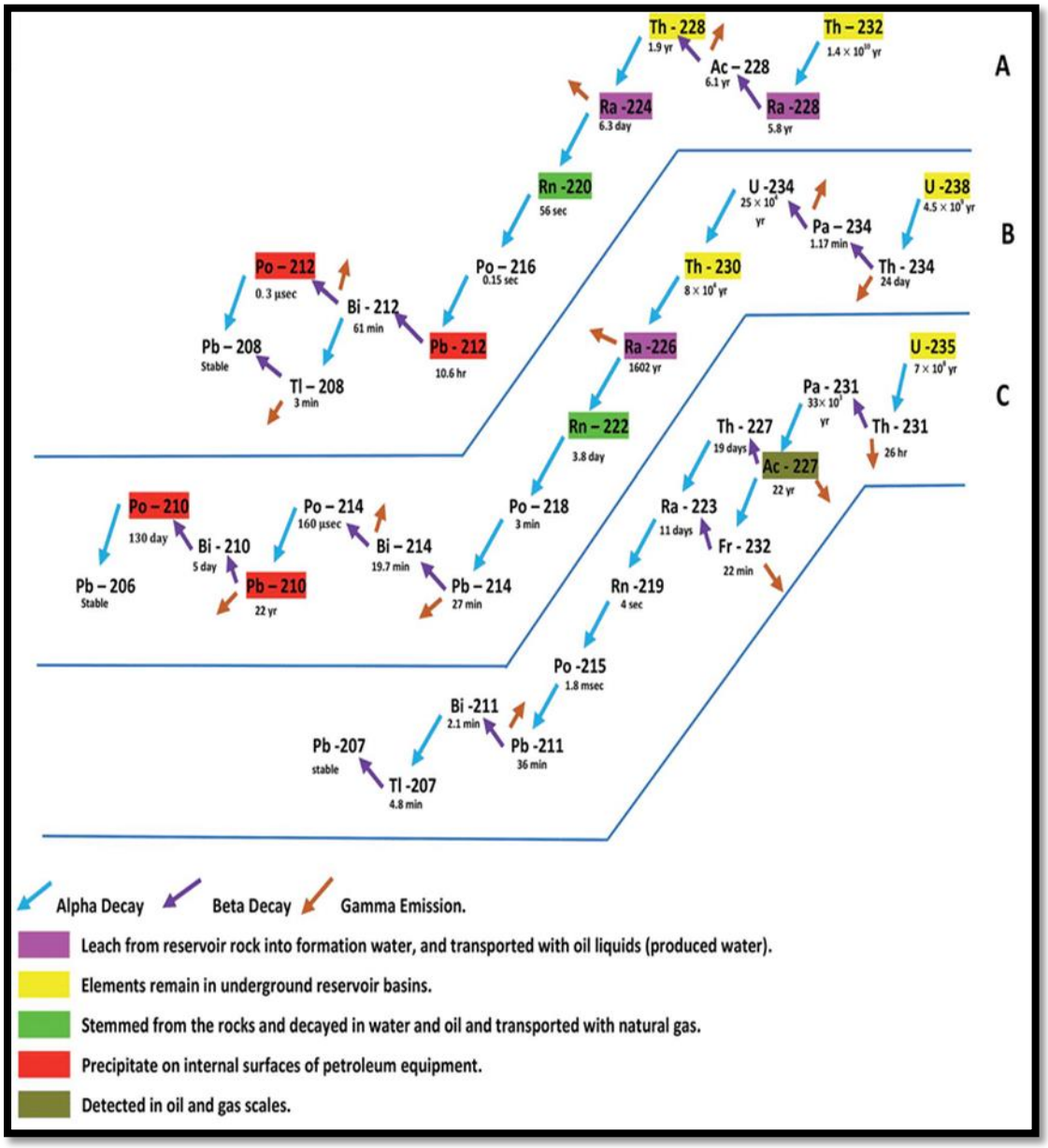

Figure (1.1): ^{238}U, ^{232}Th and ^{235}U decay series [13].

1.3.3 Internal Radiation

Internal radiation is an essential and very important element for the proper function of all organs in the body. It is the substance responsible for the electricity in the body and plays an important role in skeletal [14]. It is made up of radioactive elements that are naturally found in the human body. The essential sources of inward radiation exposures are potassium and carbon. Potassium is a fundamental mineral forever. The potassium ^{40}K isotope (0.01 percent of all potassium) is normally radioactive. It enters the human body through the evolved way of life [10]**.** Carbon makes up around 23 percent, by weight, of the human body. Grandiose radiation produces carbon ^{14}C, which is a little level of all carbon. Carbon enters the body through both the evolved way of life and by breathing [14]**.**

1.4 Humans-Invented Radiation Sources

Therapeutic methods, such as suggestive X-rays, nuclear drugs, and radiation treatment, are by far the most important source of man-made radiation exposure to the general population. A portion of the significant isotopes would be (^{131}I, ^{99}Tc, ^{60}Co, ^{192}Ir, ^{137}Cs, and others). Individuals in the open are exposed to radiation from shopper items, for example, tobacco (polonium ^{210}Po), building materials, burnable powers (gas, coal), ophthalmic glass, TVs, iridescent watches and dials (tritium), air terminal X-rays frameworks, smoke indicators (americium), street development materials, electron tubes, fluorescent light starters, lamp mantles (thorium), and so on [15]**.**

People who are occupationally exposed are exposed in different ways depending on their jobs and the sources with which they work. Dosimeters, which are pocket-sized equipment that quantify radiation exposure, are used to carefully monitor these people's exposure to

radiation. Cobalt-60, cesium-137, americium-241, and other isotopes are among those to be concerned about [16].

1.5 Radioactivity in Water

The most important source of life is water. Despite the fact that water covers 70% of the Earth's surface, only 0.3% of the total water supply can be used and is fit for everyday use. Water accounts for 70-75 percent of a person's entire body weight. Interactions with aquifer rock, near-by uranium tailing, oil uptake, and fertilizer leaching may be the result of uranium, radium, and radon in groundwater [17]. Once such radionuclides are in groundwater, they may be introduced into the atmosphere through domestic, popular and industrial use. The radioactive elements can enter the human body in a number of ways, both direct and indirect. The direct method entails drinking or eating radionuclide-contaminated vegetables from groundwater, whereas the indirect route entails drinking polluted water or feeding contaminated hay to livestock. Indirect ingestion, on the other hand, is widely thought to be safe for health due to the minimal dose obtained [18]. The health threats may occur by digging, rein and bone formation or cancer as deposition of radionuclide particles. Readily, radon gas is emitted from water or plutonium tailings and ingested by people. Radon isotopes mostly produce radioactivity in the form of radiation, that cannot break through the skin's outer layers. Thus, these radionuclides are dangerous only if swallowed or inhaled into the body. The health concerns could include radioactive dust accumulation from mining, aggregation in the reins and bones, or cancer [19]. The U.S. Environmental Protection Agency (EPA) categorizes uranium, radium and radon as "carcinogenic to humans". Lung cancer may be increased by inhaling uranium and radium dust and radon gas from water or uranium tailings as well. The EPA and the WHO have suggested (distinctly) limits for isotope concentrations in water of

drinking, based on speculation of individual yearly radiation and kind of radiation. The potion is checked in Sieverts (Sv) or in milliSieverts (mSv), when 1 Sv=1 Joule/ kg. The United Nations Expert Committee on the Nuclear Radiation Impact has estimated the global mean annual dose per person to approximately 3.0 mSv / y. 80% of the annual dosage is calculated using a naturally occurring radionuclide, 19.6% from medical diagnosis and 0.4% from other anthropogenic origins [20]**.** Dangerous radionuclide levels require different cleanup procedures supervised by the EPA. Polluted areas should be tracked regularly, and samples should be taken with the recorded date and time. It is therefore important to interact to the public in a consistent language and to explain the danger level in the different circumstances [21]**.**

1.6 Physiochemical Properties of Water

Human population growth, industrialization, agricultural fertilizer use, and other man-made activities all contribute to increased water pollution. The physicochemical characteristics of water include "temperature, pH, electrical conductivity (EC), total dissolved solids (TDS), turbidity, dissolved oxygen (DO), total alkalinity (TA), total hardness (TH), calcium (Ca^{++}), magnesium (Mg^{++}), potassium (K^{+}), and chloride (Cl^{-})" [22].

1.6.1 Potential of Hydrogen (pH)

pH amount of water is the quantity of hydrogen ions in water and is used to express the intensity of acids or alkaline conditions. The hydrolysis of salts of powerful bases and weakly acids, or the opposite, in aqueous solutions is the most common cause of pH variations below 7. Dissolved gases like CO_2, hydrogen sulfide, and ammonia impact the pH of water. Water with a pH of 7 is neutral, while water with a less than 7 is acidic, but also water with a hydrogen ions greater than 7 is alkaline. Tuberculosis is caused by acidic water, while incrustation is caused by

alkaline water. The water of drinking contains the pH that must be between 6.50 and 8.50. Water with a pH of less than 4 has a sour taste, whereas water that contains the pH of more than 8.50 has a bitter taste. It also hastens the production of scale in water heating equipment and lowers chlorine's germicidal efficacy. The lower the pH, the more the pipes corrode, and hazardous metals such as Zn, Pb, and Cu are liberated [23]. The pH of water is influenced by two factors: the bedrock and soil composition through which it travels. A body of water's pH can also be affected by the quantity of plant growth and organic matter present. Individuals, corporations, and communities dumping chemicals into bodies of water is another factor that impacts the pH of a body of water. Excess dissolved metals in solution will have a severe impact on aquatic species' health as well as poison people if these fluids are consumed [24],[25].

1.6.2 Total Dissolved Solids (TDS)

TDS in water are composed of mainly chemical, inorganic salts, sulphates and bicarbonates of Ca, Mg, K and Na. If small amount of organic matter is present, they also contribute to TDS. TDS in water is a result of natural processes and the release of wastewater. Concentrations of TDS are a major feature to be considered when ground water sources are tapped. High concentrations of TDS make the water brackish or saline and impart a disagreeable metallic taste to drinking water. Anthor problem includes hardening of water and scale formation in conduits, boilers and solar water heaters. Minerals, gases, and organic substances dissolved in water can produce an aesthetically unappealing color, taste, and odor. Significant health effects associated with ingestion of TDS have not been recorded. Some compounds have been proved to be

poisonous, and some of the soluble organic elements have been known to cause cancer [26].

1.6.3 Electrical Conductivity (EC)

"Electrical conductivity (EC)" refers to a normalized indicator of a water's capability to carry electricity across natural waterways, and it is heavily influenced by dissolved particles. Siemens per meter (S/m) is a unit of measurement for electrical conductivity.

The majority of freshwater sources will have a conductivity of 0.001-0.1 S/m. An oversupply of dissolved salts due to inadequate irrigation management, minerals from rain water runoff, or other discharges could be the source of EC. The amount of total dissolved solids (TDS) in natural waters is measured by EC in the field. Because measuring TDS in the field is challenging, the electrical conductivity of the water is utilized as a proxy [27]. Portable meters can be used to determine the electrical conductivity of water in a quick and economical manner. Electrical conductivity is no longer directly proportional to salt concentration once it reaches a particular threshold, this is due to the formation of ion pairs. Higher TDS will not result in equally higher electrical conductivity above this level because ion couples diminish each other's charge. The electrical conductivity of water is affected by its temperature, and it rises by 2% to 3% for every degree Celsius that the temperature rises. Many EC meters now automatically normalize readings to 25 degrees Celsius. While electrical conductivity is a decent predictor of total salinity, it doesn't tell you anything about the ion composition of the water. Sewage discharges from sewers and industry, agricultural runoff, and acid mine drainage are all linked to high EC. Heavy metal poisoning can be caused by high EC in drinking water combined with harmful trace metals [28].

1.7 Previous Studies

Several investigations have been performed to explore and estimate the amounts of radioactive elements such as uranium, radon, and physiochemical parameters in water samples, and some of these measurements have been made by the EPA, IAEA, and ICRP using various techniques. In addition, several research investigations looked into the radioactivity-related issues of uranium and radon in water; The following are some of the studies that have been abstracted:

1.7.1 Uranium in Water

● **In 2015, A. Ammir *et al*.,** [29] The amounts of ^{238}U, ^{232}Th, and their daughter products were measured in samples of water gathered from numerous oil fields and sources in northern Iraq. The concentrations of ^{238}U and ^{232}Th were found to be 0.20 to 3.50 ppm and 0.03 to 1.83 ppm, in that order. Due to the necessary levels and calculated yearly effective dosage, which were assessed using CR-39, the majority of the output water from the investigated oil fields is not acceptable for any specific reason.

● **In 2015, A. Liesch *et al*.,** [30] Studied of uranium concentrations in groundwater in Baden, Germany. The number has been studied 1935 regions were taken, The results show that 1.6 percent of all water samples filtered using membrane filtration and evaluated for uranium exceed the German regulatory limit for drinking water (10 µg/L), The same samples were examined for a variety of additional characteristics using ICP-MS.

●**In 2016, H. Virk.,** [31] Studied the natural uranium concentration in groundwater of India ,groundwater samples collected from sixteen sites, The concentration of uranium in the samples of water samples from the examined communities ranges from 9.72 to 186.61 µg/L with an mean

value of 69.54 μg/L).The uranium was measured using an LED Flourimeter.

● **In 2017, M. Amrane.,** [32] The concentrations of uranium and thorium in water samples were evaluated at twenty distinct sampling stations throughout Morocco. The activity concentration of uranium and thorium in water were explored to be between "12 to 37 Bq/m^3 and 2 to 10 Bq/m^3 , correspondingly. All of the river water samples analyzed had a pH of 7.5 to 8.75, which was slightly alkaline.

● **In 2018, M. Rohit *et al*.,** [33] Determined uranium concentration in collected groundwater samples utilized for household and agricultural purposes in India. The obtained results of uranium concentration in the studied samples differed from 0.03 to 19.19 μg/L with an average value of 2.83μg/L. the results analyzed by LED flourimeter.

● **In 2019, A. Abojassim *et al*.,** [34] In surface water samples from An-Najaf, Iraq, uranium concentrations and isotopes were determined using CR-39 detector, as well as the annual effective dose. The average uranium concentration in the Al-Manathera and Al-Heerra districts were 1.750±0.202 μg/L and 1.07±0.152 μg/L, respectively, according to the findings. In Al-Manathera, the average activity of ^{238}U, ^{235}U, and ^{234}U were 6.48±0.250, 0.100±0.011, and 2.18±0.252 Bq/L, respectively, whereas in Al-Heerra, they were 1.27±0.188, 0.061±0.008, and 1.33±0.189 Bq/L. Solid-state nuclear track detectors (CR-39) were employed to determine the results.

● **In 2019, A. Al-Bayati.,** [5] Uranium concentrations were measured in water samples taken from the Al-Tuwaitha region of Baghdad, Iraq. In this study, the uranium concentrations ranged from "(0.6±0.33 mg/L) to (2.51±0.49 mg/L), with a weighted average of (1.262±0.402 mg/L)". The

findings displayed that the uranium concentration in the samples of water tested was greater than the WHO and ICRP-suggested safe level. The uranium concentration was determined by calculating the paths of nuclear divi fragments utilizing the CR-39 detector.

● **In 2019, I. Sekudewicz and M. Gasiorowski.,** [35] Studied the isotopes of uranium and polonium in tap water and groundwater in the Warsaw, Poland. Surface intakes had mean values of 0.12, 3.91, and 2.75 mBq/dm^3, while deep water intakes had mean values of 0.25, 0.24, and 0.20 mBq/dm^3 of concentrations ^{210}Po, ^{234}U and ^{238}U, respectively. The technique used to determine uranium were (Ortec) alpha particle spectrometer with silicon detectors. The annual dosage absorbed by a resident as a result of drinking water consumption was determined using polonium and uranium activity measurements.

● **In 2019, T. Sharma *et al.*** [36] The seasonal change of uranium distribution in samples taken from groundwater of the Punjab districts of "Amritsar, Gurdaspur, and Pathankot" was investigated. The consequences of uranium was obtained by using LED fluorimeter. Pre-monsoon uranium concentrations in ground water samples were 8.6 µg/L, 4.3 µg/L, and 3.0 µg/L, correspondingly, and 8.8 µg/L, 4.9 µg/L, and 3.4 µg/L, correspondingly, during the monsoon to estimate the health impact on persons living in these areas, an assessment of associated radiological risks, chemical dangers, and effective radiation dose for various age groups was done.

● **In 2020, A. Abojassim and H. Neama.,** [37] Studied concentrations of uranium to twenty four samples of groundwater which collected from Kufa city, Al-Najaf governorate, Iraq. The technique that was used to obtain uranium concentrations was solid state nuclear track detector (CR-39). The findings demonstrate that the mean value of uranium

concentrations and uranium isotopes "^{238}U, ^{235}U, and ^{234}U 1.20± 0.04 µg/L, 1.48±0.06 Bq/L, 0.069±0.002 Bq/L and 1.49±0.06Bq/L", in that order.

● **In 2021, T. Al-Zaalimiu and A. Al-Hamzawi.,** [38] Studied concentrations of uranium to samples of tap water which collected from Muthanaa governorate, Iraq. The technique that was used to obtain uranium concentrations was solid state nuclear track detector (CR-39). The results show the highest value of uranium concentrations in tap water sample was 4.05±0.16 µg/L while the lowest value was 2.02±0.13 µg/L. The findings demonstrate that the uranium concentrations were within the safe limit.

1.7.2 Radon in Water

● **In 2015, A. Abojassim *et al*.,** [39] Studied concentrations of radon gas to one hundred and thirty six of tap water samples gathered from thirty four sites of Baghdad, Iraq. The results of radon concentration using the electronic radon detector RAD-7 vary from (0.012) to (0.283) Bq/L, with a mean value of (0.111) Bq/L. The annual effective dose in ingestion (stomach) and inhalation (lungs) per person is also calculated for children and adults.

● **In 2016, L. Najam *et al*.,** [40] The concentrations of radon gas in samples of tap water taken immediately from Dhi-Qar governorate, Iraq, were determined. The high average radon concentration in samples of water was discovered in the AL-Refai region (0.223±0.03 Bq/L), wh the low average radon gas concentration was discovered in the AL-Fajr area (0.108±0.01 Bq/L), with an average value of (0.175±0.03 Bq/L). The maximum yearly efficiant dosage (AED) in samples of tap water is detected in the AL-Refai area (0.814 µSv/y), but the low value (0.394 µSv/y) is detected in the AL-Fajr area (0.394 µSv/y), with an average

value of (0.640±0.1 µSv/y). Finally, the findings were analyzed by using (CR-39) detector.

● **In 2016, M. Al-jnaby.,** [41] Studied the radon concentrations in thirty eigth samples of drinking water gathered from residential tap water randomly in the thirteen different colleges sites, Babylon, Iraq. The radon concentrations measured vary from (0.193 Bq/L) to (0.036 Bq/L), with a mean of (0.115 Bq/L). The Radon concentrations measured are substantially within the range of the EPA's maximum contamination level of (11.1 Bq/L). Total yearly efficient potion originating from radon in water of drinking was (0.413 mSv/y). The measurements is done by using the RAD- H_2O method.

● **In 2017, M. Seoud.,** [42] Measured the concentrations of radon in mineral drinking water (bottled) collected from state of Kuwait, nuclear track detector (CR-39) was the technique used to obtained results of radon concentrations. In the state of Kuwait, a total of ten different famous models of bottled natural mineral drinking water were collected from the local market and are widely marketed. In bottled mineral drinking water, the average radon concentration is 2.97±1.44 Bq/L, with a range of 1.02 Bq/L to 6.05 Bq/L. The mean efficient dosage in each liter and annual effective dose from radon consumed by drinking water are "29.72 nSv/L and 21.69 µSv/y", correspondingly, for an individual consumer.

● **In 2018, J. Rasouli and S. Khosravi.** [43] In Bukan, Iran, researchers investigated radon gas pollution of drinking water, as well as the radiological risk to human health that occurs from consuming contaminated water. Water samples had radon concentrations ranging from 0.79±0.18 Bq/L to 11.87±1.43 Bq/L, which were found to be below the acceptable limit and slightly harmful to drink. These water samples had yearly effective dosage values ranging from 1.27 µSv/y to 32.67

μSv/y. An electronic solid state radon detector (RAD-7) was utilized to quantify the radon level in specific drinking water samples.

● **In 2019, O. Ntim *et al*.,** [44] Determined concentrations of radon and annual effective dose to 50 Ghanaian bottled water samples of Greater Accra, Ghana. In all analyzed water, the range and mean radon concentrations were 0.03 to 0.09 Bq/L and 0.06±0.01 Bq/L correspondingly. Measurements of radon concentrations were done by using RAD7-H_2O. The annual effective dose and measured radon concentrations were found within the "United States Environmental Protection Agency (US-EPA)".

● **In 2019, E. El-Araby *et al*.,** [45] The level of radon in samples of drinking and ground water gathered from several positions in the Saudi Arabian city of Jazan was measured. Radon levels in groundwater and drinking water were found to be 2.47±0.14 and 2.95±0.22 Bq/L, correspondingly. The measured mean of the whole yearly efficient dosage from drinking and inhaling ground water was 24.25±1.33 and 28.99±2.12 μSv/y, correspondingly, using the sealed cup approach.

● **In 2019, I. Al-Alawy and A. Hasan.,** [46] Studied the concentrations of radon in underground water samples in Karbala, Iraq by using (SSNTD-CR-39). The results were that highest were 4.152±2.2 Bq/L, where lowest were 2.165±1.6 Bq/L. The maximum Annual Effective Dose (AED) were 14.34±3.5 μSv/y, whereas the minimal value were 8.66±3.1μSv/y. Radon level concentrations, in the investigated groundwater samples was less compare with allowed permissible value.

● **In 2020, A. Abojassim *et al*.,** [47] Measured the concentrations of ^{222}Rn in groundwater samples collected from city of Najaf in Iraq. Monitoring system was RAD-7 (Durridge institution the USA) and CR-39 detector. With RAD-7, the average radon concentrations in groundwater samples ranged from (174.5±24.242 Bq/m^3) to

(2000.5±165.8 Bq/m^3), whereas employing CR-39, they ranged from (179.101±55.286 Bq/m^3) to (557.772±166.546 Bq/m^3). In addition, the yearly efficient dosage in all groundwater samples was lower than the allowed level, according to the findings.

● **In 2021, N. Kadhim *et al.*,** [48] Studied ^{222}Rn concentrations in drinking water samples collected from Iraqi market. Study is done by using RAD-7 detector. The results of radon concentrations were ranged from 28.4±2.7 mBq/L to 283±0.34 mBq/L. The results of radon concentrations were within the global allowed limits.

1.7.3 Physiochemical Properties of Water

● **In 2015, H. Amanial.** [49] Physicochemical properties of water in Arbamnch, Ethiopia. The physicochemical factors such as pH, the whole dissolved solids (TDS), the whole suspended solids (TSS), electrical conductivity (EC), the whole hardness, alkalinity, Cl^-, F^-, Na^+, K^+, Ca^{2+}, NO_3^- $NO_2^-$and Mg^{2+} were studied. The obtained results of each measured parameter were compared with the normalized values. Except for Cl^-, total alkalinity, and F^-, all of the parameters were found to be within the safe limit ranges. However, the Cl^- content was determined to be higher than the allowed limit.

● **In 2016, S. Singh and A. Hussian.** [50] Measured the quality index of water (WQI) for measuring the quality of drinking water for the last employers. A groundwater research was conducted for the purpose, with forty seven samples of groundwater collected from twenty five blocks in Greater Noida in India. The samples were submitted to an overall physicochemical and biological study of eleven parameters, including " hydrogen ion concentration, calcium, magnesium, chloride, nitrate, sulphate, total dissolved solids, fluorides, bicarbonate, sodium, and potassium" in order to construct the WQI. For the same, the WQI index was calculated, with values ranging from 53.69 to 267.85. The WQI

readings indicated that the water in the industrialized region was of very poor quality.

● **In 2017, S. Abd El-Aziz.** [51] Studied the water quality of groundwater for drinking and irrigation purposes in Aligeelat, Libya. pH, total dissolved solids (TDS), and electrical conductivity are examples of physicochemical characteristics. The pH of the water ranged from 6.98 to 7.49, with a mean of 7.17 and a normal deviation of 0.16. Groundwater samples had turbidity values ranging from 0.24 to 3.5 NTU, with a mean of 1.00 NTU and a normal deviation of 0.83 NTU. The EC of groundwater samples ranged from 2160 to 9020 S/cm at 25 degrees Celsius, with an average of 4691 S/cm and a normal deviation of 1993.28 S/cm. The average TDS level in the groundwater samples tested was 3175.2 mg/L, with a range of 1447.7 to 5979.1 mg/L. The (pH) and electrical conductivity (EC) were measured within a short period employing an Elico pH meter and a conductivity meter, correspondingly, due to the vulnerability of groundwater to environmental shifts. The whole dissolved solids were measured utilizing a TDS meter (TDS).

● **In 2018, N. Qaseem and M. Al-Barwary.** [52] Studied the physico-chemical parameters of groundwater in Zakho, Duhok governorate, Iraq. The samples were investigated for "electrical conductivity (EC), total alkalinity (TA), total dissolved solids (TDS), pH, nitrate ($NO3^-$), total hardness (TH), and chlorides" using conventional procedures (American Public Health Association). Statistical examination of the observed values revealed an important variation in the water quality of the wells.

● **In 2019, S. Abdullah *et al*.,** [53] Studied the Physico-chemical characteristics andwater quality of water samples collected fromAl-Sweiib river, Basrah, Iraq. There are 12 parameters were analyzed such as "pH, TDS, water temperature, EC, turbidity, TH, Mg^{+2}, DO, BOD, Ca^{+2},Cl^- and alkalinity". In the study area, the lowest rates (C) were

reported in January (11.4 °C) and the highest (32 °C) in August. The lowest value of hydrogen ion (pH) concentration (7.07) was recorded in August, and the highest (7.95) was recorded in February. TDS levels ranged from 1169.6 mg/L in December to 1655 mg/L in August. In November, the electrical conductivity (EC) of the samples ranged from 1.38 mS/cm to 2.30 mS/cm. Hanna instruments (a water resistant HI-9146) were used to measure these variables directly.

● **In 2020, A. Hussein *et al.,*** [54] Studied the quality index of water (WQI), in the environment laboratory of the surface water and agricultural directorate in AL-Najaf, Iraq, thirteen samples were collected and six physicochemical parameters were examined like TDS, Ca^{+2},Ec, Cl^{-}, So_4^{-2} and pH. Surface water samples had a water quality index ranging from 53.5092 to 87.5235. The three sorts of WQI values that result can be categorized (good, moderate, and poor water). According to Iraqi criteria, bad water for irrigation appeared in the north eastern, middle, and north western regions of the country, accounting for 12.689651 percent, while good and moderate water accounted for 20.174312- 67.136037 percent of the study area, respectively.

● **In 2021, A. Soceanu *et al.,*** [55] Studied the physico-chemical parameters of groundwater in Romania. The samples were investigated for "electrical conductivity (EC), total alkalinity (TA), total dissolved solids (TDS), pH, nitrate (NO_3^{-}), total hardness (TH), and chlorides" the results of pH were slightly alkaline. The results of physio-chemical properties were within the Romanian permissible limit.

1.8 Motivations of the Study

There are a number of motivations for which the study area (Dhi-Qar governorate) was chosen and the reason for choosing water as samples to be studied radiologically, the motivations can be summarized as follows:

1. Many regions in the Dhi-Qar governorate that have been bombarded in the recent wars that Iraq was exposed to in the previous period. Water's importance and direct impact on people's, animals', and agricultural crops' life.
2. Lack of comprehensive and integrated radiological study of water in Dhi-Qar governorate (tap water, marshes, stations, surface, groundwater, and RO water).
3. The incidence of cancerous diseases has increased recently, especially in the southern regions of Iraq, with high numbers recorded compared to previous times.

1.9 Aims of the Study

The essential goal of the current research is to evaluate alpha emitters in samples of water gathered from different sites of "Dhi-Qar governorate". The study is done by using soild state nuclear track detectors (CR-39), also, there are many specific objectives as follows:

1. Determine uranium concentration by employing solid state nuclear track detectors (CR-39) and calculated uranium isotopes such as ^{238}U, ^{235}U and ^{234}U using theoretical equations as well as estimated the annual effective dose using theoretical equations according to UNSCEAR 2000.
2. Determine radon concentrations using two SSNTD and RAD-7. Also, using theoretical method to assess annual effective dose (AED) for adult age old.
3. Calculate Uranium-238 and Radium-226 concentrations using theoretical method according to values of radon concentrations.
4. Assessment of health impact to humans residing in these regions using different theoretical equations.

5. Comparing with global accepted limits which recommended by international organizations.
6. Calculation of the hazard quotient (HQ) radiological and chemical toxicity risk and excess cancer risk (ECR) of all water samples.
7. Measuring some of the physiochemical characteristics of water like (pH ,TDS and EC) and studying its relationship with radioactive elements such as uranium and radon.
8. Drawn to establish of alpha emitters map to be a reference to the next studies using GIS technical.
9. Study a theoretical properties (structural and optical) of the polymeric nuclear track detectors (CR-39) using the theory of functional density (DFT) along with functional hybrid of B3LYP-SDD at ground state and time-dependent (TD-DFT) with the same functional and bases set for exaction state.
10. Assessment effect of alpha particle passing through CR-39 on the electronic properties such as the total energy ($E_{Tot.}$), high occupied molecular orbital energy (E_{HOMO}), lower unoccupied molecular orbital energy (E_{LUMO}), the energy gap (E_{gap}) ($E_g = E_{LUMO} - E_{HOMO}$) and the values of virial ratio($-V/T$) for the studied systems according to Koopman's theorem.
11. Study of molecular electrostatic potential surfaces , IR-Spectra ,UV-Vis spectra of the system result from passing increased alpha particle through CR-39.

CHAPTER TWO

THEORITICAL PART

Chapter Two
Theoretical Part

2.1 Introduction

Radon, radium, and uranium are in the same group because they are radionuclides. They are major unstable components that are highly involved in the release of ionizing radiation. These three elements occur naturally in the environment [56]. When radioactive materials are released, these substances fall into two main states, first, they either change to different isotopes, or to a completely different element. Uranium and radium are found in various types of rock as solids, while radon is present as a gas radon can be found in dissolved water or in the air. Since radionuclides are usually associated with rocks, wells of rocky water may have higher levels of radionuclides than shallow or drilled wells [57]. CR-39 detector is one of the most popular types of "Solid State Nuclear Track Detectors (SSNTDs)" and is a thermoplastic modulation made by polymerization of the allyldiglycol carbonate monomer [58]. Studying the properties of the nuclear track detectors are very interesting to provide information that helps us to comprehend the mechanism of interaction of radiation with matter, also possibility of improving these detectors to be more efficient [59]. As a result, it is important to understand the chemical and physical properties such as electronic, structural, geometric and optical characteristics of chemical systems. Nowadays, the quantum approach calculations with computational techniques are widely and important method because it is advanced, accurate, reliable methods and effective tools for investigating the properties of many chemical materials [60],[61].

2.2 Alpha Particles

Alpha particles are emitted from heavy radioactive atoms and it is released with a velocity of about 1/20 that of light and energy varying from 4 to 9 MeV [62]. Furthermore, the alpha particle emitters have ordinarily the least penetrating ability to pass through deeply into a skin or a material. Consequently, they can easily be stopped ; however, they possess the ability to break chemical bonds (which can cause chemical or biological damage or destroy living cells) when they strike a molecule due to their mass, size, and charge. Generally, Alpha particle's penetration distance relies on the energy with which they are emitted and the material through which they are penetrating. Thus, while its can be halted or absorbed by thin barriers such as a piece of tissue or skin. A typical alpha particle emitter is uranium (^{238}U), radium (^{226}Ra), and radon (^{222}Rn) [63]. The term radioactive half-life indicates to the required time for a half radioactive material to decay. With respect to radon is characterized of having a short radioactive half-life where it requires only about four days, the half -lives of the most common radium and uranium isotopes, ^{226}Ra and ^{238}U, are about 1,620 years and 4.5 billion years, respectively as illustrated in Figure (2.1) [64].

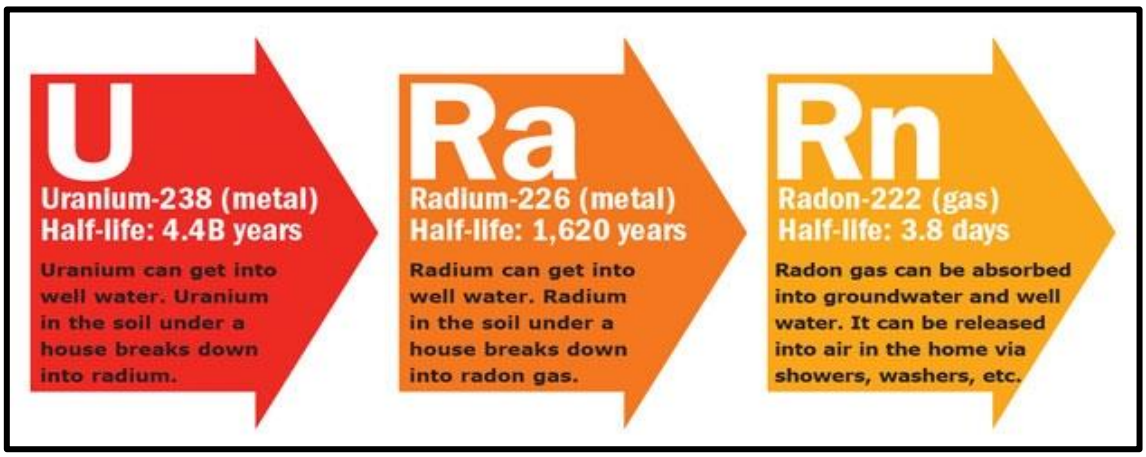

Figure (2.1): Uranium-238 decay [64]**.**

2.3 Source of Alpha Particles

2.3.1 Uranium

Uranium refers to the heavy known natural component, with an atomic number of 92. It possesses a specific density of 18.7 grams per cubic centimeter. Naturally, it's a little radioactive [65],[66]. Uranium is a heavy element that can be found in soils, rocks, seas, and oceans in many chemical forms. Uranium is also found in food and water of drinking. Normally, the men body has 90 µg of uranium through regular absorptions of air, water, and food with 66 percent of it found in the skeleton, 16 percent in the liver, 8 percent in the kidneys, and 10 percent in various parts [67].

Uranium's chemical composition (such as U_3O_8, UO_2, UO_3 or UF_6), is almost entirely responsible for the uranium's behavior in the environment and human body, and that behavior in turn is based partially on solubility. If a compound is not soluble in water, it is somewhat difficult to incorporate biologically. The oxides of uranium (U_3O_8, UO_2 or UO_3) are not soluble in water but the fluorides and nitrates of uranium (UCl_4, UF_6, $UO_2(NO_3)_2 \bullet {}_6H_2O$) are somewhat water soluble, Primary uranium ores[68].

2.3.1.1 Source of Uranium

Uranium does not exist in its metallic state in the environment, but rather as uranium compounds. Uranium compounds have a wide range of solubility. The most prevalent uranium oxides are UO_2, an anoxic insoluble chemical existed in minerals, and UO_3, a moderately soluble molecule existed on the surfaces of water. The chemical structure of uranium compounds impacts how quickly they spread through the environment and their chemical toxicity [14]. A summary was indicated by "The International Commission on Radiological Protection (ICRP)"

that the effectiveness concentrations of ^{238}U and ^{235}U of ordinary source in numerous ambient materials, as shown in Table (2.1).

Table (2.1): ^{238}U and ^{235}U activity concentrations from natural origin in several environmental materials [10].

Material	Activity concentration			
	^{238}U		^{235}U	
	Reference value	Range	Reference value	Range
Soil (Bq/mg)	35×10^{-6}	$(1– 690)\times10^{-6}$	__	__
Air (μBq/m3)	1	0.02 – 18	0.05	__
Drinking water (Bq/mg)	1×10^{-9}	9×10^{-11} - 150×10^{-6}	4×10^{-11}	0.4×10^{-9} – 0.5×10^{-6}
Leafy vegetables (Bq/mg)	20×10^{-9}	6×10^{-9} - 2.2×10^{-6}	1×10^{-9}	0.7×10^{-9} – 1.2×10^{-9}
Root vegetables (Bq/mg)	3×10^{-9}	0.4×10^{-9} - 2.9×10^{-6}	0.1×10^{-9}	5×10^{-11} – 0.6×10^{-9}
Milk products (Bq/mg)	1×10^{-9}	0.1×10^{-9} - 17×10^{-9}	5×10^{-11}	5×10^{-11} – 0.6×10^{-9}
Meat products (Bq/mg)	2×10^{-9}	0.8×10^{-9}- 20×10^{-9}	5×10^{-11}	2×10^{-11} – 0.5×10^{-9}

2.3.1.2 Uranium Isotopes

There are many isotopes of uranium in nature, but the three most important are ^{238}U, ^{235}U, and ^{234}U. As demonstrated in Table (2.2), all uranium isotopes are radioactive. [66].

Table (2.2): Normal uranium isotopes [67]**.**

Normal Uranium Isotopes						
Isotopes	Natural abundance (%)	No. of Protons	No. of Neutron	Half-life (in years)	Type of emission	Decay Energy (MeV)
^{238}U	99.27	92	146	4.5 billion	Alpha	4.270
^{235}U	0.72	92	143	700 million	Alpha	4.679
^{234}U	0.0055	92	142	245000	Alpha	4.859

2.3.1.3 Health Effect of Uranium

There are two reasons indicate the riskiness of uranium to humans and animals for two reasons: it is a heavy metal with toxic chemical impacts, as well as a radioactive alpha-emitter. Uranium possesses greater toxicity as a result of high Linear Energetic Transfer (LET) radiance, tissue deposition (kidneys, bones, lungs, and blood), and a 5000-day removal period.

The radiance restrict through which various health impacts begin (radiance–carcinogenic risk) is determined by the amount and duration of infection ("how much and how long"), as well as other operators including " age, sex, previous health status, exposure to other materials, genetic predisposition and radio sensitivity (lack of indicators), diet, and stress" [16]. The reduction of uranium and its products poses a risk of radioactive contamination. External sources, such as uranium-contaminated areas or leaking tanks, or interior sources, such as inspiration of UOx dust or absorption of water and food, can all cause higher hazard radiation [69]. Humans are most commonly exposed to uranium by inhalation, ingestion, and injury. Uranium particles inhaled will move via lymph nodes and lungs, increasing the danger of cancer in the lungs. While uranium is ingested, it can build up in the bone, raising the risk cancer in the bone or in the red bone marrow, increasing the chance of bone cancer (leukemia). Uranium can also be present in soft tissues like the gonads, raising the chance of inherited health defect like birth disorder [70]. Uranium levels in the kidney which cause moderate renal malfunction are less than 3 µg/g, which are utilized as limitations of occupational expositions, although short-lived or serious kidney uranium levels are around 1 µg/g. Uranium is deposited in bone, however there isn't enough information to say if high uranium intakes are harmful to the

bones. Due to the impacts of alpha-particle irradiation, we now have proof that uranium can directly harm DNA [69].

2.3.2 Radium

Radium, a naturally occurring radioactive element present in uranium and thorium components in the earth's crust, was discovered by Marie and Pierre Curie. Radium was used in many applications such as its use as a self-illuminating material in dial clocks, medical diagnoses and therapy (radiation therapy and brachytherapy). The most abundant of the radium isotopes is ^{226}Ra, that is a natural arises as a decay product of ^{238}U. ^{226}Ra is an alkaline earth metal with physiological and environmental qualities similar to calcium and barium, making it an important radiotoxic radionuclide. Radium would so compete with calcium and be deposited as a substitute for it in materials where the latter is in lower concentration, as it happens bones. With ^{226}Ra being an alpha-emitter and having a half-life about 1620 years, it is of utmost interest because when deposited in internal organs of humans, it is known to cause severe radiation damage resulting from the alpha particles and short lived daughter radionuclides of high specific activity emitted in its decay process [71]. Such severe radiation damage may cause cancer as in the case of the early radium dial painters. ^{226}Ra is also a large pollution in mine and milling trashes, such as uranium mill tailings, since it sticks totally to the particles of soil, rocks and seeps into ground water according to its capacity in order to make soluble sulphates, chlorides, and carbonates, and is a fundamental pollution in mine and milling trashes. Since ^{226}Ra represents easily soluble and deposited in bone tissue when taken up, it is necessary to monitor its uptake in ground and natural waters, by the fauna of these waters [72].

2.3.2.1 Source of Radium

Groundwater and Ra-bearing interact of components like rocks, soil, ore bodies, and other materials are natural sources of radium in groundwater. The solubility and accessibility of nuclides in the rocks by which groundwater percolates, rock penetrability, the existence of ionic elements, the acidity of the medium, and other parameters, all impact the concentration of ^{226}Ra and its parent nuclides in percolating groundwater [73]. Radium and other normal existed radionuclides can also be emitted immediately by the use of radioactive elements like uranium and thorium in the nuclear fuel cycle. Due to the existence of uranium and its long-term lived daughter productions in the minerals, this is also correct for the mining and processing of other economically relevant minerals, such as phosphate minerals like "apatite, copper, gold, lignite, coal, and other ores" [74].

2.3.2.2 Radium Isotopes

In the environment, there are 4 normal occurrence of radium radioactive isotopes which weights of 228, 226, 224, and 223. Radium-224 and radium-228 arise from thorium 232 decay chain, while radium-226 is result from the dissolution of uranium-238. The uranium-235 decay series produces radium-223 as a byproduct. Radium-224 and radium-223 have a very short life period (i.e., they release half of their radiance) estimated in days. [73]. On the other hand, the other isotopes are very steady. Radium-226 will live more than 1600 years, while radium- 228 will live little more than 6 years [75],[76].

2.3.2.3 Health Effect of Radium

Radium causes lung, bone, skull, and nasal passage cancers when it is inhaled. At large amounts of inner exposure, radium has been demonstrated to induce the cancer of bone cancer in animals as well as humans. The first examples of radium-226 and 228 develop cancer in

bone were discovered among watch dial painters in the United States in the early twentieth century. Radium causes a variety of bone cancers that affect various bones throughout the body [77]. Due to the relative size of their bones, animals that are shown to radium have a bit various division of cancers in bone than humans. Additionally, there are 3 basic categories or kinds of radiation induced cancer in bone. Each one is determined by the sort of cell that has been destroyed and turned into cancer [77].

2.3.3 Radon

Radon, with the chemical formula Rn, atomic number 86, and mass number 222, is a radioactive gas that occurs spontaneously. Moreover, it lives 3.82 days [78]. Radon is a tasteless, colorless, odorless, and chemically inert gas. Only specialized equipment may be used to measure it. Radon is also fairly soluble in water and organic solvents, thus water running through radon-containing rocks and sand can absorb it [79]. A detailed list of radon's physical and chemical characteristicss are given in Table (2.3) [80].

Table (2.3): Radon's physical and chemical characteristics [80].

Properties	Value
Atomic Number	86
Relative Atomic Mass	222 g mol^{-1}
Density	9.73 g m^{-3}
Melting point	−71 °C, −96 °F
Boiling point	−61.7 °C, −79.1 °F
Electron configuration	$4f^{14}\ 5d^{10}\ 6s^2\ 6p^6$
Half-life	3.82 days
Ionizing potential	10.749 eV
State at 20°C	Gas
Group name	Noble gas
Group in periodic table	18
Period in periodic table	6

2.3.3.1 Sources of Radon

Emissions account for at least 80 percent of the radon in the atmosphere comes from the soil, which are obtained from rocks. These rocks contain uranium, and radon is produced via the decay of ^{238}U through ^{226}Ra [81]. Radon is a gas with significantly more mobility than uranium and radium, which are fixed in rocks and soils. Granite, shale, and phosphate (mineral) are among the rocks and soils that contain high amounts of uranium and retain natural deposits of radon. Radon may more readily escape the rocks and soils by escaping through cracks and fissures in rocks and into the pore spaces between grains of soil. When radon is found in drinking water, it is considered a public health risk. The human species gets its water from both surface and ground water. Because it travels through rock and soil formations and dissolves various chemicals, minerals, and radioactive elements, ground water is more radioactive than surface water [80]. Radon levels in water are mostly determined by the source of radon, which might be natural processes, industrial or agricultural operations, or an increase in human activity in the region where the wells are located [79]. Radon possesses a high solubility in water and this decreases with increasing temperature. The disappearance of dissolved radioactive ^{226}Ra and immediate release of radon from the minerals matrix harboring member of the uranium disappeared series are two independent sources of radon derivation in water. Due to difference in mobilization from rock and water chemistry, usually ^{226}Ra and ^{222}Rn are not in radioactive equilibrium with each other in water, ^{226}Ra is rather insoluble element and the concentration of radon in water is larger than radium [82].

2.3.3.2 Radon Isotopes

There are three major radon's isotopes. These represent ^{222}Rn (called radon that is a member of the ^{238}U decayed series), ^{220}Rn (named

thoron that is a member of the ^{232}Th decayed series), and ^{219}Rn (named radon that is a member of the ^{238}U decayed series) (named actinon that is a member of ^{235}U decayed series). The most prevalent isotope of the element radon is ^{222}Rn, according to science. The phrases radon and ^{222}Rn are often interchanged in the literature.[45] that half-life is 3.82 [83].

2.3.3.3 Health Effect of Radon

The damage induced by alpha-particles is the primary source of radon's negative health consequences. The prospective consequences will be determined by the degree of exposure. The most significant danger posed by high radon levels is a higher chance of lung cancer. Radon, being a noble gas, is quickly expelled; nevertheless, radon offspring mix with other molecules in the air, as well as dust, aerosols, or smoke particles, and readily deposit in the lungs' airways. The progeny release ionizing radiance as alpha particles when trapped there, which can harm the cells lining the airways [84]. There is an immediate proof of a relationship between radon exposure and lung cancer in human research. As a result, radon was divided as a Group 1 carcinogen according to the "WHO's International Agency for Research on Cancer" [85]. Based on the rate of radon concentration in the nation and the approach of measurement, the average of the whole existed cancers in lung due to radon is considered to be between 3-14 percent. Lung cancer does not affect everyone who breaths radon decay products. The quantity of radon, the duration of exposure, and the individual's smoking behaviors all have a role in a person's risk of lung cancer caused by radon [35].

2.4 Solid State Nuclear Track Detectors (SSNTDs)

SSNTDs are mostly utilized in several technological applications for the detection of charged particles ranging from protons to heavy ions, as well as fluencies in environmental dosimeters. SSNTDs have been used to assess radon concentrations for a long time. These detectors come

in a variety of shapes and sizes, including inorganic crystals, glassware, and polymers [86].

2.4.1 Types of Solid State Nuclear Track Detector

2.4.1.1 Inorganic Detectors

Inorganic detectors are compounds that lack carbon and hydrogen in their structure, resulting in a "ionic link" between their atoms. Table (2.4) shows the chemical composition of several types of inorganic nuclear track detectors.[87].

Table (2.4): Chemical composition of inorganic nuclear track detectors [87]**.**

No.	Detectors	Chemical Composition
1	Zircon	$ZrSiO_4$
2	Quartz	SiO_2
3	Mica(Biotite) Mica (Muscovite)	$K(Mg, Fe)_3\ AlSi_3O_{10}\ (OH)_2$ $KAl_3Si_3O_{10}\ (OH)_2$
4	Fluorite	$CaF_{10}\ (OH)_2$
5	Soda Lime Glass	$23SiO_2\ 5Na_2O\ 5CaO\ Al_2O_3$
6	Olivine	$MgFeSiO_4$
7	Calcite	$CaCo_3$

2.4.1.2 Organic Detectors

Organic detectors are formed when carbon and hydrogen enter in their compositions, and created a "covalent bond" between its atoms. Table (2.5) shows some kinds of the organic detectors and their chemical composition [88].

Table (2.5): Chemical composition of organic nuclear track detectors [88]**.**

No.	Detectors	Chemical Composition
1	Polyester	$C_{17}H_9O_2$
2	Polyimide	$C_{11}H_4O_4N_2$
3	Cellulose, Cellulose Nitrate Cellulose Triacetate	$C_6H_8O_9N_2$ $C_3H_4O_2$

4	Polycarbonate (Lexan, Makrofol)	$C_{16}H_{14}O_3$
5	Plexiglass	$C_5H_8O_2$
6	Polyallyldiglycol Carbonate (CR-39)	$C_{12}H_{18}O_7$

2.4.2 CR-39 Detector

A typical solid state nuclear track detector is CR-39 (Polyallyldiglycol Carbonate) (SSNTD). The CR-39 detector is widely utilized in several fields, including nuclear physics, radon dosimetry, and radiobiological researches. Its density is 1.32 $g.cm^{-1}$. The chemical form for CR-39 may be written as ($C_{12}H_{18}O_7$). It is illustrated in Figure (2.2) [89].

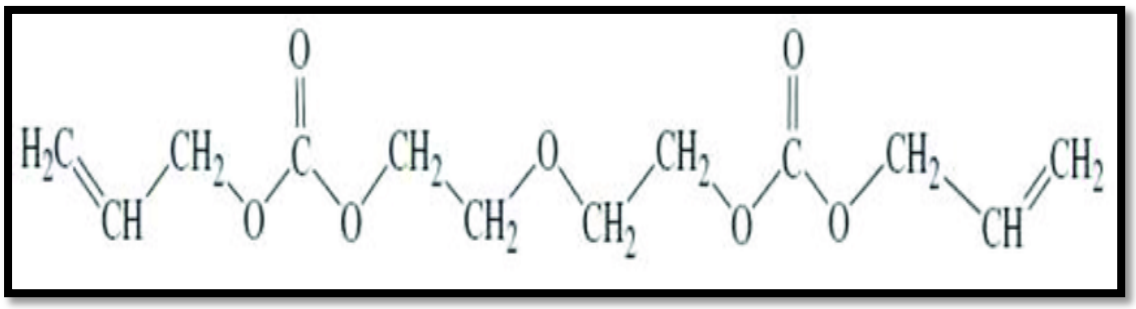

Figure (2.2): CR-39 detector [89].

In comparison to other detectors, the CR-39 has a high efficiency for recording tracks, and it has several features such as being optically transparent, very sensitive to radiation, extremely isotropic and homogenous, and having a non-solvent chemical etchant, among others [90].

2.4.3 Chemical Etching

Chemical etching of plastic detectors is often done in a temperature-controlled bath. The most often used etchant for plastics is an aqueous solution of NaOH (or KOH), with the rate of concentrations from 1 to 12. The time it takes to etch might range from a few seconds to

several hours. It changes depending on the particular etching circumstances, such as temperature and etchant concentration [91].

2.4.4 Plastic Nuclear Detectors (TASTRAK)

Poly allyldiglycol carbonate (PADC) plastic, also known as CR-39, serves as a solid-state nuclear track detector which is highly sensitive to alpha particles. It is manufactured by Track Analysis Systems Ltd. at Bristol University under the trade name TASTRAK. Alpha-particle detection with TASTRAK carried out in this laboratory provides spectroscopic information. The shape and dimensions of a-particle tracks are measured, either manually or by automated image analysis, and these measurements are used to derive for each track the dip angle and range in the plastic [92].

2.5 RAD-7 Detector

RAD-7 represents a semiconductor material (often silicon) which transforms alpha radiance to an electrical signal immediately. The interior sample cell of RAD-7 points out to a (0.7 liters) hemisphere in a combination of an electrical conductor on the interior. The planar Silicon alpha detector, which is solid state and ion implanted, is at the center of the hemisphere, as illustrated in Figure (2.3). It works on the basis of charged alpha emitters being electrostatically collected on the surface of a silicon solid-state detector and then detected via spectroscopic analysis [43]. A total of four five-minute counting cycles are executed by RAD-7, bringing the total analysis duration to 30 minutes [93].

Figure (2.3): RAD-7 detector [93]**.**

2.6 Density Functional Theory (DFT)

A mathematical model, that is called "The Density Functional Theory (DFT), is used to study the electronic structure and behavior of many-electron systems in physics and chemistry. DFT demonstrates that the features of a many electron system may be deduced from electron density distribution information using functional. In computational physics and chemistry, DFT is the most widely used and adaptable approach. Furthermore, DFT has proven to be a very effective method for calculating material ground state properties. The opening point of density theory was made by Thomas and Fermi model established in 1927. Thomas-Fermi model calculated the energy of an atom by the half of the kinetic energy of the atom as an electron function density [94].

DFT method computes properties of a many particle system as a functional of electron density or probability density $\rho(\vec{r})$. $\rho(\vec{r})$ that means the probability of electrons in volume element $d\vec{r}$ with any spin for a given state. It is dependent on only three coordinates self-sufficiently of the number of electrons of the system [95]:

$$N = \int \rho(\vec{r})d\vec{r} \qquad (2.1)$$

The ground state energy and all other ground state electronic characteristics, which are exceptionally determined via the electron density, are important notions in DFT.

In 1964, Hohenberg and Kohn (HK) proved two important theorems to establish the principles of DFT as a quantum mechanical method [96].They proved that the ground state of a lot of electron system can be determined through the ground state electron density $\rho(\vec{r})$ [97].

According to these theorems, the ground state energy functional $E_V[\rho]$ can be labeled as in the following [98]

$$E_V[\rho] = \int \rho(\vec{r})\, V_{ext}(\vec{r})d\vec{r} + F_{HK}[\rho] \qquad (2.2)$$

$F_{HK}[\rho]$ represents a functional of $\rho(\vec{r})$to be determined which contains kinetic energy and all the electron connections. $F_{HK}[\rho]$ refers to the HK functional of density independent of the external potential $V_{ext.}(\vec{r})$. Considering of the particle preservation, the difference of ground state energy satisfies to the following principle [98],[96].

$$\delta\left\{E_V[\rho] - \kappa\left[\int \rho(\vec{r})d\vec{r} - N\right]\right\} = 0 \qquad (2.3)$$

which gives:

$$K = \frac{\delta E_V[\rho]}{\delta\rho(\vec{r})} = V_{ext.}(\vec{r}) + \frac{\delta F_{HK}[\rho]}{\delta\rho(\vec{r})} \qquad (2.4)$$

Where K indicates the chemical potential. The ground state electron characteristics of a many-electron system can be calculated exactly. HK theorems did not give the real expression of energy functional $F_{HK}[\rho]$, in

which kinetic functional and exchange-correlation functional were not known [99]. The time-dependent density functional theory (TD-DFT) spreads the important idea of the ground state DFT which can be used to examine the excited-state properties of a system in the presence of time-dependent potentials, such as electric or magnetic fields. The influence of fields on molecules can be studied with TD-DFT as an application for representative excitation energies, oscillator strength, wavelength, molecular orbital character and electronic transitions of the molecules. The theoretical of TD-DFT based on the Runge-Gross theorem (R-G theorem) in 1984 [100],[101].

2.7 Hybrid Functionals

The hybrid exchange-correlation functionals occupy a private site in the molecular applications of the DFT and nowadays it is very popular used in computational physics and chemistry [102]. These functionals combine the exchange-correlation with the Generalized Gradient Approximation (GGA) and an exact exchange functional. The most widely hybrid functional, B3LYP uses Becke's1988 exchange functional (E_X^{B88}) and Lee-Yang-Parr correlation functional (E_C^{LYP}) as gradient rectifications to the topical density approximation LDA exchange and correlation functionals. The exchange-correlation term of B3LYP is shown as in the following form [103].

$$\mathrm{E_{XC}^{B3LYP}} = (1-\mathrm{a})\mathrm{E_X^{LSDA}} + \mathrm{aE_{XC}^{HF}} + \mathrm{bE_X^{B88}} + \mathrm{cE_C^{LYP}} + (1-\mathrm{c})\mathrm{E_C^{LSDA}} \quad (2.5)$$

When the three parameters (a =0.20, b=0.72 and c=0.81), these values were found by fitting the experimental data. The first parameter (a) specifies the quantity of exact exchange, while the second and third parameters (b) and (c) determine the contribution of exchange and correlation, respectively.

2.8 Basis Sets

A basis set in theoretical physical and chemistry refers to a group of mathematical functions utilized to clarify the shape of the molecular orbitals. Both ab-initio and DFT methods employ basis sets to mathematically specify the molecular orbitals in a system. Although it is possible to develop a basis set from scratch, the majority of computations are performed using pre-existing basis sets. The reliability of the findings is confirmed by the type of performing calculations and the chosen basis sets. Slater-type Orbitals (STOs) and Gaussian-type Orbitals (GTOs) represent the two sorts of basis sets (GTOs) [104].

2.9 The Software

All theoretical calculations in this study were done by employing the Gaussian 09 package of Programs, Gauss View 5.0.8, Gauss Sum 3.0 and other assistant programs. These programs are described as below:

2.9.1 Gaussian 09 (G09) Program

The Gaussian program is a computational software package initially published by John Pople in 1970. The Gaussian program is a quantum mechanical software suite that is quite high-end. The "09" mentions to the year 2009 in which the software was published [105].

All of the major molecular modeling approaches, such as molecular mechanics, ab-initio, semi-empirical, HF, and DFT, may be run using Gaussian. Furthermore, with this application, excited state computations may be performed using a variety of methods. The name is derived from Gaussian is derived from the usage of Gaussian Type Orbitals, which Gaussian's creator, John Pople, devised to address the computing issues that Slater Type Orbitals posed. Pople, along with other bright scholars like as S.F. Boys and Isaiah Shavitt, noticed that substituting a sequence of Gaussian functions for the Slater function would substantially simplify

the rest of the Schrödinger equation computation. For this achievement, Pople (1998) received the Nobel Prize in Chemistry (together with Walter Kohn) [104],[105].

2.9.2 Gauss View Program

Gaussian View was built to import Gaussian program input files and show Gaussian program output files in a three-dimensional picture. Gaussian View is not a calculating software, but it does make working with the Gaussian software easier and offers three primary advantages to users.. First, allow the user to draw molecules, even the large ones, as well as rotate, transfer, and change their size with ease, and utilize the mouse. Second, the Gaussian view allows for multiple Gaussian calculations, as well as complicated input preparation for ordinary tasks and sophisticated methods. Third, the Gaussian perspective allows for the examination of Gaussian computations using a range of geometrical tools, such as balanced molecular patterns and electronic density surfaces [104],[105].

CHAPTER THREE

PRACTICL PART

Chapter Three
Practical Part

3.1 Introduction

The practical part will be explained in this chapter. A review of the materials and methodology that were used to measure uranium and radon levels in different water samples collected from Dhi-Qar governorate. The chapter also provides materials and methods used to collect and prepare water samples and the reasons for choosing this region. The samples collected from six types of water (tap water in residential districts, surface water, groundwater, RO water, stations water, and marshes water).

3.2 Area of Study

Dhi-Qar province is located on the Euphrates river's banks, 370 kilometers southeast of Baghdad, Iraq's capital see Figure (3.1). The city is situated in latitudes of 31°14'N and longitudes of 46°19' E. Dhi-Qar, the city, is around 9 meters above sea level. It borders the provinces of Basrah, Missan, Muthanna, Qadissiya, and Wassit and covers 13,552 km^2. It has a population of 1,450,200 people [106]. Marshes are large bodies of water that are dispersed across the city area of this governorate (or Iraq marshes). It is situated in the mesopotamian's lower basin, amid the enormous floodplain marshes produced by the system of Tigris-Euphrates river, and makes up a significant portion of the city's overall region. The marshes are regarded as a unique environment in the Middle East [107]. The rivers Tigris and Euphrates are Iraq's principal water sources since ancient times [108]. Dhi- Qar's water has a significant salty content and comes from two different sources. The major source is saline water from the Euphrates river, with sweet water from the Al-Garaf River as a secondary supply (a branch of the Tigris river). [109].

Figure (3.1): Area of study (Dhi-Qar governorate).

3.3 Collecting and Preparing of Samples

A whole number of samples of water that are (125 sample) were obtained from various places around the Dhi-Qar governorate. The water samples are separated into six categories, as shown below.

1. Thirty samples (Tap water) as shown in Figure (3.2).
2. Twenty samples (Marshes water) as shown in Figure (3.3).
3. Twenty samples (Stations water) as shown in Figure (3.4).
4. Fifteen samples (Surface water) as shown in Figure (3.5).
5. Twenty samples (Groundwater) as shown in Figure (3.6).
6. Twenty samples (RO water) as shown in Figure (3.7).

In November 2019, samples were taken in order to define the amounts of uranium isotopes, radon, and different physicochemical characteristics in the water of those places. Approximately 1 liter of water was collected for each site, it is divided into groups with three different sizes, the first with a size of 60 ml to measure uranium, the size of 250 ml is to account radon (passive method) and the latter is in the size of 250 ml to measure radon directly (active method). For six sets of samples, coordinates were utilized to calculate the ground position of any item employing the GPS (Global Positioning System), that refers to a satellite navigation system utilized to detect the location of any item on the ground, as shown in Tables (3.1) to (3.6), respectively. Also, all six groups have been designed by GIS technical (ArcGIS 10.7.1), as shown in Figures (3.2) to (3.7), respectively. Water samples were measured directly without any preparation. The collected samples were stored for about one month prior to counting. The storing is carried out in order to achieve a secular equilibrium within the uranium chain between ^{222}Rn and its parent ^{226}Ra [6].

Table (3.1): The coordinates of the sites for tap water.

No.	Symbol code	Location name	Coordinates in meter	
			E	N
1	T1	AL ISQAN ALQADIM	3434731.419	618518.0556
2	T2	AL SALIHIA	3436023.542	620757.3464
3	T3	AL SHARQIA	3435526.572	620260.3758
4	T4	AL SHAELA	3434035.660	618313.4207
5	T5	AL SHIYBANEI	3434743.112	617582.5817
6	T6	AL ISQAN AL SINAEI	3431351.228	622340.4906
7	T7	DWR SAYD HAMZA	3430330.848	623351.5368
8	T8	AL ZAEILAT	3431996.793	620591.2945
9	T9	TINA	3434789.701	619064.1782
10	T10	AL MUHIDIA	3434258.885	619562.3284
11	T11	AL SIKAK	3432855.136	617648.8068
12	T12	AL THAWRA	3433606.554	617008.5137
13	T13	AL MANSURIA	3433945.222	616156.5534
14	T14	AL AMIR	3434469.098	616310.0121
15	T15	SHARIE BAGHDAD	3434537.89	617818.1406
16	T16	AL BASHAYIR	3436273.56	618479.6004
17	T17	AL SARAY	3435919.018	619326.2691
18	T18	AL SHUMUKH	3433765.305	618733.601
19	T19	AL ASKARI	3436908.562	621321.232
20	T20	SUMER (1)	3436548.728	619749.6034
21	T21	SUMER(2)	3437717.742	619692.5846
22	T22	AL SHUHADA	3438691.673	621025.9424
23	T23	AL FADA	3437752.526	622295.531
24	T24	AL TADHIYAH	3435839.447	621698.4186
25	T25	UR (1)	3437114.833	618486.7653
26	T26	UR (2)	3437572.812	618834.5978
27	T27	AL ADRUH AL MAHALIYA	3435433.643	618799.8145
28	T28	AL ZAYTON	3436088.916	618631.1675
29	T29	MADINAT AL SADR	3439439.21	618770.0741
30	T30	AL MUTANAZAH	3434897.462	617973.3342

Table (3.2): The coordinates of the sites for marshes water.

No.	Sample code	Coordinates in meter	Coordinates in meter	
			E	N
1	M1	Al Hammar (1)	3423844.376	654415.7051
2	M2	Al Chebaish	3426517.09	691183.2842
3	M3	Al Hammar (2)	3415623.427	660066.1326
4	M4	Khamisiyah	3413042.597	637344.9429
5	M5	Umm Nakhleh (1)	3411880.887	655177.0162
6	M6	AZ 24 (1)	3429183.925	669031.9446
7	M7	AZ 24 (2)	3429011.683	662999.8945
8	M8	M2 (1)	3417001.011	642576.9555

⟶ Next

9	M9	M2 (2)	3421305.502	646570.623
10	M10	M2 (3)	3413756.998	644133.0137
11	M11	M5 (1)	3411267.205	651681.0563
12	M12	M5 (2)	3417553.837	650435.7798
13	M13	BC3 (1)	3416229.18	689095.8178
14	M14	BC3 (2)	3420895.183	690157.4907
15	M15	BC4	3420450.804	677629.3178
16	M16	Umm Nakhleh (2)	3412761.755	660587.4567
17	M17	Late public estuary	3424229.869	626025.4302
18	M18	Al Hafar	3422945.385	665727.7155
19	M19	M4	3424329.9	637887.6142
20	M20	Abu Subat	3432427.442	692371.959

Table (3.3): The coordinates of the sites for stations water.

No.	Sample code	Location name	Coordinates in mater	
			E	N
1	ST1	7 ATHAR	3438654	622626.8
2	ST2	AL MUTANAZA	3435193	617181.5
3	ST3	ABU ALSHWUJ	3441013	618516.5
4	ST4	AL SIDARIN	3438830	622352.9
5	ST5	AL FADAA	3438787	622432.1
6	ST6	AL MANSURIA	3435209	617237.6
7	ST7	AL AIQTISADIIYN	3435198	617200
8	ST8	AL MUJAMEAT ALSEBEA	3438440	622618.1
9	ST9	AL SHAAMIA	3439909	618604.7
10	ST10	NOOR AL ZAHRAA	3441116	619292.6

Table (3.4): The coordinates of the sites for surface water.

No.	Sample code	Coordinates in mater	
		E	N
1	S1	3434288	620681.8
2	S2	3434581	620415.9
3	S3	3434546	620038.9
4	S4	3434780	619868.2
5	S5	3434740	619594.4
6	S6	3434919	619507.1
7	S7	3434871	619269
8	S8	3435061	619114.2
9	S9	3435038	618852.2
10	S10	3435153	618725.2
11	S11	3435133	618606.2
12	S12	3435300	618554.6
13	S13	3435276	618439.5

⟶ Next

14	S14	3435407	618419.6
15	S15	3435351	618332.3

Table (3.5):The coordinates of the sites for groundwater.

No.	Sample Code	Coordinate in matter	
		E	N
1	G1	3461453	614594.8
2	G2	3461359	614540.6
3	G3	3461344	614462.1
4	G4	3461441	614320
5	G5	3461681	614063.9
6	G6	3461892	613920
7	G7	3462012	614133.1
8	G8	3461750	614346.2
9	G9	3461688	614435.9
10	G10	3461428	613748
11	G11	3461410	613953.6
12	G12	3461768	613495.6
13	G13	3461920	613647
14	G14	3461916	613512.4
15	G15	3461757	613303.1
16	G16	3461284	614125.6
17	G17	3461503	614198.5
18	G18	3461471	614484.5
19	G19	3461355	614411.6
20	G20	3461905	614077

Table (3.6): The coordinates of the sites for RO water.

No.	Sample code	Location name	Coordinates in mater	
			E	N
1	RO1	AL MURTHDHA	3435221	617310.3
2	RO2	AL SARIE	3434601	620881
3	RO3	AL SALSIBIL	3434332	620461.7
4	RO4	ALL NIAZ	3438809	622324.4
5	RO5	AL JAMIEA(1)	3435719	617265.5
6	RO6	AL JAMIEA(2)	3435634	617106.8
7	RO7	AL FADHLIA(1)	3425522	628339.8
8	RO8	AL FADHLIA(2)	3425449	628219
9	RO9	AL ISKAN	3431673	621196.6
10	RO10	AL BITAT	3421020	637930.9
11	RO11	AL GHADIR	3441895	618722.1
12	RO12	AL QARYA(1)	3443105	618335.3
13	RO13	AL QARYA(2)	3443339	618217.9
14	RO14	AL NOOR	3434171	620804.6

⟶ Next

15	RO15	AL RASUL	3440842	618767.2
16	RO16	BASHAYIR	3436097	618113.4
17	RO17	AL HABOBI	3435712	619538.3
18	RO18	AL ADRUH AL MAHALIYA	3435896	618716.9
19	RO19	AL SHUHADA	3438360	621902
20	RO20	UR	3437220	617996

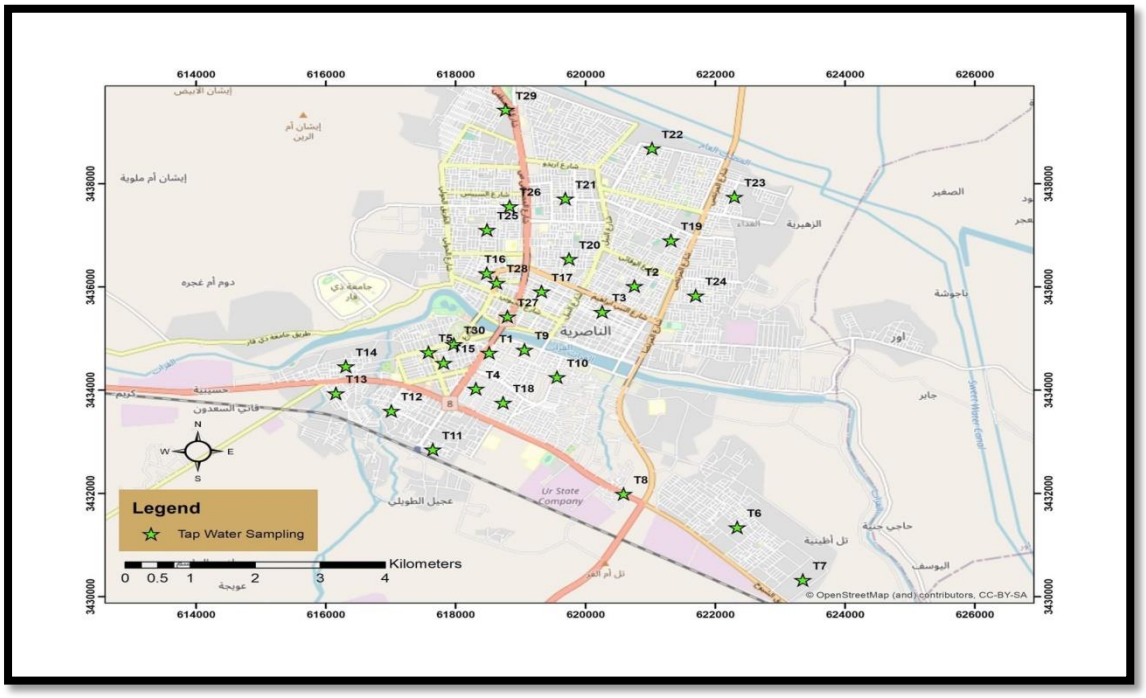

Figure (3.2): Samples positions of tap water.

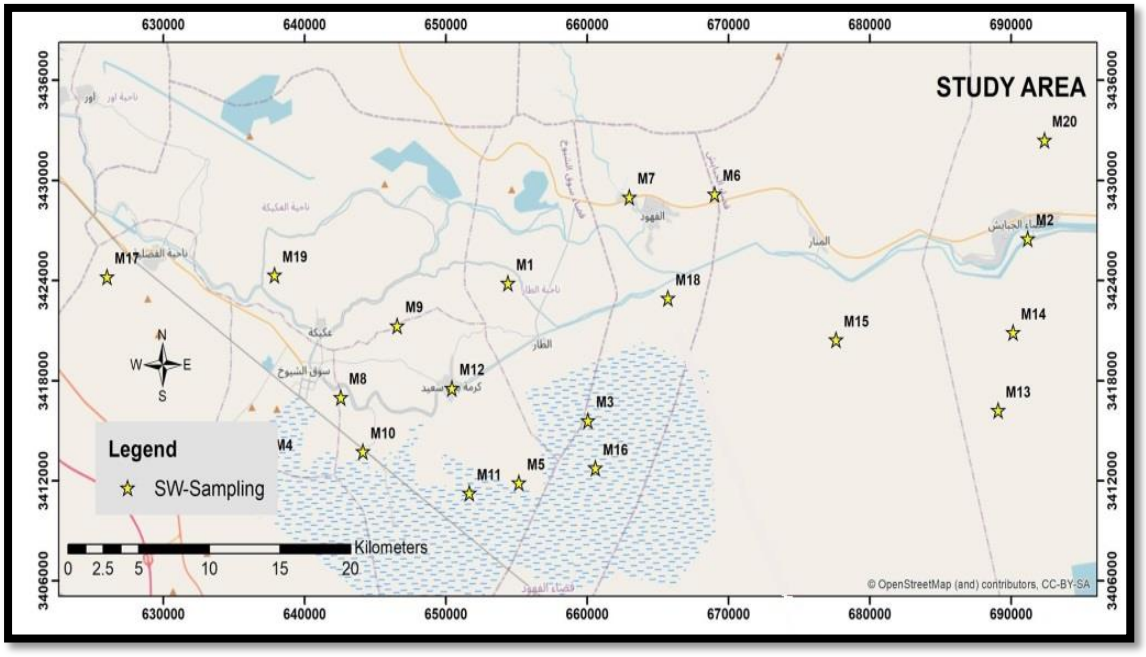

Figure (3.3): Samples positions of marshes water.

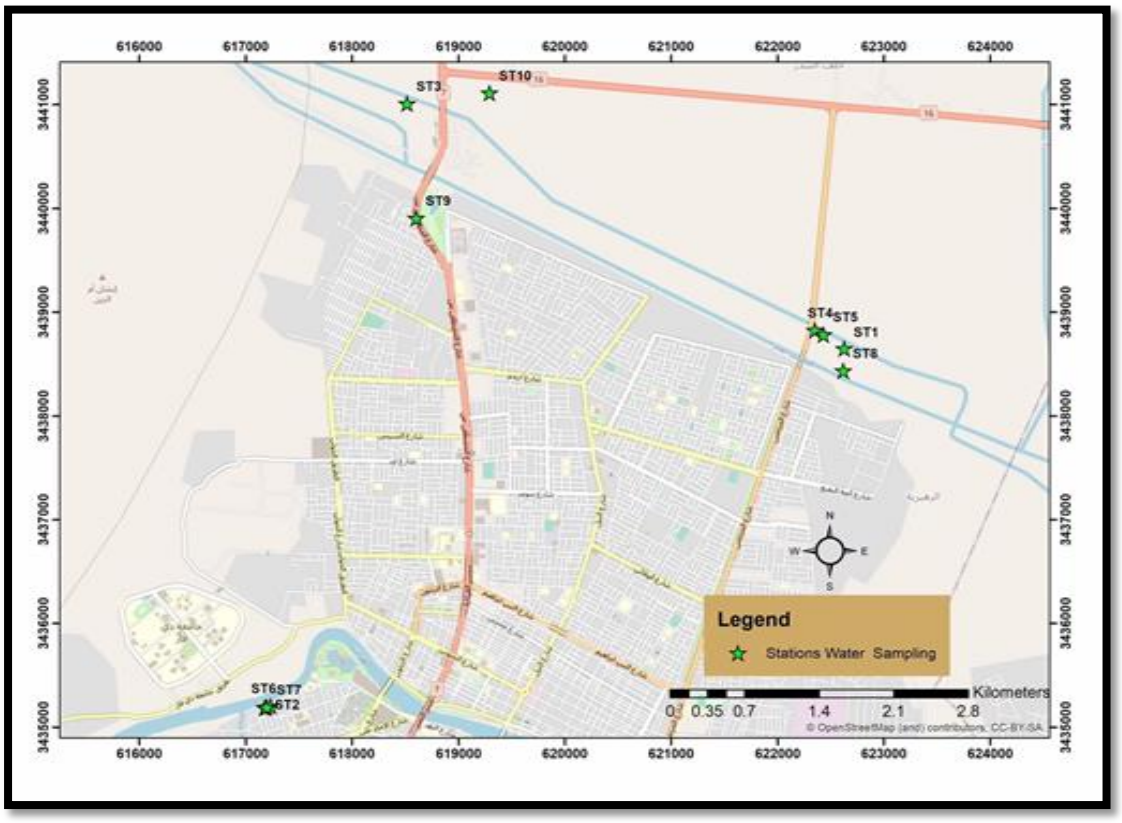

Figure (3.4): Samples positions of stations water.

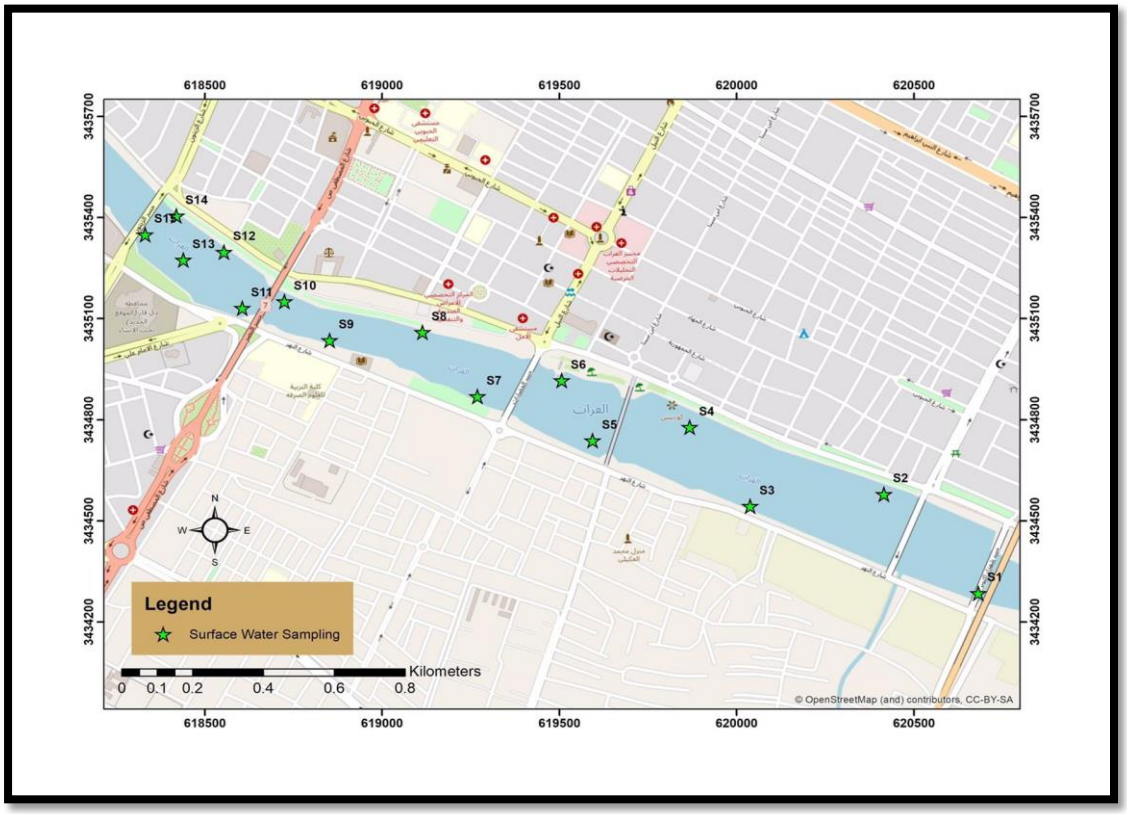

Figure (3.5): Samples positions of surface water.

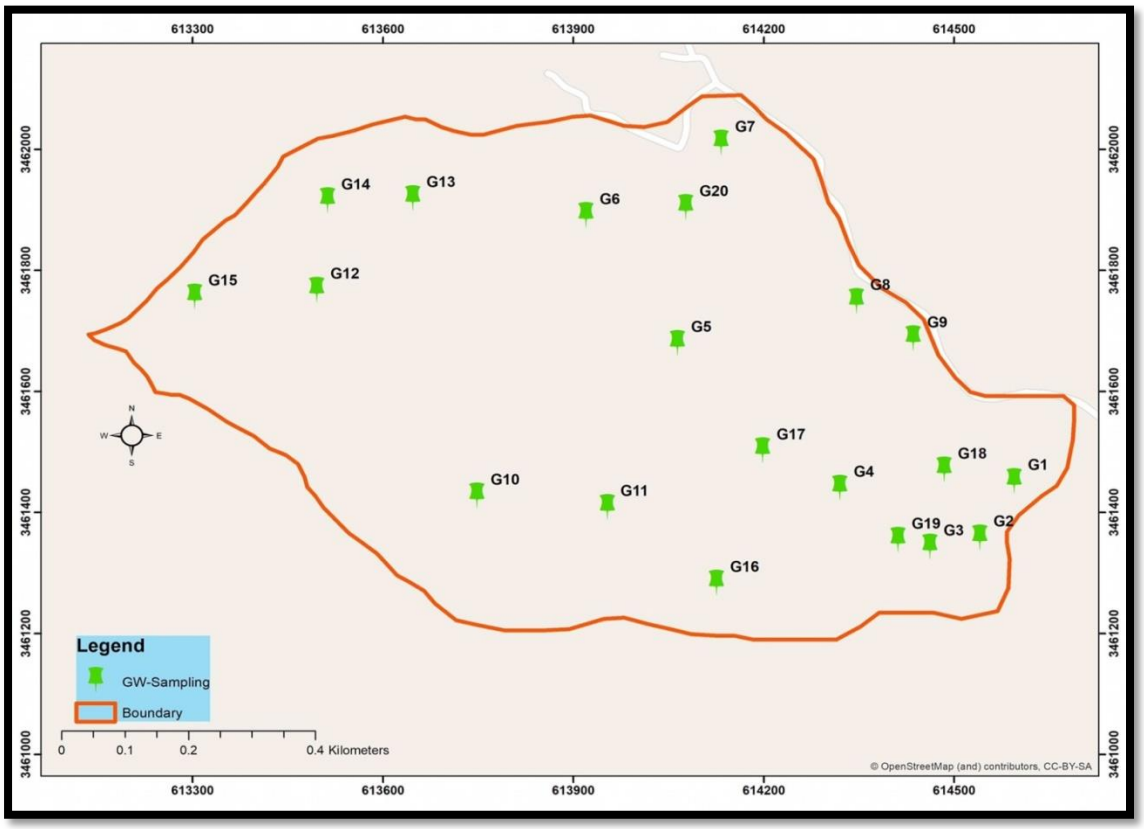

Figure (3.6): Samples positions of groundwater.

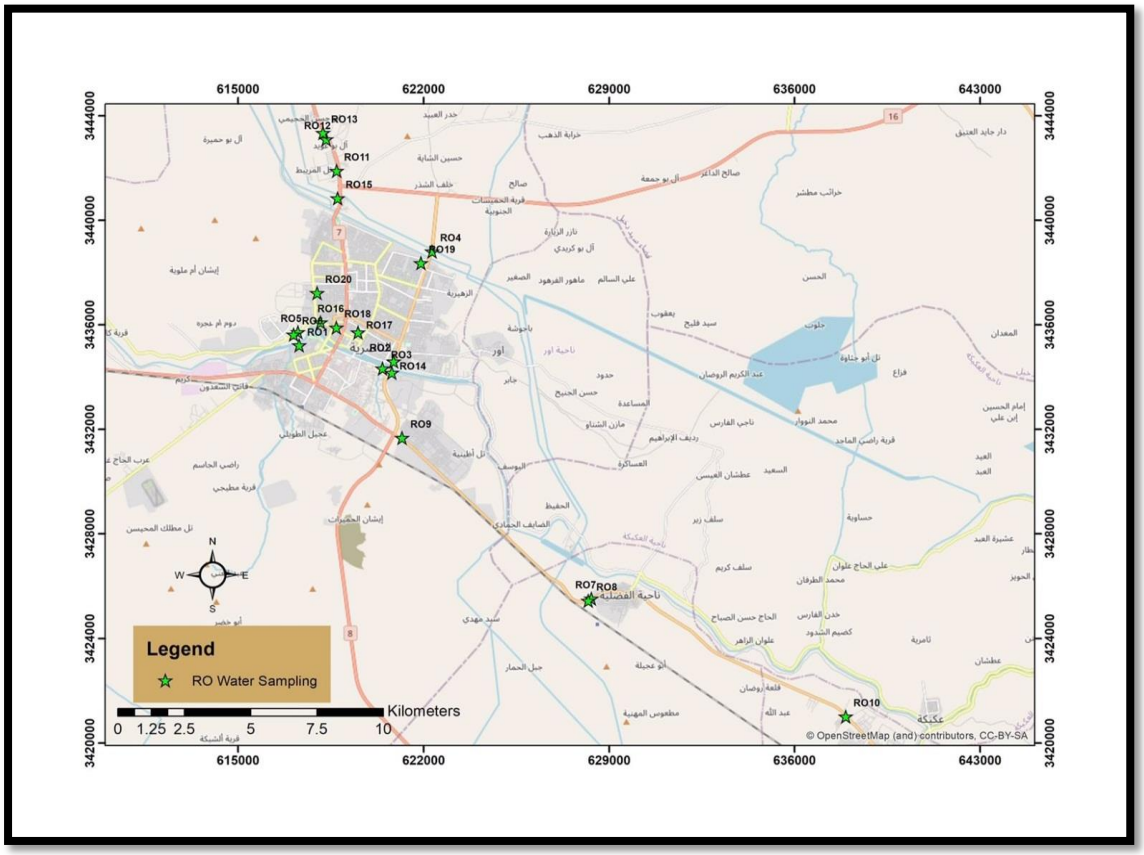

Figure (3.7): Samples positions of RO water samples.

3.4 Experimental Setup

In current study, the experiential setup is assorted into two method according to the uranium concentrations and radon concentrations, as following:

3.4.1 Uranium Concentration Calculation

The detector name CR-39 ($C_{12}H_{18}O_7$) and it was purchased from TASTRAK Analysis System, Ltd., UK: TASTRACK. A sheet of CR-39 detector was 2.5 cm × 2.5 cm dimensions, thickness 1mm, with code for each sheets contain code and number to fit TASL image system. The intensity of the sheet was approximately 1.32 g/cm^3. The dimensions of the sealed plastic cans were with height of 6.5 cm and diameter of 3.5 cm, the sample name and storage date were written Figure (3.8) show the plastic container used in the current study. The detector (CR-39) were put at the bottom of the containers by adhesive tape then the containers were filled with water samples. The cover of the containers were tightened with layer of adhesive tape to prevent radon gas from leaking out. The water samples were stored for a period of 70 days. The current study adopted the long-term method of irradiation. When the time of irradiation is end, the detectors are pick up from the containers to begin with chemical etching process. The method to account the uranium concentrations for the samples of water in the current study in the two areas of research, were the standard method sources. The standard solutions prepared for uranium was carried out using uranium octoxide U_3O_8 as the reference method [110]. In the standard solution, the quantities of uranium are calculated using special uranium dosimeters. The same specification was used for the container in which the standard source were set and the same irradiation period was used as indicated in the study [110].

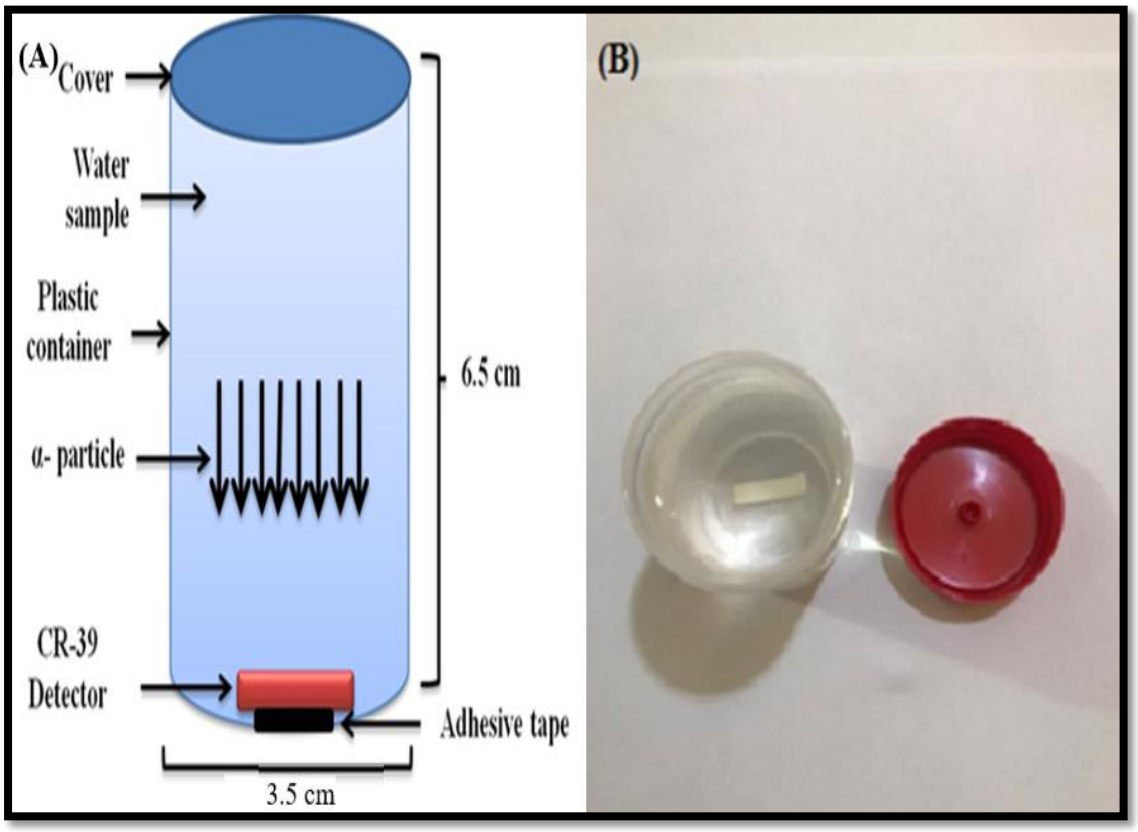

Figure (3.8): Dosimeter container for uranium measurements; A) diagram of container. B)cylindrical polyethylene sample container.

3.4.2 Radon Concentration Calculation

3.4.2.1Using CR-39

0.25 L of water samples were collected in plastic cups with radius (3.5cm), length (18 cm), and volume (1000 ml) as shown in Figure (3.9). CR-39 detectors (Ltd., UK: TASTRACK) was utilized in this investigation. A piece of the CR-39 detector was positioned at the bottom of each cover of the cylinders. A thin sponge was placed to reduce moisture and prevent thoron from passing through and reaching the detector. The samples were set at the bottom of the cylinders, then the cylinders were sealed, and stored at room temperature for 90 days (exposure time) [111].

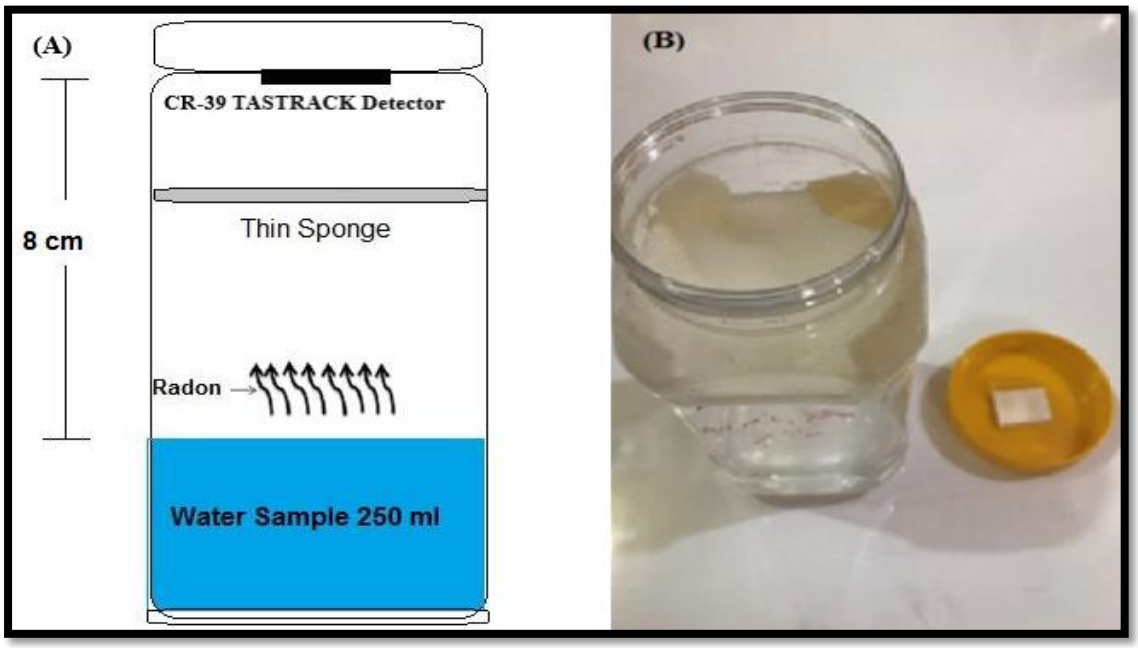

Figure (3.9): Dosimeter container for radon measurements; A) diagram of container. B) cylindrical polyethylene sample container.

3.4.2.2 Employing RAD-7

The RAD-H_2O detector is an add-on for the RAD-7 detector, that is designed to monitor the gas exists in water at a variety of concentrations. The results must be acquired through sixty munities after obtaining the sample, and sterilization must be performed (i.e., the moisture must be less than sixty percent), after that the concentration of radon within water must be calculated via Grab system by placing a Pump on it. To elicit radon from the sample, the pump runs for 5 minutes in each session, then radon will be drawn and delivered to the RAD7 detector to be measured. Later on, it pauses for five minutes and reaches equilibrium, and then the four other sessions are repeated to have a total test of 30 minutes (i.e., measuring radon concentration, moisture, temperature, and normal deviation) [112]. The operational number, the 4-circuit diagram, the cumulative spectrum, and the number of turning are also included [14]. In a sample of 250 ml, the ratio of radon elimination from water in the air ring is 94 percent, which is quite high. The

schematic diagram of the RAD-H_2O supplement is shown in Figure (3.10) [10],[11].

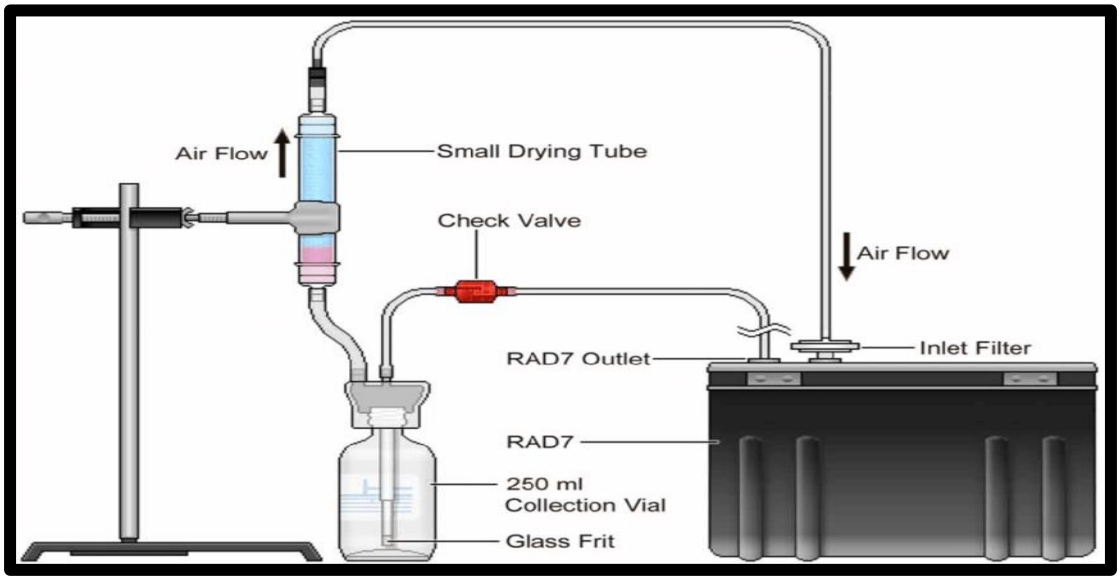

Figure (3.10): RAD-H_2O detector [113]**.**

3.5 Chemical Etching

The following formula were used to prepare the etching solution [119]:

$$\boldsymbol{W = Weq \times N \times V} \qquad (\mathbf{3.1})$$

where:

w : represents the weight of NaOH required to make the given normality (100 gm) ready.

w_{eq} is equivalent weight of NaOH (which it is equal = 40).

N is normality (Which it is equal 6.25 N for CR-39 detector)

V is the volume of distilled water (0.4 Litter).

The etchant compartment has a total volume of 400 ml contains the NaOH solution with 6.25 N. This system is closed to assembly except for tiny ventilation at the top of the condenser tube preventing any change of the condenser tube. Throughout the experiment etchant normality (concentration) due to evaporation. The detectors were placed inside the glass pyrex by connecting them with wires see Figure (3.11), then the

pyrex was placed inside the water bath (water path type (HH-420) made in Germany which includes a thermostat and it can be operated over a range of (0- 100 ºC ±1), as shown in Figure (3.12).When the temperature of the water bath reached 70 ºC, 5 hours were calculated as the most suitable conditions [111]. The detectors were removed from the solution by forceps and washed with distilled water, dried and saved by plastic boxes to ready for microscopy processing. Figures (3.11) and (3.12) shows a picture of the water bath and the chemical etching process.

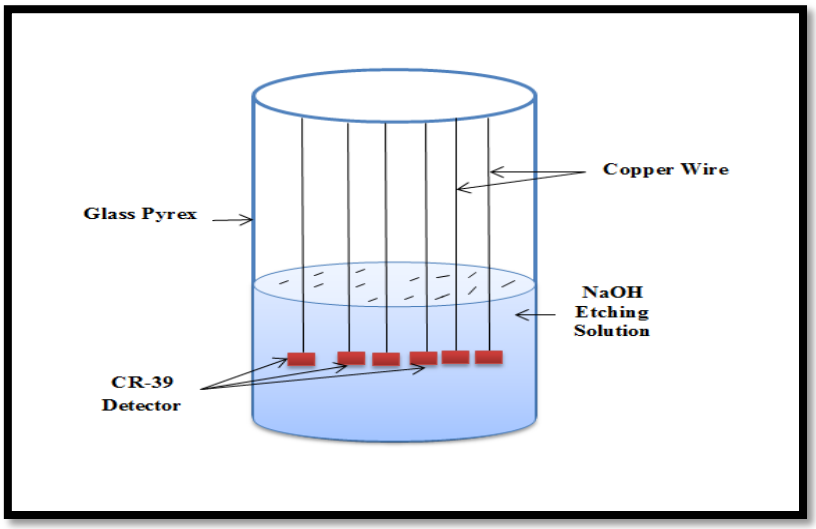

Figure (3.11): Mechanism of chemical etching.

Figure (3.12): Digital water path HH-420.

3.6 Microscopy Processing

In this study, a microscopic treatment was performed to calculate the concentrations of uranium and radon by three methods, two of which were practical and the last was theoretical. The purpose of diversifying microscopic treatment methods to be familiar with all internationally known methods of performing processing such data. The use of all methods tells us about the accuracy and efficiency of each method in conducting the calculations and the time required to extract and process data.

3.6.1 Manual Counting

The microscopy processing manually is done by using the optical microscope is of the type (Novel, china) . The magnifying power of the microscope that used to count tracks of (400X), where the object piece (40X). The detector surface dividing to ten areas of view to count the alpha particle and taking a multiple picture of each region by using of digital camera connecting with computer via cable USB after install the camera program on the computer to count number of tracks, as shown in Figure (3.13).

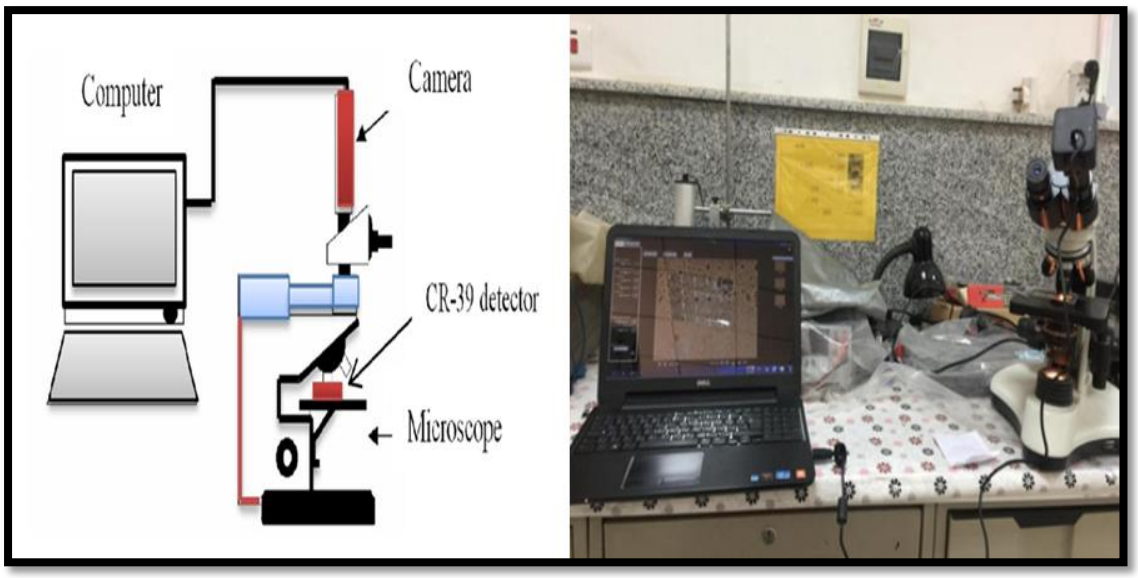

Figure (3.13): Microscopy processing manually.

3.6.2 TASL Counting

As a complete laboratory system, the TASLIMAGE dosimetry system refers to a system that includes "a microscope based analysis system, an etch tank, a drying cabinet, trays, and a computer" that runs the analysis software [12], see Figure (3.14). The general characteristics of the radon dosimetry system will be discussed. The TASLIMAGE is a track analysis device based on a microscope that uses high quality Nikon optics to accomplish remarkable track and background feature discrimination. The technology is one-of-a-kind in that it analyzes and classifies any single track before calculating the dosage. The algorithm that distinguishes an etched track from a background feature as shown in Figures (3.14) and (3.15), whether it's a scratch, a hair, or anything else, does so by analyzing 31 distinct criteria related to track characteristics. The method might be used in research as a totally automated readout system or for single plastic analysis. To create a dosage measurement for any slice of plastic in the automated mode, that is generally used for dosimetry services, simply a single click is required [114]. Individual plastics can also be analyzed using a user interface that offers a variety of choices for in-depth research. The scan data is translated to a dosage measurement automatically, and the findings are stored in a database. The system can read “Auto scan” type plastics or be adapted for any size plastic, including automated ID scanning, in addition to our own unique TASTRAK format detectors. TASL has progressed TASTRAK, an exceptionally sensitive PADC plastic that enables for effective background track recognition. TASLIMAGE system specifications [115]:

1- Dimensions (W×H×D): 486 x 440 x 640 mm

2- Stage area: 203 × 203 mm

3- Throughput: One minute is required for each detector to be analyzed.

4- Radon detectors: There are up to 49 radon detectors each tray of radon detectors.

5- Optics: Nikon standard sextuple nosepiece, Nikon CFI LU Plan Epi 20x objective, Nikon L-IM focusing unit.

The TASLIMAGE system was used to automatically scan, identify, and count etched detectors PADC. It comprises a motorized scanning stand with 3 axis monitored by software, an apochromatic optical microscope with Nikon optics of high quality, a scanning (etching) framework, an analysis control software, and a dedicated computer (CR-39). The track density for any measured detector may be automatically recorded using the given detector correspondance number.

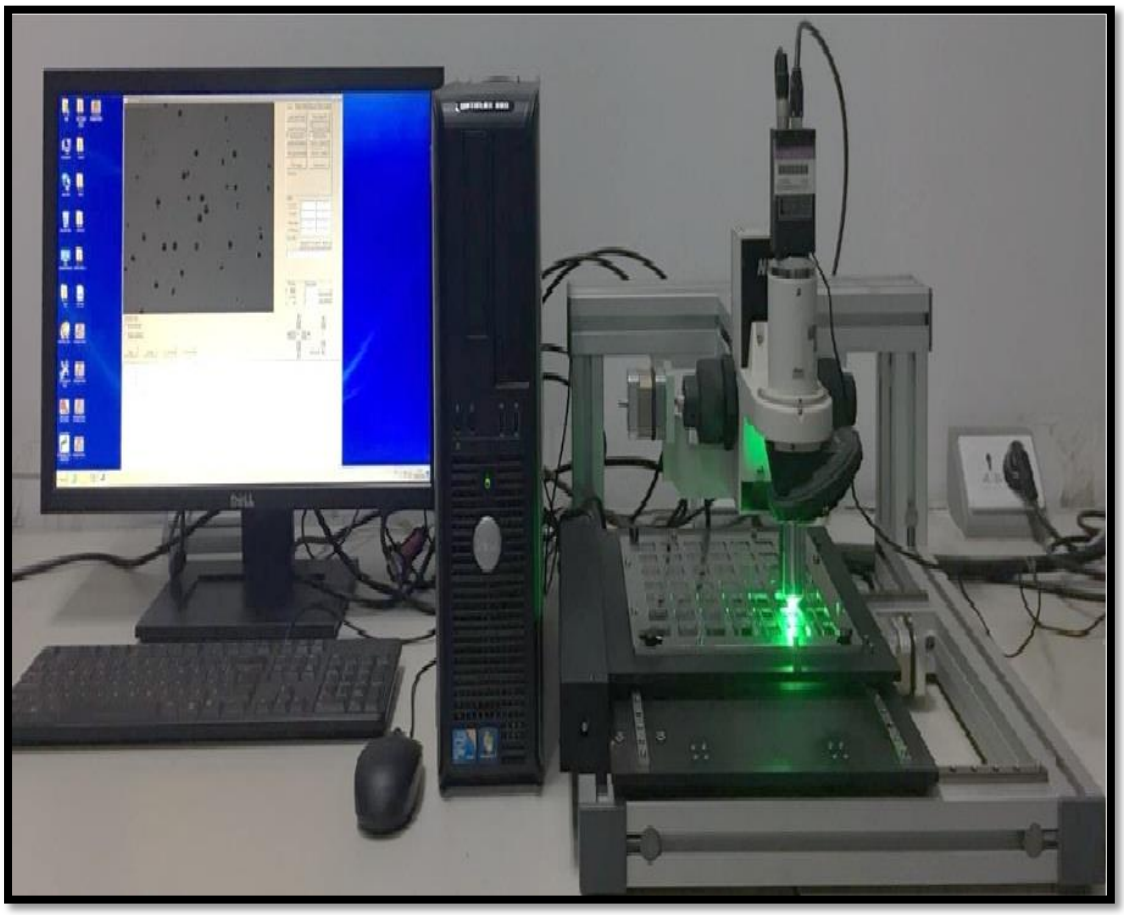

Figure (3.14): TASLIMAGE dosimetry system [116]**.**

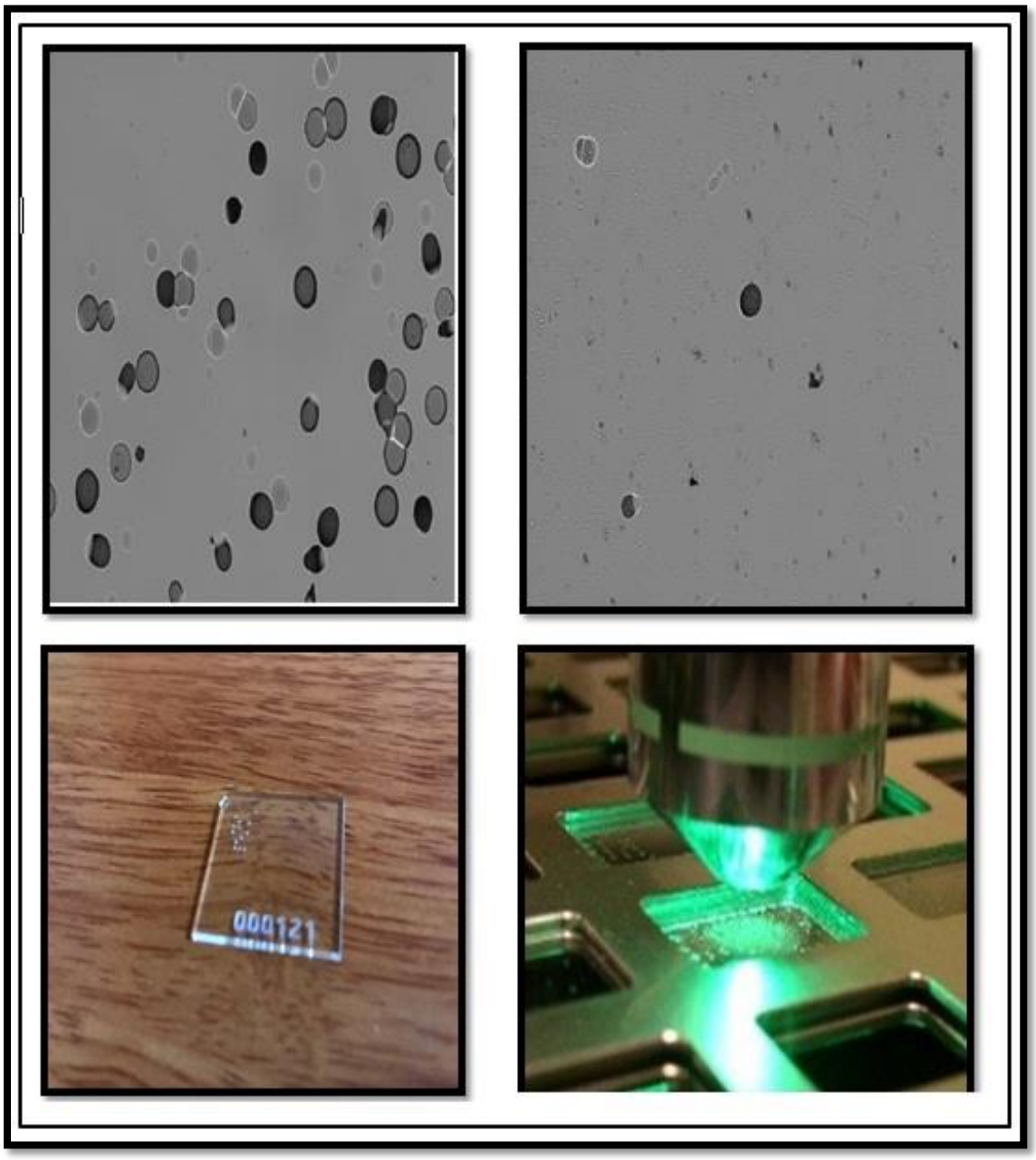

Figure (3.15): Spots of alpha particle and auto processing to code CR-39 detector.

3.6.3 CR-39-D2 Counting

A theoretical program has been progressed to count the number of nuclear tracks (alpha particles) using the Matlab-2014 program see Figure (3.16). Nevertheless, before the development, the program had the ability to download and calculate only one image, which was known as (CR-39-D1) [117], while the current program had the ability to process, download and calculate the number of nuclear tracks to ten images and

read it automatically, which is called (CR-39-D2). The mechanism work of this program, where first the images obtained from dividing the detector are loaded into several regions as in Figure (3.17,a), and then rely on special sensitive functions in the Matlab-2014 program such as the (Gray) function, which works to convert the image to gray, so that the program can sense the nuclear tracks (alpha particles) as in Figure (3.17, b). The next stage, in which the image is converted into a binary image, as in Figure (3.17, c), and then the inverse of the binary image is taken (inverted binary image)as in Figure (3.17, d) so that the program can isolate the nuclear tracks (alpha particles) from the impurities on the detector (the radioactive background), The final stage includes calculating the number of nuclear tracks in the image and measuring their diameters through the (center) function, which is characterized by its ability to sensitive circular shapes and measure their diameters. The last image shows the last stage in the program, and it shows the original image with the diameter of each nuclear trace being printed on the original image, and the number of nuclear traces is displayed. The results can be displayed in the form of the (Excel) program. Figure (3.16) shows the interface of the program and notes the number of images that have been uploaded to be processed automatically. The process of downloading the images and passing them through the various stages of the program is done after processing 50 pictures, reading and analyzing them automatically a few minutes, relying on the number of tracks on the picture.

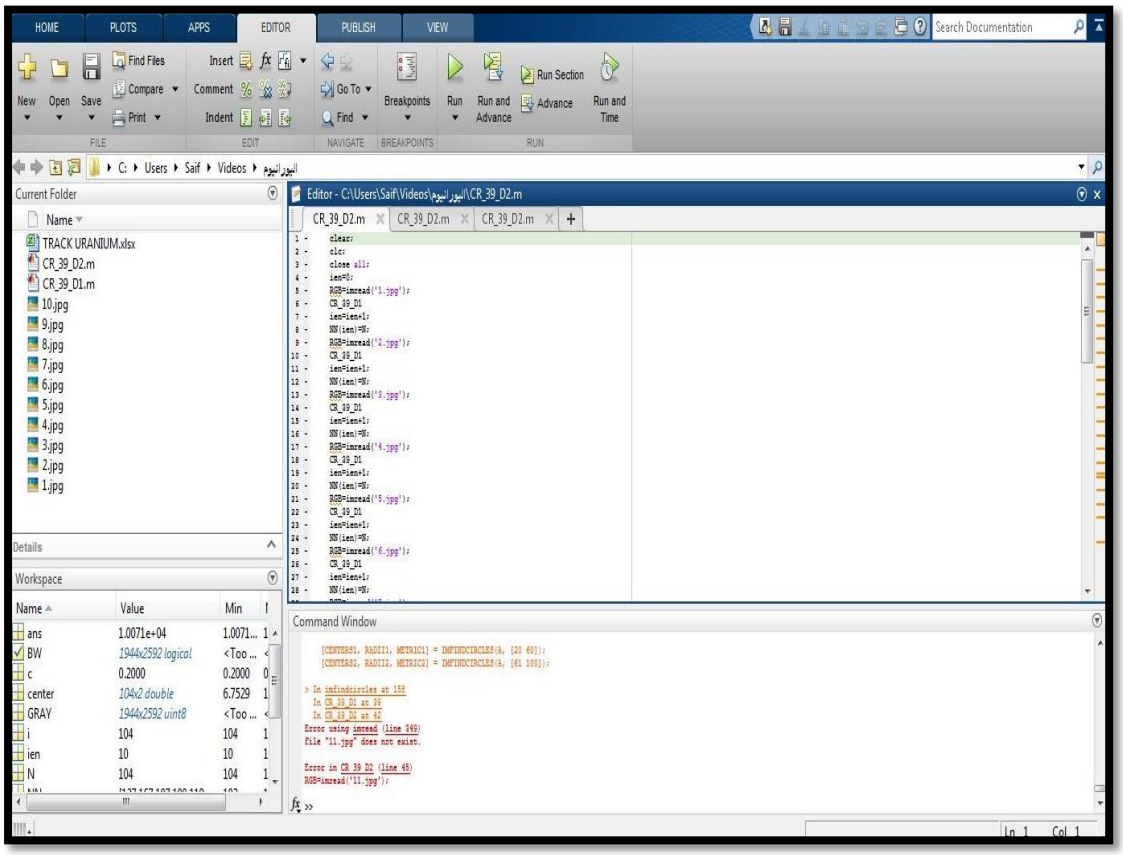

Figure (3.16): The CR-39-D2 program interference.

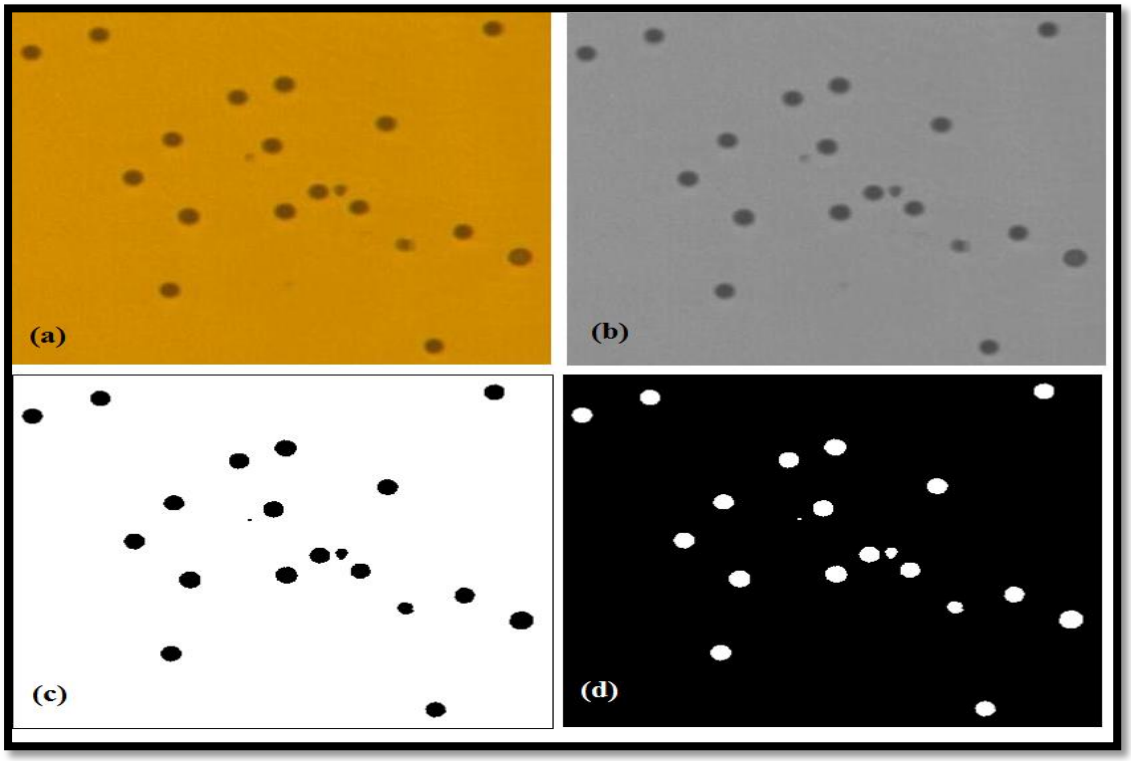

Figure (3.17): The stages of reading and count the tracks on CR-39 detector.

3.7 Theoretical Calculations

3.7.1 Uranium Levels

The tracks density (ρ) in unit (track/cm^2) using CR-39 detector was calculated using the following relation [110],[118]:

$$\textbf{Track density } (\rho) = \frac{\textbf{Average number of total pits (tracks)}}{\textbf{Area of field}(cm^2)} \qquad (3.2)$$

The amounts of uranium (UC) in water samples (ppb or µg / L) are determined by using the following relation [110],[34]:

$$\frac{C_x}{\rho_x} = \frac{C_s}{\rho_s} \qquad (3.3)$$

Where C_x is uranium concentration in unidentified sample, $C_s$uranium concentration in standard samples, while, ρ_x and ρ_s in unidentified and normal samples is monitored, correspondingly.

Special uranium dosimeters were used to test uranium concentrations in water (ppb or µg/L), as illustrated in Figure (3.18).

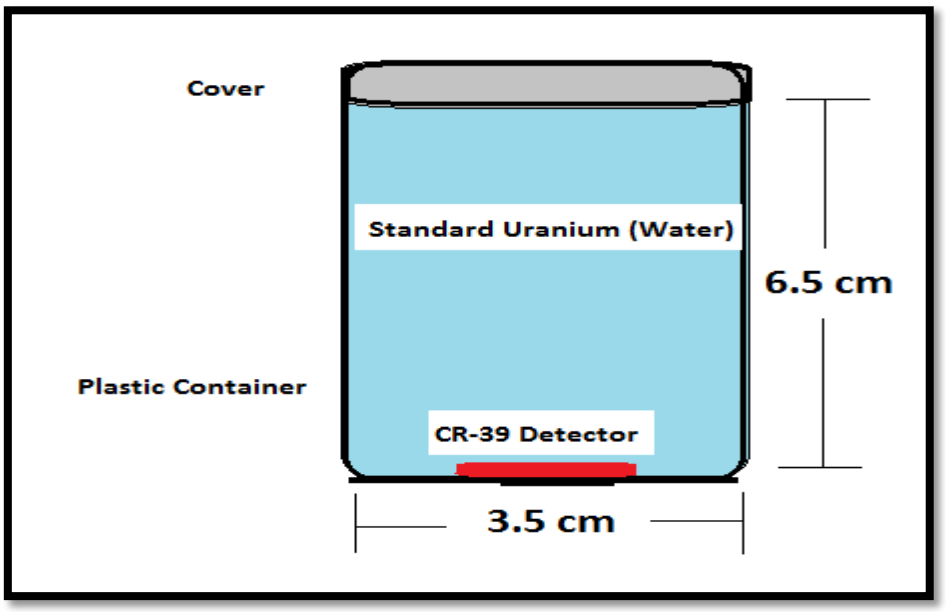

Figure (3.18): Special uranium dosimeters [110],[37],[119].

The uranium content was measured using the calibration curve as shown in Figure (3.19) for water samples of both research areas according to previous studies [110],[118],[120].

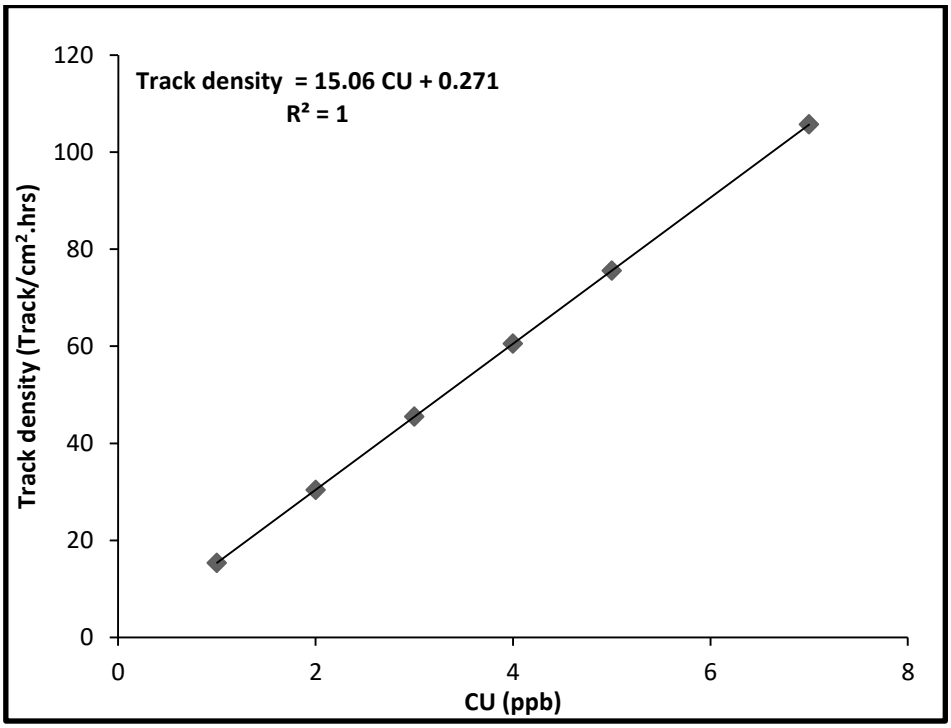

Figure (3.19): Calibration curve for uranium levels[110]**,**[118]**,**[120]**.**

3.7.1.1 Uranium Isotopes

The specific activity of uranium (A) in water samples can be calculated for uranium isotopes (^{238}U, ^{235}U and ^{234}U) by determining the uranium concentrations (UC), specific activity for uranium (S.P.A.) and the mass fraction of them (I.A.M) using the following equation [118],[110]:

$$\boldsymbol{A\left(\frac{Bq}{L}\right) = UC\left(\frac{mg}{L}\right) \times I.A.M(\%) \times S.P.A.\left(\frac{Bq}{mg}\right)} \qquad (\mathbf{3.4})$$

Where A shows the particular activity (Bq/L), I.A.M represents the isotopic affluence (percentage) via mass fraction, and S.P.A represents the particular activity [120]. The radioactive characteristics of normal

uranium isotopes for I.A.M and S.P.A were used in present study that published in the previous studies see Table (3.7) [120], [10],.

Table (3.7): Radioactive characteristics of normal uranium isotopes [120],[10].

Isotope	Particular activity for Uranium (S.P.A.) (Bq/mg)	Isotopic Affluence Mass fraction (I.A.M.) (%)
^{238}U	12.44	99.2745
^{235}U	80	0.72
^{234}U	230,700	0.0055

3.7.1.2 Radiological Risks of Uranium

3.7.1.2.1 Annual Effective Dose (E_T)

E_T (Sv/y) is the annual effective dosage for the inhabitance (after calculating the ^{238}U, ^{235}U and ^{234}U emanating from the ingestion of drinking water measure by using the following equation [110],[118]

$$E_T\left(\frac{Sv}{y}\right) = A\left(\frac{Bq}{L}\right) \times 365(d) \times C_w\left(\frac{L}{d}\right) \times e(g)\left(\frac{Bq}{y}\right) \quad (3.5)$$

Where, e(g) represents the dosage coefficients (Sv/Bq) for ^{238}U ($4.5x10^{-8}$), ^{235}U ($4.7x10^{-8}$) and ^{234}U ($4.9x10^{-8}$), C_w represents consumption ratio of water (2L/d) [121].

3.7.1.2.2 Excess Cancer Risk (ECR)

The excess cancer risk (ECR) was evaluated employing uranium level in Bq/L (Bq/L= 1 µg/L of uranium equals to 0.02528 Bq/L [122] and risk factor as following according to USEPA [123].

$$Excess\ cancer\ risk = uranium\ level\ of\ water(Bq/L) \times risk\ factor\left(6.07 \times 10^{-5}\ per\ \frac{Bq}{L}\right) \quad (3.6)$$

Finally, the risk factor was 6.07×10^{-5} per Bq/L [124].

3.7.1.3 Chemical Toxicity

The chemical/non-carcinogenic risk for uranium was described using the following relations in terms of Lifetime Average Daily Dose (LADD) and Hazard Quotient (HQ) [25]:

$$\boldsymbol{LADD}\left(\frac{\boldsymbol{\mu g}}{\boldsymbol{kg.day}}\right)=\frac{\boldsymbol{EPC}\left(\frac{\boldsymbol{\mu g}}{\boldsymbol{L}}\right)\times\boldsymbol{IR}\left(\frac{\boldsymbol{L}}{\boldsymbol{day}}\right)\times\boldsymbol{EF}(\frac{\boldsymbol{days}}{\boldsymbol{y}})\times\boldsymbol{D}(\boldsymbol{y})}{\boldsymbol{AT}(\boldsymbol{year})\times\boldsymbol{W}(\boldsymbol{kg})} \qquad (\mathbf{3.7})$$

In the mentioned Equation ; EPC refers to the exposure point concentration of uranium in water (μg/L), IR represents ingestion rate (1.38L/day), EF is ingestion occurrence (365days/ y), D =Duration (69.89 y), AT = Average time and W is the ideal body weight (70 kg) [33].

$$\boldsymbol{HQ}=\frac{\boldsymbol{LADD}\,(\frac{\boldsymbol{\mu g}}{\boldsymbol{kg.day}})}{\boldsymbol{RFD}\,(\frac{\boldsymbol{\mu g}}{\boldsymbol{kg.day}})} \qquad (\mathbf{3.8})$$

Where RFD points out to the limitation of the reference dosage taken as 0.6 μg/kg.day [125].

3.7.2 Radon Concentrations

^{222}Rn concentrations in the air of the space of the tube $\boldsymbol{(C_{Rn}^{a})}$ was calculated using the following formula [126]:

$$\boldsymbol{C_{Rn}^{a}}\left(\frac{\boldsymbol{Bq}}{\boldsymbol{m^3}}\right)=\frac{\boldsymbol{\rho}}{\boldsymbol{K\,t}} \qquad (\mathbf{3.9})$$

Where **ρ** refers the track density on the detector (Tr/cm^2), **t** represents the period of the exposure (90 day), and *K* is the calibration factor. The calibration factor for the detectors for which had a range from (0.5-3) days for the Radium-226 (Radon source) whose activity is 3.3 kBq was counted to be (0.2217±0.033) (track/cm^2)/(Bq.day/m^3). This value are agreed well with the reported values in many works [127],[128].

The concentration of the radon of the sample (C_{Rn}^{s}), can be calculated using following equation [129]:

$$C_{Rn}^{s}\left(\frac{Bq}{m^3}\right) = \frac{C_{Rn}^{a}\lambda_{Rn}\, h\, t}{l} \qquad (3.10)$$

Where λ_{Rn} refers the decay constant of ^{222}Rn (0.1814 d^{-1}), h points out to the distance from the sample flat to the detector, **t** is the exposure time, and l is the thickness of the sample in the tube.

The activity concentration of radon inside sample $(C_{Rn}^{s,ac})$ was determined using the following relation [130]:

$$C_{Rn}^{s,ac}\left(\frac{Bq}{L}\right) = \frac{C_{Rn}^{s}\, l\, A^{s}}{M^{s}} \qquad (3.11)$$

Where $\mathbf{A^s}$ refers to the surface area of the sample and $\mathbf{M^s}$ is the mass of the investigated sample.

3.7.2.1 Radium and Uranium Concentrations

Radium activity concentration (^{226}Ra) within the sample $(C_{Ra}^{s,ac})$ was determined using the relation [131]:

$$C_{Ra}^{s,ac}\left(\frac{Bq}{L}\right) = \frac{C_{Rn}^{a}\, h\, A^{s}}{M^{s}} \qquad (3.12)$$

The concentration of uranium (C_{U}^{s}) in ppm is provided by following relation [132],[133]:

$$C_{U}^{s}(ppm) = \frac{M_{U}^{s}}{M^{s}} \qquad (3.13)$$

Where, M_U^S is the mass of uranium in the sample.

3.7.2.2 Radiological Risk of Radon

3.7.2.2.1 Annual Effective Dose (AED)

The annual effective dose (AED) in accordance with the ingestion of ^{222}Rn and ^{226}Ra at the time of drinking water for adults was calculated by using the following equation [10],[110],[118] :

$$AED\left(\frac{Sv}{y}\right) = C\left(\frac{Bq}{L}\right) \times WC\left(\frac{L}{y}\right) \times DCF\left(\frac{Sv}{Bq}\right) \qquad (3.14)$$

Where C represents the concentration of radionuclide activity (^{222}Rn and ^{226}Ra), WC is the consumption of yearly water for a person (2 L/d) [134] and DCF refers to the ingestion dose changed determinant for the identical radionuclide, which it is equal for radon-222 and radium-226 ingestion by people as 0.0035 µSv/Bq and 0.28 µSv/Bq [10],[135].

3.7.2.2.2 Lifetime Cancer Risk

The lifetime cancer risk in accordance with ingestion of ^{222}Rn and ^{226}Ra from samples was measured by using the following equation [136]:

$$\boldsymbol{Lifetime\ cancer\ risk = AED \times DL \times RF} \qquad (\mathbf{3.15})$$

Where DL refers to the period of life (70 year) and RF shows the risk factor (0.055 Sv^{-1}) suggested via the ICRP [137].

3.8 Physiochemical Parameters

Twenty samples of water (marshes) were transferred to the laboratory of center for restoration of Iraqi marshes and wetlands in Dhi-Qar governorate , Iraq for the purpose of measuring the physical and chemical properties of selected water. the current study includes determination of pH, electrical conductivity, total dissolved salts. Some physical and chemical properties were measured directly with special measuring devices, such as pH, total dissolved salts, electrical conductivity.

The physiochemical properties of water such as (pH, TDS ,EC) was measured for 20 water samples by using a multimeter of American origin (YSI 6820 V2). The V2 sondes are a tried-and-true generation of YSI multi-parameter sensors. The optical sensors from YSI contain an integrated bio fouling wiper, a corrosion-resistant titanium wiper shaft, and interchangeable seals, making them perfect for contamination

situations. Use a YSI 650 multi parameter display system for long-term deployment or a YSI 650 multi parameter display system for sampling. For unattended sampling, the 6820 V2-2 requires an external power supply. After calibrating the meter with various solutions, measure a wide range of parameters for long-term monitoring, profiling, or sampling in fresh, marine, or contaminated water [138]. Figure (3.20) shows the multimeter device .

Figure (3.20): Physiochemical properties multimeter (YSI 6820 V2-2) [138]**.**

CHAPTER FOUR

RESULTS AND DISCUSSIONS

Chapter Four
Results and Discussions

4.1 Introduction

This chapter includes the results for uranium and radon concentrations which calculated depend on three different techniques, radon dosemetry (TASL), manually processing (microscopic) and digital count program by using MATLAB (CR-39-D2). Radon concentrations also measured by active device (RAD-7) for ground water in current study. In the present research, various risk factors including "the radiological risk, Annual Effective Dose (E_T) of uranium isotopes, the excess cancer risks, the chemical toxicity risk, Lifetime Average Daily Dose (LADD) and Quotient of Hazard (HQ)" were calculated. These risk factors, presented by this study, which could be resulted from the daily consumption of water by the inhabitants as drinking water, were determined risk of average internal effective dosage (AED) and cancer risk throughout a lifetime in accordance with ingesting of ^{222}Rn and ^{226}Ra in water also measured in current study. Physiochemical parameters were measured for marshes water samples including hydrogen ion concentration (pH), electrical conductivity (EC), total dissolved solids (TDS).

Theoretical study have been achieved by measuring ,the structural electronic and optical properties of the polymeric nuclear track detectors (CR-39) effected by different number atoms of radon gas as source of alpha particles, by using the density functional theory (DFT) approach was used with functional hybrid (B3LYP) at SDD bases set in ground state and the time-dependent (TD-DFT) with same functional and bases set for exaction state properties. The results illustrated in following Tables regarding radiological risks and chemical toxicity are calculated based on the uranium and radon concentrations of the TASL technique:

4.2 Uranium Concentrations

The results of uranium concentration , the activity of uranium isotopes (A), annual effective dose (E_T), excess cancer risk (ECR), lifetime average daily dose (LADD) and hazard quotient (HQ) in water samples will divided according to the type of water as follows.

4.2.1 Tap Water

Thirty samples of tap water were gathered from various locations around the Dhi-Qar governorate, with the goal of measuring uranium quantities released from the water. Uranium isotopes concentration and radioactivity of its isotopes (^{238}U, ^{235}U, and ^{234}U) in the water, were shown in Table (4.1). From this table, it was found that uranium concentrations of the samples, were found to be ranged from (0.77±0.068 μg/L to 1.20±0.084 μg/L) with 0.89±0.021 μg/L as an average. The activity uranium isotopes in Bq/L: for ^{238}U were ranged from 0.95 to 1.48, with an average 1.10±0.02, ^{235}U were ranged from 0.044 to 0.069, with an average 0.051±0.001 and for ^{234}U were ranged from 0.960 to 1.497, with an average 1.118±0.02. The greatest concentration of uranium was discovered in sample T1, while the lowest concentration was discovered in sample T16. Natural uranium values were estimated by combining the three uranium isotopes (^{238}U, ^{235}U, and ^{234}U) in unit Bq/L, which vary from 1.96 to 3.05, with an average of 2.27±0.05.

Table (4.1): Concentrations of uranium and its isotopes of tap water.

No.	Code of Sample	Concentration of Uranium (μg/l)	Uranium activity isotopes (Bq/L)			Natural uranium (Bq/L)
			^{238}U	^{235}U	^{234}U	
1	T1	1.20±0.084	1.48	0.069	1.497	3.05
2	T2	0.87±0.072	1.07	0.050	1.081	2.20
3	T3	0.83±0.070	1.02	0.048	1.029	2.10
4	T4	0.93±0.074	1.15	0.054	1.158	2.36
5	T5	0.81±0.069	1.00	0.047	1.012	2.06
6	T6	0.98±0.076	1.21	0.056	1.216	2.48

⟶ Next

7	T7	0.95±0.075	1.18	0.055	1.186	2.42
8	T8	0.81±0.069	1.00	0.047	1.007	2.05
9	T9	0.86±0.071	1.06	0.049	1.067	2.17
10	T10	0.88±0.072	1.09	0.051	1.098	2.24
11	T11	1.18±0.083	1.45	0.068	1.464	2.98
12	T12	1.16±0.083	1.43	0.067	1.439	2.93
13	T13	0.82±0.070	1.01	0.047	1.020	2.08
14	T14	0.86±0.071	1.06	0.050	1.073	2.19
15	T15	0.79±0.068	0.98	0.046	0.985	2.01
16	T16	0.80±0.069	0.99	0.046	1.001	2.04
17	T17	0.87±0.072	1.07	0.050	1.084	2.21
18	T18	0.99±0.077	1.23	0.057	1.238	2.52
19	T19	1.02±0.078	1.26	0.059	1.268	2.58
20	T20	0.82±0.070	1.01	0.047	1.023	2.08
21	T21	0.78±0.068	0.96	0.045	0.968	1.97
22	T22	0.94±0.075	1.16	0.054	1.175	2.39
23	T23	0.84±0.071	1.04	0.049	1.051	2.14
24	T24	0.78±0.068	0.97	0.045	0.976	1.99
25	T25	0.77±0.068	0.95	0.044	0.960	1.96
26	T26	0.83±0.070	1.03	0.048	1.037	2.11
27	T27	0.84±0.070	1.03	0.048	1.042	2.12
28	T28	1.02±0.078	1.26	0.059	1.268	2.58
29	T29	0.80±0.069	0.98	0.046	0.993	2.02
30	T30	0.92±0.074	1.14	0.053	1.147	2.34
Minimum		**0.77±0.068**	**0.95**	**0.044**	**0.960**	**1.96**
Maximum		**1.20±0.084**	**1.48**	**0.069**	**1.497**	**3.05**
Average±S.E		**0.89±0.021**	**1.10±0.02**	**0.051±0.001**	**1.118±0.02**	**2.27±0.05**

Figures (4.1) show the map of UC in the tap water samples. The maps were created using ArcGIS 10.7.1 and a GIS method (different colors were utilized to tell the difference among high, medium, and low amounts).

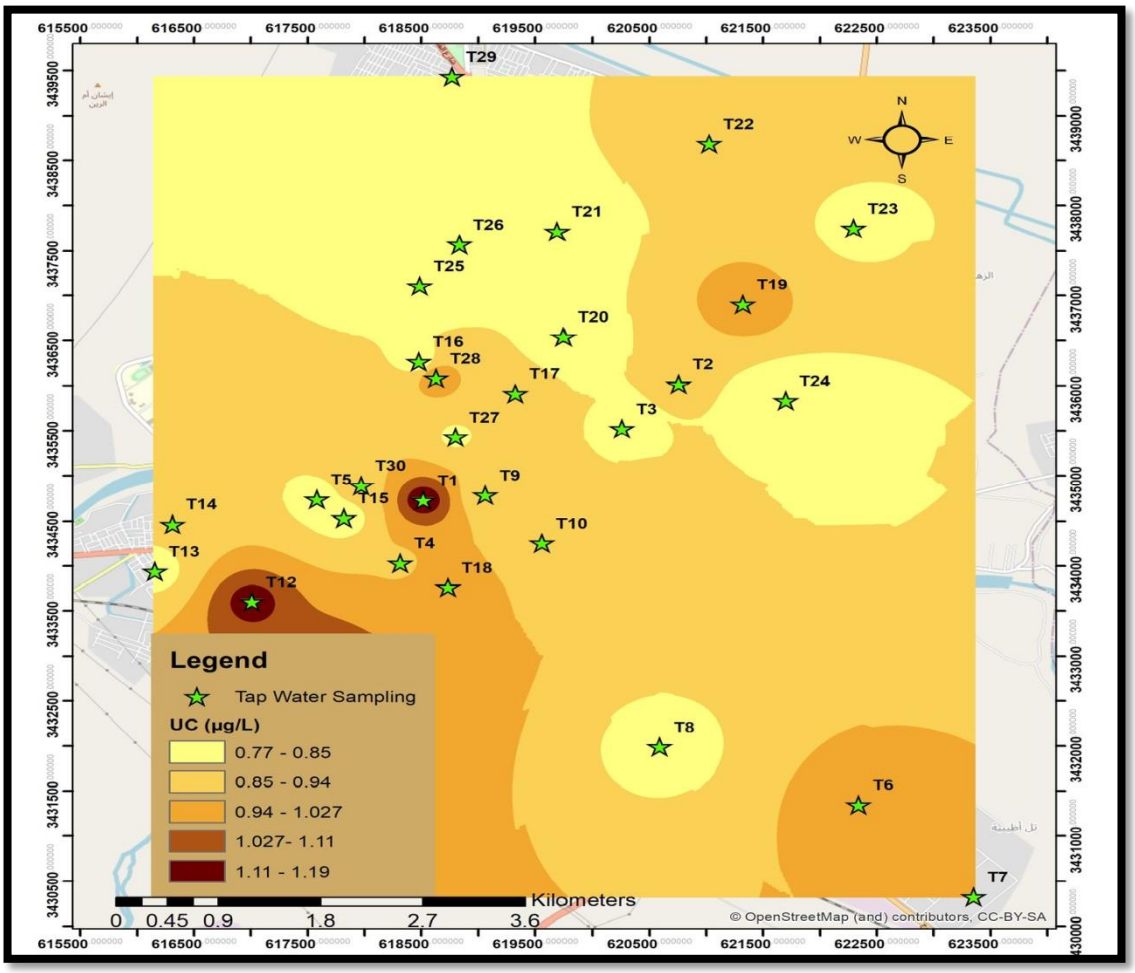

Figure (4.1): The map of the uranium concentrations of tap water.

The radiological risk variables (annual effective dose and excess cancer risk) for the samples of water are shown in Table (4.2). In the collected water samples, the average annual effective dose (E_T) to the population occupants throughout a year (according to uranium isotopes activity ^{238}U, ^{235}U, and ^{234}U) was 36.43±0.86 µSv/y, 1.77±0.04 µSv/y, and 40.01±0.95 µSv/y, respectively. The total range of annual effective dose in mSv/y, on the other hand, was 0.067 to 0.105, with an average of 0.078±0.001. Other radiological concerns, such as an increased cancer risk, were assessed as presented in Table (4.2). The total excess cancer risk in the present research ranges from (0.204×10^{-3}) to (0.318×10^{-3}), with an average value of $(0.237\pm0.005) \times 10^{-3}$.

Table (4.2): The radiological risks results of tap water.

No.	Code of Sample	Annual average of dose effective (μSv/y)			Total (mSv/y)	Excess Cancer Risk×10^{-3}
		^{238}U	^{235}U	^{234}U		
1	T1	48.75	2.37	53.55	0.105	0.318
2	T2	35.20	1.71	38.67	0.076	0.230
3	T3	33.50	1.63	36.80	0.072	0.219
4	T4	37.72	1.84	41.43	0.081	0.246
5	T5	32.96	1.61	36.20	0.071	0.215
6	T6	39.60	1.93	43.50	0.085	0.259
7	T7	38.61	1.88	42.41	0.083	0.252
8	T8	32.78	1.60	36.01	0.070	0.214
9	T9	34.76	1.69	38.18	0.075	0.227
10	T10	35.74	1.74	39.26	0.077	0.233
11	T11	47.67	2.32	52.37	0.102	0.311
12	T12	46.87	2.28	51.48	0.101	0.306
13	T13	33.23	1.62	36.50	0.071	0.217
14	T14	34.93	1.70	38.37	0.075	0.228
15	T15	32.06	1.56	35.22	0.069	0.209
16	T16	32.60	1.59	35.81	0.070	0.213
17	T17	35.29	1.72	38.77	0.076	0.231
18	T18	40.32	1.96	44.29	0.087	0.263
19	T19	41.30	2.01	45.37	0.089	0.270
20	T20	33.32	1.62	36.60	0.072	0.218
21	T21	31.53	1.54	34.63	0.068	0.206
22	T22	38.25	1.86	42.02	0.082	0.250
23	T23	34.22	1.67	37.58	0.073	0.224
24	T24	31.79	1.55	34.92	0.068	0.208
25	T25	31.26	1.52	34.33	0.067	0.204
26	T26	33.77	1.64	37.09	0.073	0.221
27	T27	33.95	1.65	37.29	0.073	0.222
28	T28	41.30	2.01	45.37	0.089	0.270
29	T29	32.33	1.58	35.52	0.069	0.211
30	T30	37.36	1.82	41.03	0.080	0.244
Minimum		**31.26**	**1.52**	**34.33**	**0.067**	**0.204**
Maximum		**48.75**	**2.37**	**53.55**	**0.105**	**0.318**
Average±S.E		**36.43±0.86**	**1.77±0.04**	**40.01±0.95**	**0.078±0.001**	**0.237±0.005**

The risks of uranium in tap water samples owing to chemical toxicity, the LADD and HQ, are shown in Table (4.3). The estimated LADD, which was measured in (μg/kg.day) units and is based on oral chemical ingestion through tap water, has been detected in the range of 0.0250 to 0.0390, with an average of 0.0291±0.0006, whereas the value of HQ has been detected to be in the range of 0.0417 to 0.0650, with an average of 0.0485±0.001.

Table (4.3): The chemical toxicity results of tap water.

No.	Sample Code	LADD (μg/kg.day)	HQ
1	T1	0.0390	0.0650
2	T2	0.0282	0.0469
3	T3	0.0268	0.0447
4	T4	0.0302	0.0503
5	T5	0.0264	0.0440
6	T6	0.0317	0.0528
7	T7	0.0309	0.0515
8	T8	0.0262	0.0437
9	T9	0.0278	0.0463
10	T10	0.0286	0.0477
11	T11	0.0381	0.0636
12	T12	0.0375	0.0625
13	T13	0.0266	0.0443
14	T14	0.0280	0.0466
15	T15	0.0257	0.0428
16	T16	0.0261	0.0435
17	T17	0.0282	0.0471
18	T18	0.0323	0.0538
19	T19	0.0330	0.0551
20	T20	0.0267	0.0444
21	T21	0.0252	0.0420
22	T22	0.0306	0.0510
23	T23	0.0274	0.0456
24	T24	0.0254	0.0424
25	T25	0.0250	0.0417

⟶ Next

26	T26	0.0270	0.0450
27	T27	0.0272	0.0453
28	T28	0.0330	0.0551
29	T29	0.0259	0.0431
30	T30	0.0299	0.0498
Minimum		**0.0250**	**0.0417**
Maximum		**0.0390**	**0.0650**
Average±S.E		**0.0291±0.0006**	**0.0485±0.001**

4.2.2 Marshes Water

Twenty marsh surface water samples were gathered from different locations within the (Ahwar) marshes in order to determine the uranium concentration released from the samples water. Uranium isotopes concentration and radioactivity of its isotopes (^{238}U, ^{235}U, and ^{234}U) in the water, were shown in Table (4.4). According to this data, the uranium concentrations of the samples in the current investigation varied from 0.87±0.072 μg/L to 1.89±0.093 μg/L, with an average of 1.23±0.05 μg/L. The activity uranium isotopes in Bq/L: for ^{238}U were ranged from 1.07 to 2.33, with an average 1.51±0.06, ^{235}U were ranged from 0.050 to 0.109, with an average 0.07±0.002 and for ^{234}U were ranged from 1.084 to 2.355, with an average 1.53±0.06. It was also noticed that the sample M4 (AZ 24(2)) had the greatest uranium concentration, whereas the sample M7 had the lowest (Khamisiyah). Natural uranium values were determined by combining the three uranium isotopes (^{238}U, ^{235}U, and ^{234}U) in unit Bq/L, which varied from 2.20 to 4.79, with an average of 3.12±0.13.

Table (4.4): Concentrations of uranium and its isotopes of marshes water.

No.	Code of Sample	Concentration of Uranium (µg/L)	Uranium activity isotopes (Bq/L)			Natural uranium (Bq/L)
			^{238}U	^{235}U	^{234}U	
1	M1	1.06±0.079	1.31	0.061	1.321	2.69
2	M2	1.25±0.083	1.54	0.072	1.557	3.17
3	M3	1.13±0.081	1.40	0.065	1.408	2.87
4	M4	1.89±0.093	2.33	0.109	2.355	4.79
5	M5	0.98±0.076	1.21	0.056	1.221	2.49
6	M6	1.20±0.081	1.48	0.069	1.495	3.04
7	M7	0.87±0.072	1.07	0.050	1.084	2.20
8	M8	1.39±0.090	1.72	0.080	1.732	3.53
9	M9	1.37±0.084	1.69	0.079	1.707	3.48
10	M10	1.47±0.093	1.82	0.085	1.831	3.74
11	M11	1.40±0.091	1.73	0.081	1.744	3.56
12	M12	1.31±0.092	1.62	0.075	1.632	3.33
13	M13	1.35±0.092	1.67	0.078	1.682	3.43
14	M14	1.17±0.077	1.44	0.067	1.458	2.97
15	M15	1.27±0.079	1.57	0.073	1.582	3.23
16	M16	0.96±0.073	1.19	0.055	1.196	2.44
17	M17	0.99±0.077	1.22	0.057	1.233	2.51
18	M18	0.93±0.071	1.15	0.054	1.159	2.36
19	M19	1.28±0.081	1.58	0.074	1.595	3.25
20	M20	1.33±0.088	1.64	0.077	1.657	3.37
Minimum		**0.87±0.072**	**1.07**	**0.050**	**1.084**	**2.20**
Maximum		**1.89±0.093**	**2.33**	**0.109**	**2.355**	**4.79**
Average±S.E		**1.23±0.05**	**1.51±0.06**	**0.07±0.002**	**1.53±0.06**	**3.12±0.13**

Figures (4.2) show the map of UC in the marshes water samples. The maps were designed by GIS technique, with ArcGIS 10.7.1 (different colors have been utilized to tell the difference among high, medium, and low amounts).

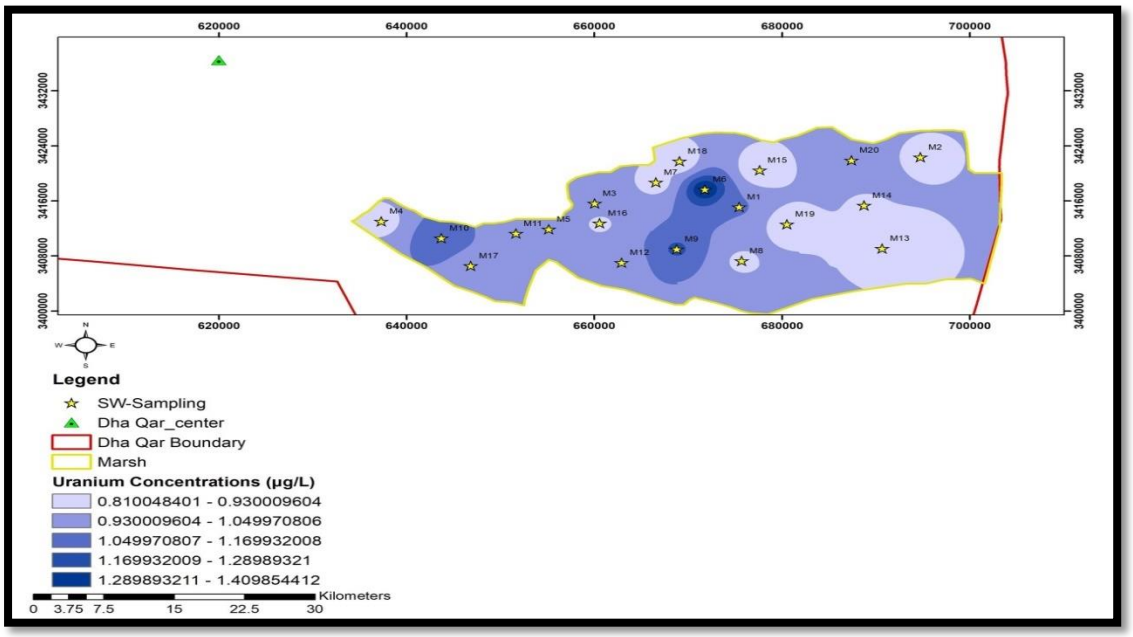

Figure (4.2): The map of the uranium concentrations of marshes water.

The radiological risks variables (effective annual dose and excess cancer risk) for the samples of water taken from ahwar are shown in Table (4.5). The average annual effective dosage (E_T) to the population of wetlands residents throughout a year was 49.90±2.08 µSv/y, 2.43±0.10 µSv/y, and 58.81±2.29 µSv/y, respectively, in the collected water samples (owing to uranium isotopes activity ^{238}U, ^{235}U, and ^{234}U). The entire range of yearly effective dosage in mSv/y, on the other hand, was 0.076 to 0.165, with an average of 0.107±0.004. Other radiological concerns, such as an increased cancer risk, were assessed as presented in Table (4.5). The total excess cancer risk in the present research ranges from (0.231×10^{-3}) to (0.501×10^{-3}), with an average value of (0.326 ± 0.013) $\times10^{-3}$.

Table (4.5): The radiological risks results of marshes water.

No.	Code of Sample	Annual average of dose effective (µSv/y)			Total (mSv/y)	Excess Cancer Risk$\times10^{-3}$
		^{238}U	^{235}U	^{234}U		
1	M1	43.00	2.09	47.24	0.092	0.281
2	M2	50.71	2.47	55.70	0.109	0.331

⟶ Next

3	M3	45.84	2.23	50.35	0.098	0.299
4	M4	76.67	3.74	84.22	0.165	0.501
5	M5	39.76	1.94	43.67	0.085	0.260
6	M6	48.68	2.37	53.47	0.105	0.318
7	M7	35.29	1.72	38.77	0.076	0.231
8	M8	56.39	2.75	61.94	0.121	0.368
9	M9	55.58	2.71	61.05	0.119	0.363
10	M10	59.64	2.91	65.51	0.128	0.390
11	M11	56.80	2.77	62.39	0.122	0.371
12	M12	53.15	2.59	58.38	0.114	0.347
13	M13	54.77	2.67	60.16	0.118	0.358
14	M14	47.47	2.31	52.14	0.102	0.310
15	M15	51.52	2.51	56.59	0.111	0.337
16	M16	38.95	1.90	42.78	0.084	0.254
17	M17	40.16	1.96	44.12	0.086	0.262
18	M18	37.73	1.84	41.44	0.081	0.246
19	M19	51.93	2.53	57.04	0.111	0.339
20	M20	53.96	2.63	59.27	0.116	0.352
Minimum		**35.29**	**1.72**	**38.77**	**0.076**	**0.231**
Maximum		**76.67**	**3.74**	**84.22**	**0.165**	**0.501**
Average±S.E		**49.90±2.08**	**2.43±0.10**	**58.81±2.29**	**0.107±0.004**	**0.326±0.013**

The risks of uranium in marshes water samples owing to chemical toxicity, the LADD and HQ, are shown in Table (4.6). The evaluated LADD, that is based on oral intake of the chemical through contaminated water, in (µg/kg.day) unit, has been detected in the range of 0.0282 to 0.0613, with an average of 0.040±0.001, whereas the HQ value was found to be in the range of 0.0471 to 0.1022, with an average of 0.066±0.002.

Table (4.6): The chemical toxicity results of marshes water .

No.	Sample Code	LADD (µg/kg.day)	HQ
1	M1	0.0344	0.0573
2	M2	0.0406	0.0676
3	M3	0.0367	0.0611
4	M4	0.0613	0.1022
5	M5	0.0318	0.0530

⟶ Next

6	M6	0.0390	0.0649
7	M7	0.0282	0.0471
8	M8	0.0451	0.0752
9	M9	0.0445	0.0741
10	M10	0.0477	0.0795
11	M11	0.0454	0.0757
12	M12	0.0425	0.0709
13	M13	0.0438	0.0730
14	M14	0.0380	0.0633
15	M15	0.0412	0.0687
16	M16	0.0312	0.0519
17	M17	0.0321	0.0536
18	M18	0.0302	0.0503
19	M19	0.0415	0.0692
20	M20	0.0432	0.0720
Minimum		**0.0282**	**0.0471**
Maximum		**0.0613**	**0.1022**
Average±S.E		**0.040±0.001**	**0.066±0.002**

4.2.3 Stations Water

Assess uranium concentrations released from the samples of water, twenty samples of stations water were gathered from various locations in the Dhi-Qar governorate. Uranium isotopes concentration and radioactivity of its isotopes (^{238}U, ^{235}U, and ^{234}U) in the water, were shown in Table (4.7) . From this table, it was found that uranium concentrations of the samples, were found to be ranged (0.75±0.067 μg/L to 1.03±0.078 μg/L) with 0.840±0.016 μg/L as an average. The activity of uranium isotopes in Bq/L: for ^{238}U were ranged from 0.93 to 1.27, with an average 1.03±0.01, ^{235}U were ranged from 0.043 to 0.059, with an average 0.048±0.0009 and for ^{234}U were ranged from 0.935 to 1.282, with a average 1.046±0.02. It was also discovered that the sample ST4 had the greatest uranium concentration, whereas the sample ST1 had the lowest. Natural uranium values were determined by combining the three

uranium isotopes (^{238}U, ^{235}U, and ^{234}U) in unit Bq/L, which vary from 1.91 to 2.61, with an average of 2.13±0.04.

Table (4.7): Concentrations of uranium and its isotopes of stations water.

No.	Code of Sample	Concentration of Uranium (µg/L)	Uranium activity isotopes (Bq/L)			Natural uranium (Bq/L)
			^{238}U	^{235}U	^{234}U	
1	ST1	0.79±0.068	0.98	0.046	0.987	2.01
2	ST2	0.77±0.067	0.95	0.044	0.957	1.95
3	ST3	0.98±0.076	1.21	0.056	1.219	2.48
4	ST4	1.03±0.078	1.27	0.059	1.282	2.61
5	ST5	0.93±0.074	1.14	0.053	1.153	2.35
6	ST6	0.90±0.073	1.11	0.052	1.122	2.29
7	ST7	0.86±0.071	1.06	0.049	1.067	2.17
8	ST8	0.82±0.070	1.01	0.047	1.020	2.08
9	ST9	0.77±0.068	0.95	0.044	0.960	1.96
10	ST10	0.83±0.070	1.03	0.048	1.037	2.11
11	ST11	0.87±0.072	1.07	0.050	1.078	2.20
12	ST12	0.76±0.067	0.94	0.044	0.952	1.94
13	ST13	0.78±0.068	0.97	0.045	0.974	1.98
14	ST14	0.84±0.071	1.04	0.048	1.048	2.14
15	ST15	0.88±0.072	1.08	0.050	1.092	2.23
16	ST16	0.75±0.067	0.93	0.043	0.935	1.91
17	ST17	0.76±0.067	0.94	0.044	0.946	1.93
18	ST18	0.85±0.071	1.05	0.049	1.062	2.16
19	ST19	0.81±0.069	1.00	0.046	1.004	2.05
20	ST20	0.82±0.070	1.02	0.047	1.026	2.09
Minimum		**0.75±0.067**	**0.93**	**0.043**	**0.935**	**1.91**
Maximum		**1.03±0.078**	**1.27**	**0.059**	**1.282**	**2.61**
Average±S.E		**0.84±0.016**	**1.03±0.01**	**0.048±0.0009**	**1.046±0.02**	**2.13±0.04**

Figures (4.3) show the maps of UC in the stations water samples (before treatment). The maps were created using ArcGIS 10.7.1 and a GIS method (different colors have been utilized to show the difference among high, medium, and low amounts).

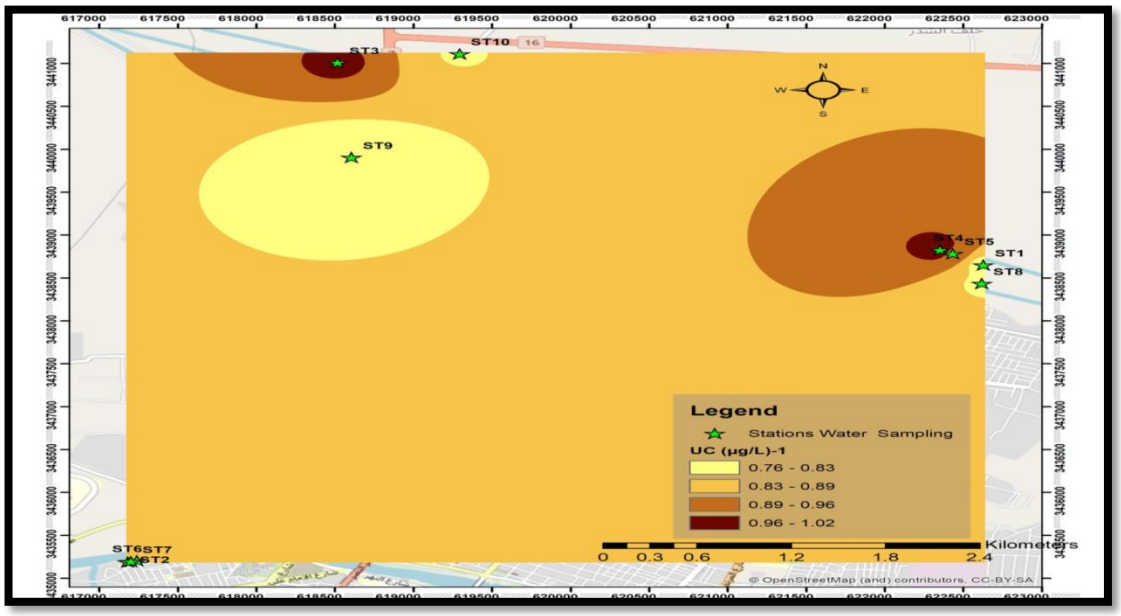

Figure (4.3): The map of the uranium concentrations of stations water (before treatment).

Figures (4.4) show the map of UC in the stations water samples (aftar treatment) . The maps were created using ArcGIS 10.7.1 and a GIS method (different colors have been utilized to tell the difference among high, medium, and low amounts).

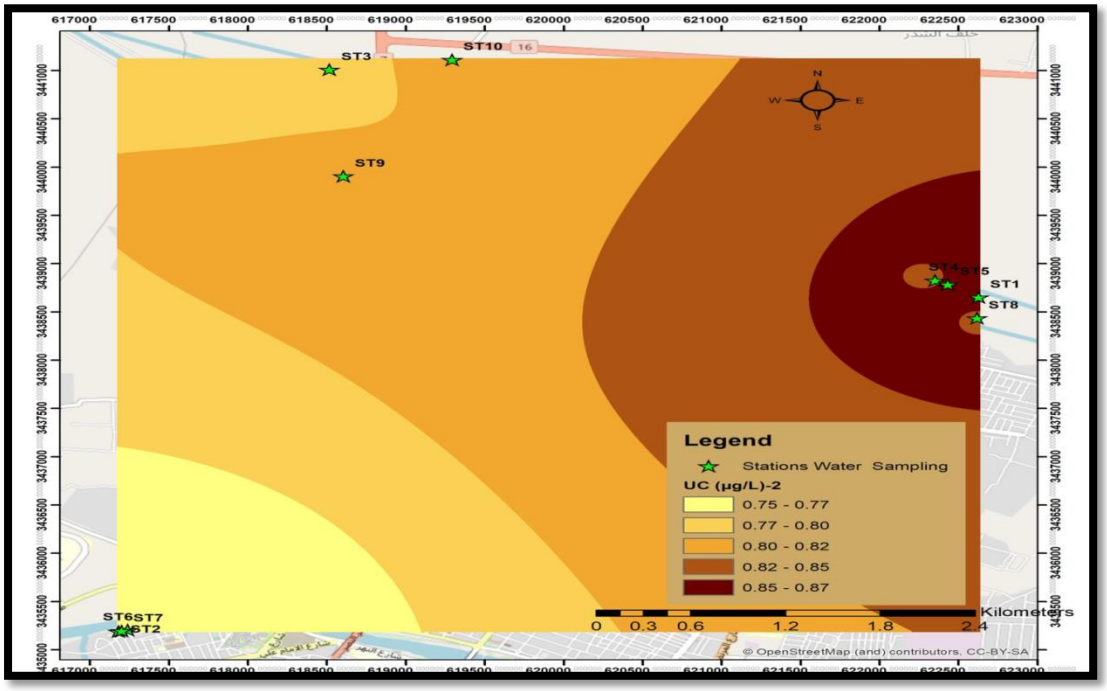

Figure (4.4): The map of the uranium concentrations of stations water (after treatment)

The radioactive risk indicators (annual effective dose and excess cancer risk) for the samples of water taken from stations water are shown in Table (4.8). In the collected water samples, the average annual effective dosage (E_T) to the population of wetlands residents throughout a year (owing to uranium isotopes activity ^{238}U, ^{235}U, and ^{234}U) was 34.06±0.66 μSv/y, 1.65±0.03 μSv/y, and 37.41±0.72 μSv/y, respectively. The range of total annual effective dose in mSv/y, on the other hand, was 0.065 to 0.090, with an average of 0.073±0.001. Other radiological risk, such as an increased cancer risk, were assessed as presented in Table (4.8). The total excess cancer risk in the present research ranges from (0.199×10^{-3}) to (0.273×10^{-3}), with an average value of (0.222±0.004) $\times10^{-3}$.

Table (4.8): The radiological risks results of stations water.

No.	Code of Sample	Annual average of dose effective (μSv/y)			Total (mSv/y)	Excess Cancer Risk×10^{-3}
		^{238}U	^{235}U	^{234}U		
1	ST1	32.15	1.57	35.32	0.069	0.210
2	ST2	31.17	1.52	34.23	0.067	0.204
3	ST3	39.69	1.93	43.60	0.085	0.259
4	ST4	41.75	2.03	45.86	0.090	0.273
5	ST5	37.54	1.83	41.23	0.081	0.245
6	ST6	36.55	1.78	40.15	0.078	0.239
7	ST7	34.76	1.69	38.18	0.075	0.227
8	ST8	33.23	1.62	36.50	0.071	0.217
9	ST9	31.26	1.52	34.33	0.067	0.204
10	ST10	33.77	1.64	37.09	0.073	0.221
11	ST11	35.11	1.71	38.57	0.075	0.229
12	ST12	30.99	1.51	34.04	0.067	0.202
13	ST13	31.70	1.54	34.83	0.068	0.207
14	ST14	34.13	1.66	37.49	0.073	0.223
15	ST15	35.56	1.73	39.06	0.076	0.232
16	ST16	30.45	1.48	33.45	0.065	0.199
17	ST17	30.81	1.50	33.84	0.066	0.201

⟶ Next

18	ST18	34.58	1.68	37.98	0.074	0.226
19	ST19	32.69	1.59	35.91	0.070	0.214
20	ST20	33.41	1.63	36.70	0.072	0.218
Minimum		**30.45**	**1.48**	**33.45**	**0.065**	**0.199**
Maximum		**41.75**	**2.03**	**45.86**	**0.090**	**0.273**
Average±S.E		**34.06±0.66**	**1.65±0.03**	**37.41±0.72**	**0.073±0.001**	**0.222±0.004**

The risks of uranium in stations water samples owing to chemical toxicity, the LADD and HQ, are shown in Table (4.9). The evaluated LADD, that is based on oral consumption of the chemical through stations water, in (µg/kg.day) unit, has been detected in the range of 0.0244 to 0.0334, with an average of 0.0272±0.0005, while the HQ value was found to be in the range of 0.0406 to 0.0557, with an average of 0.0454±0.0008.

Table (4.9): The chemical toxicity results of stations water.

No.	Sample Code	LADD (µg/kg.day)	HQ
1	ST1	0.0257	0.0429
2	ST2	0.0249	0.0416
3	ST3	0.0318	0.0529
4	ST4	0.0334	0.0557
5	ST5	0.0300	0.0501
6	ST6	0.0292	0.0487
7	ST7	0.0278	0.0463
8	ST8	0.0266	0.0443
9	ST9	0.0250	0.0417
10	ST10	0.0270	0.0450
11	ST11	0.0281	0.0468
12	ST12	0.0248	0.0413
13	ST13	0.0254	0.0423
14	ST14	0.0273	0.0455
15	ST15	0.0285	0.0474
16	ST16	0.0244	0.0406
17	ST17	0.0246	0.0411
18	ST18	0.0277	0.0461
19	ST19	0.0262	0.0436

⟶Next

20	ST20	0.0267	0.0446
Minimum		**0.0244**	**0.0406**
Maximum		**0.0334**	**0.0557**
Average±S.E		**0.0272±0.0005**	**0.0454±0.0008**

4.2.4 Surface Water

Assessing uranium concentrations of the surface water samples, fifteen samples of surface water were gathered from various locations across the Dhi-Qar governorate. Uranium isotopes concentration and radioactivity of its isotopes (^{238}U, ^{235}U, and ^{234}U) in the water, were shown in Table (4.10). From this table, it was found that uranium concentrations of the samples, were found to be ranged (0.76±0.067 μg/L to 1.49±0.094 μg/L) with 0.87±0.04 μg/L as an average. The activity uranium isotopes in Bq/L: for ^{238}U were ranged from 0.94 to 1.84, with an average 1.07±0.05, ^{235}U were ranged from 0.044 to 0.086, with an average 0.050±0.002 and for ^{234}U were ranged from 0.943 to 1.861, with an average 1.086±0.05. It was also discovered that sample S2 had the greatest uranium content, whereas sample S7 had the lowest. Normal uranium values as Table (4.10) were determined by combining the 3 uranium isotopes (^{238}U, ^{235}U, and ^{234}U) in units of Bq/L, which vary from 1.92 to 3.79, with an average of 2.21±0.111.

Table (4.10): Concentrations of uranium and its isotopes of surface water.

No.	Code of Sample	Concentration of Uranium (μg/l)	Uranium activity isotopes (Bq/L)			Natural uranium (Bq/L)
			^{238}U	^{235}U	^{234}U	
1	S1	0.81±0.069	1.00	0.047	1.012	2.06
2	S2	1.49±0.094	1.84	0.086	1.861	3.79
3	S3	0.85±0.071	1.05	0.049	1.062	2.16
4	S4	0.95±0.075	1.18	0.055	1.186	2.42
5	S5	0.77±0.067	0.95	0.044	0.957	1.95
6	S6	0.80±0.069	0.98	0.046	0.993	2.02
7	S7	0.78±0.068	0.96	0.045	0.968	1.97

⟶ Next

8	S8	0.79±0.068	0.98	0.046	0.987	2.01
9	S9	0.83±0.070	1.03	0.048	1.040	2.12
10	S10	0.77±0.068	0.95	0.045	0.963	1.96
11	S11	0.92±0.074	1.13	0.053	1.142	2.33
12	S12	0.93±0.074	1.15	0.053	1.155	2.35
13	S13	0.85±0.071	1.04	0.049	1.053	2.15
14	S14	0.79±0.068	0.97	0.045	0.979	1.99
15	S15	0.76±0.067	0.94	0.044	0.943	1.92
Minimum		**0.76±0.067**	**0.94**	**0.044**	**0.943**	**1.92**
Maximum		**1.49±0.094**	**1.84**	**0.086**	**1.861**	**3.79**
Average±S.E		**0.87±0.04**	**1.07±0.05**	**0.050±0.002**	**1.086±0.05**	**2.21±0.11**

Figures (4.5) show the map of UC in the surface water samples. The maps were created using ArcGIS 10.7.1 and a GIS method (different colors have been utilized to tell the difference among high, medium, and low amounts).

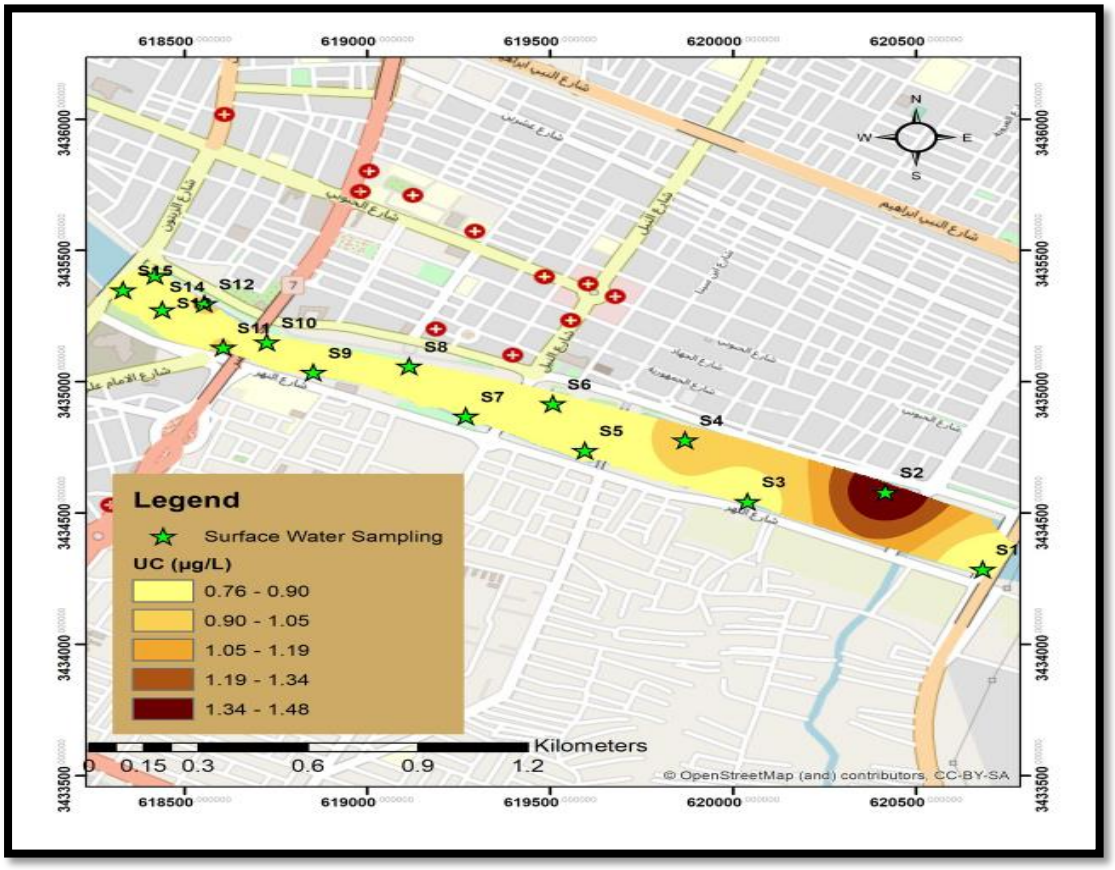

Figure (4.5): The map of the uranium concentrations of surface water.

The radiological risk indices (annual effective dose and excess cancer risk) for the collected water samples obtained from surface water are shown in Table (4.11). In the collected water samples, the average annual effective dose (E_T) to the collected surface water samples throughout a year (owing to uranium isotopes activity ^{238}U, ^{235}U, and ^{234}U) was 35.39±1.84 μSv/y, 1.72±0.08 μSv/y, and 38.87±2.02 μSv/y, respectively. The range of total annual effective dose in mSv/y, on the other hand, was 0.066 to 0.130, with an average of 0.076±0.003. Other radiological concerns, such as an excess cancer risk, were assessed as presented in Table (4.11). The total excess cancer risk in the present research ranges from (0.201×10^{-3}) to (0.396×10^{-3}), with an average value of $(0.231\pm0.012)\times10^{-3}$.

Table (4.11): The radiological risks results of surface water.

No.	Code of Sample	Annual average of dose effective (μSv/y)			Total (mSv/y)	Excess Cancer Risk×10^{-3}
		^{238}U	^{235}U	^{234}U		
1	S1	32.96	1.61	36.20	0.071	0.215
2	S2	60.59	2.95	66.56	0.130	0.396
3	S3	34.58	1.68	37.98	0.074	0.226
4	S4	38.61	1.88	42.41	0.083	0.252
5	S5	31.17	1.52	34.23	0.067	0.204
6	S6	32.33	1.58	35.52	0.069	0.211
7	S7	31.53	1.54	34.63	0.068	0.206
8	S8	32.15	1.57	35.32	0.069	0.210
9	S9	33.86	1.65	37.19	0.073	0.221
10	S10	31.35	1.53	34.43	0.067	0.205
11	S11	37.18	1.81	40.84	0.080	0.243
12	S12	37.63	1.83	41.33	0.081	0.246
13	S13	34.31	1.67	37.68	0.074	0.224
14	S14	31.88	1.55	35.02	0.068	0.208
15	S15	30.72	1.50	33.74	0.066	0.201
Minimum		**30.72**	**1.50**	**33.74**	**0.066**	**0.201**
Maximum		**60.59**	**2.95**	**66.56**	**0.130**	**0.396**
Average±S.E		**35.39±1.84**	**1.72±0.08**	**38.87±2.02**	**0.076±0.003**	**0.231±0.012**

The risks of uranium in water samples owing to chemical toxicity, the LADD and HQ, are shown in Table (4.12). The evaluaed LADD, that is based on oral consumption of the chemical through investigated water samples, in (µg/kg.day), has been detected to be in the range of 0.0246 to 0.0485, with an average of 0.0283±0.001, while the HQ value was found to be in the range of 0.0410 to 0.0808, with an average of 0.0472±0.002.

Table (4.12): The chemical toxicity results of surface water.

No.	Sample Code	LADD (µg/kg.day)	HQ
1	S1	0.0264	0.0440
2	S2	0.0485	0.0808
3	S3	0.0277	0.0461
4	S4	0.0309	0.0515
5	S5	0.0249	0.0416
6	S6	0.0259	0.0431
7	S7	0.0252	0.0420
8	S8	0.0257	0.0429
9	S9	0.0271	0.0452
10	S10	0.0251	0.0418
11	S11	0.0297	0.0496
12	S12	0.0301	0.0502
13	S13	0.0274	0.0457
14	S14	0.0255	0.0425
15	S15	0.0246	0.0410
Minimum		**0.0246**	**0.0410**
Maximum		**0.0485**	**0.0808**
Average±S.E		**0.0283±0.001**	**0.0472±0.002**

4.2.5 Groundwater

Twenty samples of water were gathered from distinctive locations throughout the Dhi-Qar governorate, with the purpose of measuring uranium concentrations of groundwater samples. Uranium isotopes concentration and radioactivity of its isotopes (^{238}U, ^{235}U, and ^{234}U) in the

water, were shown in Table (4.13). From this Table, it was found that uranium concentrations of the samples, were found to be ranged (0.77±0.068 μg/L to 1.18±0.084 μg/L) with 0.87±0.02 μg/L as an average. The activity uranium isotopes in Bq/L: for ^{238}U were ranged from 0.95 to 1.46, with an average 1.07±0.02, ^{235}U were ranged from 0.044 to 0.068, with an average 0.050±0.001 and for ^{234}U were ranged from 0.960 to 1.472, with a average 1.080±0.02. It was also discovered that the sample G16 had the greatest concentration of uranium, whereas the sample G14 had the lowest concentration. Normal uranium values were determined by combining the 3 uranium isotopes (^{238}U, ^{235}U, and ^{234}U) in units of Bq/L, which vary from 1.98 to 3.00, with an average of 2.21±0.05.

Table (4.13): Concentrations of uranium and its isotopes of groundwater.

No.	Code of Sample	Concentration of Uranium (μg/l)	Uranium activity isotopes (Bq/L)			Natural uranium (Bq/L)
			^{238}U	^{235}U	^{234}U	
1	G1	0.88±0.072	1.09	0.051	1.095	2.23
2	G2	0.79±0.068	0.97	0.045	0.982	2.00
3	G3	0.80±0.069	0.99	0.046	0.998	2.03
4	G4	0.82±0.070	1.02	0.047	1.026	2.09
5	G5	0.92±0.074	1.13	0.053	1.144	2.33
6	G6	0.85±0.071	1.05	0.049	1.056	2.15
7	G7	0.83±0.070	1.03	0.048	1.037	2.11
8	G8	0.86±0.071	1.06	0.049	1.067	2.17
9	G9	0.87±0.072	1.07	0.050	1.081	2.20
10	G10	0.81±0.069	1.00	0.047	1.012	2.06
11	G11	0.89±0.073	1.10	0.051	1.109	2.26
12	G12	0.83±0.070	1.02	0.048	1.031	2.10
13	G13	0.80±0.069	0.98	0.046	0.993	2.02
14	G14	0.77±0.068	0.95	0.044	0.960	1.96
15	G15	0.90±0.073	1.11	0.052	1.122	2.29
16	G16	1.18±0.084	1.46	0.068	1.472	3.00
17	G17	0.78±0.068	0.96	0.045	0.971	1.98
18	G18	0.95±0.075	1.17	0.054	1.177	2.40

⟶ Next

19	G19	1.12±0.082	1.39	0.065	1.401	2.85
20	G20	0.82±0.070	1.01	0.047	1.023	2.08
Minimum		**0.77±0.068**	**0.95**	**0.044**	**0.960**	**1.98**
Maximum		**1.18±0.084**	**1.46**	**0.068**	**1.472**	**3.00**
Average±S.E		**0.87±0.02**	**1.07±0.02**	**0.050±0.001**	**1.08±0.02**	**2.21±0.05**

Figures (4.6) show the map of UC in the groundwater samples. The maps were created using ArcGIS 10.7.1 and a GIS method (different colors have been utilized to demonstrate the difference among high, medium, and low amounts).

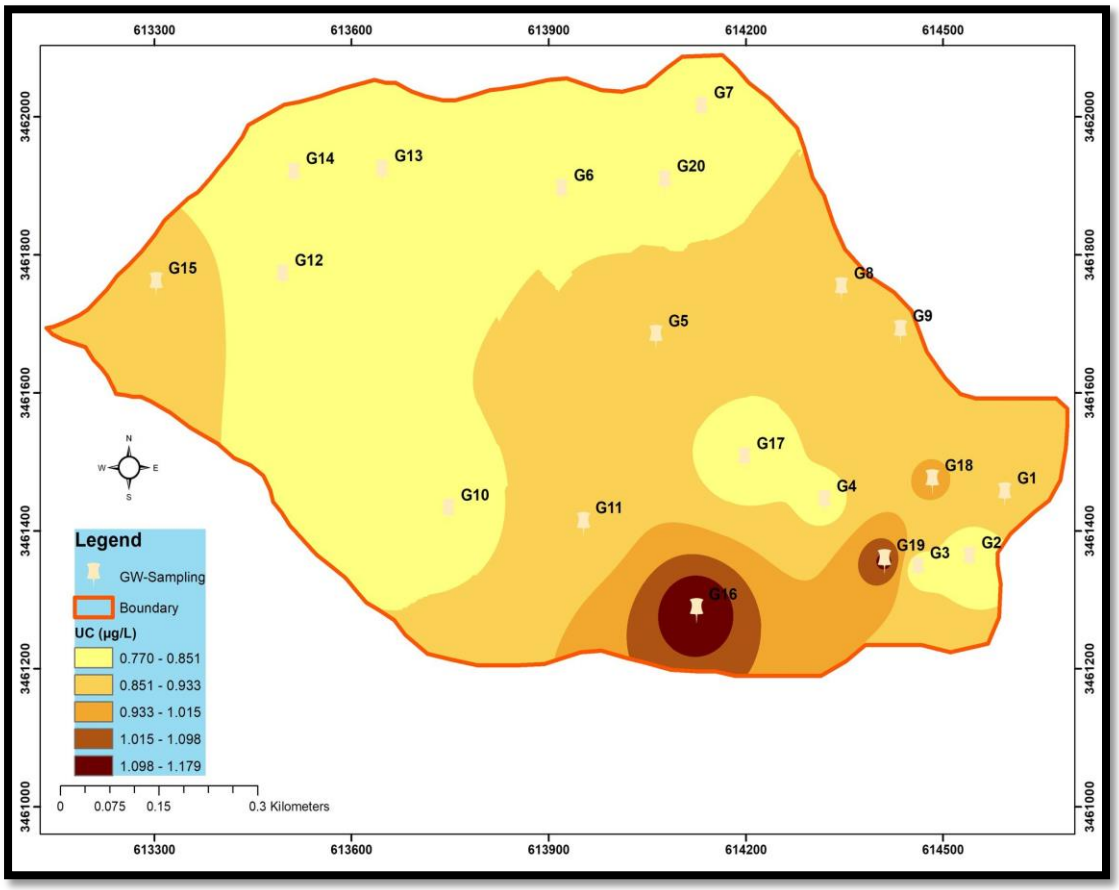

Figure (4.6): The map of the uranium concentrations of groundwater.

The radioactive risk variables (annual effective dose and excess cancer risk) for the samples water obtained from groundwater are shown in Table (4.14). In the collected water samples, the average annual effective dosage (E_T) to the population of wetlands residents throughout a

year (owing to uranium isotopes activity ^{238}U, ^{235}U, and ^{234}U) was 35.42±0.94 μSv/y, 1.72±0.04 μSv/y, and 38.91±1.03 μSv/y, respectively. The entire range of yearly effective dosage in mSv/y, on the other hand, was 0.067 to 0.103, with an average of 0.076±0.002. Other radiological concerns, such as an increased cancer risk, were assessed as presented in Table (4.14). The total excess cancer risk in the present research ranges from (0.204×10^{-3}) to (0.313×10^{-3}), with an average value of $(0.231\pm0.007)\times10^{-3}$.

Table (4.14): The radiological risks results of groundwater.

No.	Code of Sample	Annual average of dose effective (μSv/y)			Total (mSv/y)	Excess Cancer Risk×10^{-3}
		^{238}U	^{235}U	^{234}U		
1	G1	35.65	1.74	39.16	0.077	0.233
2	G2	31.97	1.56	35.12	0.069	0.209
3	G3	32.51	1.58	35.71	0.070	0.212
4	G4	33.41	1.63	36.70	0.072	0.218
5	G5	37.27	1.82	40.94	0.080	0.243
6	G6	34.40	1.68	37.78	0.074	0.225
7	G7	33.77	1.64	37.09	0.073	0.221
8	G8	34.76	1.69	38.18	0.075	0.227
9	G9	35.20	1.71	38.67	0.076	0.230
10	G10	32.96	1.61	36.20	0.071	0.215
11	G11	36.10	1.76	39.65	0.078	0.236
12	G12	33.59	1.64	36.89	0.072	0.219
13	G13	32.33	1.58	35.52	0.069	0.211
14	G14	31.26	1.52	34.33	0.067	0.204
15	G15	36.55	1.78	40.15	0.078	0.239
16	G16	47.94	2.34	52.66	0.103	0.313
17	G17	31.62	1.54	34.73	0.068	0.207
18	G18	38.34	1.87	42.12	0.082	0.250
19	G19	45.61	2.22	50.10	0.098	0.298
20	G20	33.32	1.62	36.60	0.072	0.218
Minimum		**31.26**	**1.52**	**34.33**	**0.067**	**0.204**
Maximum		**47.94**	**2.34**	**52.66**	**0.103**	**0.313**
Average±S.E		**35.42±0.94**	**1.72±0.04**	**38.91±1.03**	**0.076±0.002**	**0.231±0.006**

Table (4.15) shows the hazards of uranium in samples of water owing to chemical toxicity, as well as the LADD and HQ. The estimated LADD, which is based on oral consumption of the chemical through contaminated water, in (µg/kg.day), has been detected to be in the range of 0.0250 to 0.0384, with an average of 0.0283±0.0007, while the value of HQ was found to be in the range of 0.0417 to 0.0639, with an average of 0.0472±0.001.

Table (4.15): The chemical toxicity results of groundwater.

No.	Sample Code	LADD (µg/kg.day)	HQ
1	G1	0.0285	0.0475
2	G2	0.0256	0.0426
3	G3	0.0260	0.0434
4	G4	0.0267	0.0446
5	G5	0.0298	0.0497
6	G6	0.0275	0.0459
7	G7	0.0270	0.0450
8	G8	0.0278	0.0463
9	G9	0.0282	0.0469
10	G10	0.0264	0.0440
11	G11	0.0289	0.0481
12	G12	0.0269	0.0448
13	G13	0.0259	0.0431
14	G14	0.0250	0.0417
15	G15	0.0292	0.0487
16	G16	0.0384	0.0639
17	G17	0.0253	0.0422
18	G18	0.0307	0.0511
19	G19	0.0365	0.0608
20	G20	0.0267	0.0444
Minimum		**0.0250**	**0.0417**
Maximum		**0.0384**	**0.0639**
Average±S.E		**0.0283±0.0007**	**0.0472±0.001**

4.2.6 RO Water

Twenty samples of RO water have been gathered from distinctive locations across the Dhi-Qar governorate, with the goal of determining the uranium concentrations released from the water. Uranium isotopes concentration and radioactivity of its isotopes (^{238}U, ^{235}U, and ^{234}U) in the water, were shown in Table (4.16). From this table, it was found that uranium concentrations of the samples, were found to be ranged (0.76±0.067 μg/L to 1.46±0.093 μg/L) with 0.93±0.04 μg/L as an average. The activity uranium isotopes in Bq/L: for ^{238}U were ranged from 0.94 to 1.80, with an average 1.14±0.06, ^{235}U were ranged from 0.044 to 0.084, with an average 0.053±0.002 and for ^{234}U were ranged from 0.946 to 1.814, with a average 1.158±0.05. It was also found that the sample RO14 had the greatest concentration of uranium, whereas the sample RO17 had the lowest concentration. Natural uranium values were determined by combining the 3 uranium isotopes (^{238}U, ^{235}U, and ^{234}U) in units of Bq/L, which vary from 1.93 to 3.70, with an average of 2.36±0.11.

Table (4.16): Concentrations of uranium and its isotopes of RO water.

No.	Code of Sample	Concentration of Uranium (μg/l)	Uranium activity isotopes (Bq/L)			Natural uranium (Bq/L)
			^{238}U	^{235}U	^{234}U	
1	RO1	0.77±0.068	0.95	0.044	0.960	1.96
2	RO2	0.97±0.076	1.20	0.056	1.208	2.46
3	RO3	0.79±0.069	0.98	0.046	0.990	2.02
4	RO4	0.83±0.070	1.03	0.048	1.040	2.12
5	RO5	1.06±0.079	1.31	0.061	1.321	2.69
6	RO6	0.83±0.070	1.02	0.048	1.031	2.10
7	RO7	0.81±0.069	1.00	0.047	1.007	2.05
8	RO8	0.79±0.068	0.97	0.045	0.979	1.99
9	RO9	0.88±0.072	1.09	0.051	1.095	2.23
10	RO10	0.82±0.070	1.01	0.047	1.018	2.07
11	RO11	1.26±0.086	1.56	0.073	1.569	3.20

⟶ Next

12	RO12	1.37±0.090	1.69	0.079	1.704	3.47
13	RO13	0.78±0.068	0.96	0.045	0.971	1.98
14	RO14	1.46±0.093	1.80	0.084	1.814	3.70
15	RO15	0.96±0.075	1.19	0.055	1.197	2.44
16	RO16	0.80±0.069	0.99	0.046	1.001	2.04
17	RO17	0.76±0.067	0.94	0.044	0.946	1.93
18	RO18	0.86±0.071	1.06	0.049	1.067	2.17
19	RO19	0.77±0.068	0.96	0.045	0.965	1.97
20	RO20	1.04±0.078	1.28	0.060	1.293	2.63
Minimum		**0.76±0.067**	**0.94**	**0.044**	**0.946**	**1.93**
Maximum		**1.46±0.093**	**1.80**	**0.084**	**1.814**	**3.70**
Average±S.E		**0.93±0.04**	**1.14±0.06**	**0.053±0.002**	**1.158±0.05**	**2.36±0.11**

Figures (4.7) show the map of UC in the RO water samples. The maps were created using ArcGIS 10.7.1 and a GIS method (different colors have been utilized to show the difference among high, medium, and low amounts).

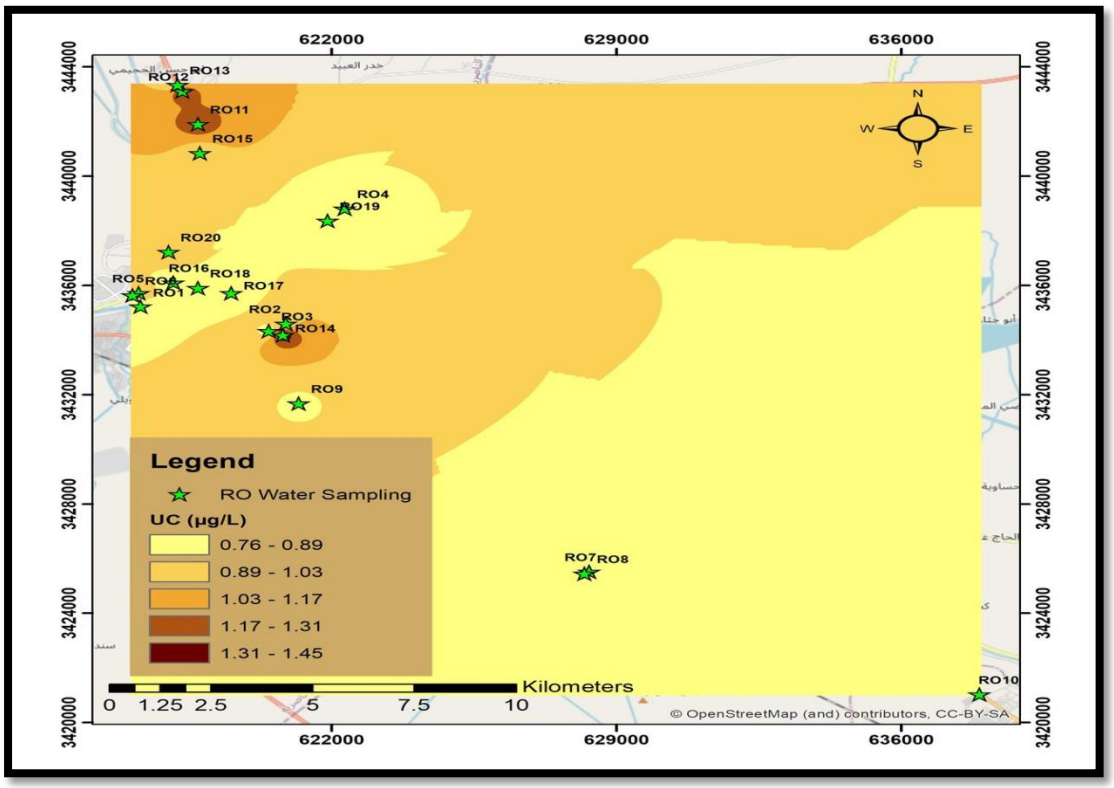

Figure (4.7): The map of the uranium concentrations of RO water.

The radioactive risk variables (annual effective dose and excess cancer risk) for the collected RO water samples are shown in Table (4.17). In the collected water samples, the average annual effective dose (E_T) to the population of wetlands residents throughout a year (owing to uranium isotopes activity ^{238}U, ^{235}U, and ^{234}U) was 37.73±1.83 μSv/y, 1.83±0.08 μSv/y, and 41.44±2.01 μSv/y, respectively. The range of total annual effective dosage in mSv/y, on the other hand, was 0.066 to 0.127, with an average of 0.080±0.003. Other radiological indices, such as an increased cancer risk, were assessed as presented in Table (4.17). The total excess cancer risk in the present research ranges from (0.201×10^{-3}) to (0.386×10^{-3}), with an average value of ($0.246 \pm 0.01) \times 10^{-3}$.

Table (4.17): The radiological risks results of RO water.

No.	Code of Sample	Annual average of dose effective (μSv/y)			Total (mSv/y)	Excess Cancer Risk×10^{-3}
		^{238}U	^{235}U	^{234}U		
1	RO1	31.26	1.52	34.33	0.067	0.204
2	RO2	39.33	1.92	43.20	0.084	0.257
3	RO3	32.24	1.57	35.42	0.069	0.211
4	RO4	33.86	1.65	37.19	0.073	0.221
5	RO5	43.01	2.10	47.24	0.092	0.281
6	RO6	33.59	1.64	36.89	0.072	0.219
7	RO7	32.78	1.60	36.01	0.070	0.214
8	RO8	31.88	1.55	35.02	0.068	0.208
9	RO9	35.65	1.74	39.16	0.077	0.233
10	RO10	33.14	1.61	36.40	0.071	0.217
11	RO11	51.08	2.49	56.11	0.110	0.334
12	RO12	55.48	2.70	60.94	0.119	0.362
13	RO13	31.62	1.54	34.73	0.068	0.207
14	RO14	59.07	2.88	64.88	0.127	0.386
15	RO15	38.97	1.90	42.81	0.084	0.255
16	RO16	32.60	1.59	35.81	0.070	0.213
17	RO17	30.81	1.50	33.84	0.066	0.201
18	RO18	34.76	1.69	38.18	0.075	0.227

⟶ Next

19	RO19	31.44	1.53	34.53	0.067	0.205
20	RO20	42.11	2.05	46.26	0.090	0.275
Minimum		**30.81**	**1.50**	**33.84**	**0.066**	**0.201**
Maximum		**59.07**	**2.88**	**64.88**	**0.127**	**0.386**
Average±S.E		**37.73±1.83**	**1.83±0.08**	**41.44±2.01**	**0.080±0.003**	**0.246±0.01**

Table (4.18) shows the risks of uranium in samples of water owing to chemical toxicity, as well as the LADD and HQ. The evaluated LADD, that is based on oral consumption of the chemical through contaminated water, in (µg/kg.day) unit, has been detected to be in the range of 0.0246 to 0.0473, with an average of 0.0301±0.001, while the HQ value was found to be in the range of 0.0411 to 0.0788, with an average of 0.0503±0.002.

Table (4.18): The chemical toxicity results of RO water.

No.	Sample Code	LADD (µg/kg.day)	HQ
1	RO1	0.0250	0.0417
2	RO2	0.0315	0.0524
3	RO3	0.0258	0.0430
4	RO4	0.0271	0.0452
5	RO5	0.0344	0.0574
6	RO6	0.0269	0.0448
7	RO7	0.0262	0.0437
8	RO8	0.0255	0.0425
9	RO9	0.0285	0.0475
10	RO10	0.0265	0.0442
11	RO11	0.0409	0.0681
12	RO12	0.0444	0.0740
13	RO13	0.0253	0.0422
14	RO14	0.0473	0.0788
15	RO15	0.0312	0.0520
16	RO16	0.0261	0.0435
17	RO17	0.0246	0.0411
18	RO18	0.0278	0.0463
19	RO19	0.0252	0.0419

⟶Next

20	RO20	0.0337	0.0562
Minimum		**0.0246**	**0.0411**
Maximum		**0.0473**	**0.0788**
Average±S.E		**0.0301±0.001**	**0.0503±0.002**

4.2.7 Discussion of Uranium Concentrations

The results illustrated in Tables (4.1), (4.4), (4.7), (4.10), (4.13) and (4.16) indicate that uranium concentration nearly differs in all water samples in the current investigation. The highest values were obtained for uranium concentrations were in samples M4, S2 and RO14, 1.89, 1.49 and 1.46 respectively. The worth of uranium concentrations (UC) in the whole samples of water (tap, marshes, station, surface, ground and RO) in the this research have been detected to be within the suggested ICRP value of 1.9 μg/L [139]. From the Table (4.19), we note that the highest average value of uranium concentration obtained in the current study is in marshes water samples was (1.23±0.05), which also was within the permissible values suggested by (ICRP).

The findings of the whole annual effective dose shows in the Tables (4.2), (4.5), (4.8), (4.11), (4.14) and (4.17), in the whole collected samples, was within 0.18 mSv/y, that is the level of dose recommended by "International Commission on Radiological Protection (ICRP) 1993"[139], and it is lower than 1 mSv/y level of activity recommended via "ICRP 1990". The maximum values of total annual effective dosage were in the samples M4, S2 and RO14, 0.165, 1.30, 1.81 respectively. The Table (4.20) of radiological risks shows that the highest average of total annual effective dose were in marshes water samples in spite of that it is within the limit of global permissible, regarding to the drinking water. These values of uranium contamination have been proposed as the acceptable amounts that do not pose a significant health risk when consumed via contaminated water throughout the lifespan. Other

radiological concerns, such as an increased cancer risk, were assessed. The water samples from the marshes had the highest average maximum value of increased cancer risk. In the current research, the total excess cancer risk in the studied region is minimal in all directions, compared to the tolerable radiological risk limit of 10^{-3} [123],[140].

The maximum value of lifetime average daily dose LADD (because of uranium ingestion) illustrated in the Tables (4.3), (4.6), (4.9), (4.12), (4.15) and (4.18), were in marshes region in sample M4 (0.0631) Through what was mentioned above, we can say that all samples under investigation (tap, marshes, station, surface, ground and RO) were low comparing to the values recommended by Water Healthy Organization (WHO), that is 0.6 μg/kg.day [141]. As well as for the values Quotient of Hazard (HQ), That were calculated in this current study have been detected to be less than the favorable level recommended by World Health Organization (1) [123].

4.2.8 Summary of Mean Uranium Concentrations

Table (4.19): Summary of uranium concentrations and its isotopes for all water samples.

Water Type		Concentration of Uranium (μg/L)	Uranium activity isotopes (Bq/L)			Natural Uranium (Bq/L)
			^{238}U	^{235}U	^{234}U	
Tap	Minimum	0.77± 0.06	0.95	0.044	0.960	1.96
	Maximum	1.20± 0.08	1.48	0.069	1.497	3.05
	Average±S.E	0.89± 0.02	1.10±0.02	0.05±0.001	1.11±0.02	2.27±0.05
Marshes	Minimum	0.87± 0.07	1.07	0.050	1.084	2.20
	Maximum	1.89± 0.09	2.33	0.109	2.355	4.79
	Average±S.E	1.23± 0.05	1.51±0.06	0.07±0.002	1.53±0.06	3.12±0.13
Station	Minimum	0.75± 0.06	0.93	0.043	0.935	1.91
	Maximum	1.03± 0.07	1.27	0.059	1.282	2.61
	Average±S.E	0.84± 0.01	1.03±0.06	0.04±0.009	1.04±0.02	2.13±0.04

⟶ Next

Surface	**Minimum**	**0.76± 0.06**	**0.94**	**0.044**	**0.943**	**1.92**
	Maximum	**1.49± 0.07**	**1.84**	**0.086**	**1.861**	**3.79**
	Average±S.E	**0.87± 0.04**	**1.07±0.05**	**0.05±0.002**	**1.08±0.05**	**2.21±0.04**
Ground	**Minimum**	**0.77± 0.06**	**0.87**	**0.041**	**0.877**	**1.79**
	Maximum	**1.18± 0.08**	**1.46**	**0.068**	**1.472**	**3.00**
	Average±S.E	**0.87± 0.02**	**1.07±0.02**	**0.05±0.001**	**1.08±0.05**	**2.21±0.04**
RO	**Minimum**	**0.76± 0.06**	**0.94**	**0.044**	**0.946**	**1.93**
	Maximum	**1.46± 0.09**	**1.80**	**0.084**	**1.814**	**3.70**
	Average±S.E	**0.93± 0.04**	**1.14±0.06**	**0.05±0.002**	**1.15±0.05**	**2.36±0.04**

Table (4.20): Summary of radiological risks for all water samples.

Water Type		**Annual average of dose effective(μSv/y)**			**Total (mS/y)**	**Excess Cancer Risk $\times 10^{-4}$**
		^{238}U	**^{235}U**	**^{234}U**		
Tap	**Minimum**	**31.26**	**1.52**	**34.33**	**0.067**	**0.204**
	Maximum	**48.75**	**2.37**	**53.55**	**0.105**	**0.318**
	Average±S.E	**36.43±0.86**	**1.77±0.04**	**40.01±0.02**	**0.078±0.001**	**0.237±0.005**
Marshes	**Minimum**	**35.29**	**1.72**	**38.77**	**0.076**	**0.231**
	Maximum	**76.67**	**3.74**	**84.22**	**0.165**	**0.501**
	Average±S.E	**49.90±0.86**	**3.43±0.10**	**58.81±2.29**	**0.107±0.004**	**0.326±0.013**
Station	**Minimum**	**30.45**	**1.48**	**33.45**	**0.065**	**0.199**
	Maximum	**41.75**	**2.03**	**45.86**	**0.090**	**0.273**
	Average±S.E	**34.06±0.66**	**1.65±0.03**	**37.41±0.72**	**0.073±0.001**	**0.222±0.004**
Surface	**Minimum**	**30.72**	**1.50**	**33.74**	**0.066**	**0.201**
	Maximum	**60.59**	**2.95**	**66.56**	**0.130**	**0.396**
	Average±S.E	**35.39±1.84**	**1.72±0.08**	**38.87±2.02**	**0.076±0.003**	**0.231±0.012**
Ground	**Minimum**	**31.26**	**1.52**	**34.33**	**0.067**	**0.204**
	Maximum	**47.94**	**2.34**	**52.66**	**0.103**	**0.313**
	Average±S.E	**35.42±0.94**	**1.72±0.04**	**38.91±1.03**	**0.076±0.002**	**0.231±0.006**
RO	**Minimum**	**30.81**	**1.50**	**33.84**	**0.066**	**0.201**
	Maximum	**59.07**	**2.88**	**64.88**	**0.127**	**0.386**
	Average±S.E	**37.73±1.83**	**1.83±0.08**	**41.44±2.01**	**0.080±0.003**	**0.246±0.01**

Table (4.21): Summary of chemical toxicity for all water samples.

Water Type		LADD(µg/kg.day)	HQ
Tap	Minimum	0.0250	0.0417
	Maximum	0.0390	0.0650
	Average±S.E	0.0291±0.0006	0.0485±0.001
Marshes	Minimum	0.0282	0.0471
	Maximum	0.0631	0.1022
	Average±S.E	0.0400±0.001	0.0660±0.001
Station	Minimum	0.0244	0.0406
	Maximum	0.0334	0.0557
	Average±S.E	0.0272±0.0006	0.0454±0.0008
Surface	Minimum	0.0246	0.0410
	Maximum	0.0485	0.0808
	Average±S.E	0.0283±0.001	0.0472±0.002
Ground	Minimum	0.0250	0.0417
	Maximum	0.0384	0.0639
	Average±S.E	0.0283±0.0007	0.0472±0.001
RO	Minimum	0.0246	0.0411
	Maximum	0.0473	0.0788
	Average±S.E	0.0301±0.001	0.0503±0.002

4.3 Radon Concentrations

4.3.1 Tap Water

Alpha emitters (^{222}Rn, ^{226}Ra, and ^{238}U) concentrations in the samples of tap water. The results of ^{222}Rn (C_{Rn}^{a}, C_{Rn}^{s}, and $C_{Rn}^{s,ac}$), ^{226}Ra, and ^{238}U concentrations in the samples of water are shown in Table (4.22). The values of C_{Rn}^{a} ranged between 81.58 Bq/m^3 in sample T6 to 1773.57 Bq/m^3 in the sample T16 with an average value of 441.61±77.02 Bq/m^3, while the values of C_{Rn}^{s} in unit kBq/m^3 and $C_{Rn}^{s,ac}$ in unit Bq/L, were ranged from 4.00 to 86.87 in the with an average value of 21.62±3.92 and from 2.12 to 46.10 with an average value of 11.47±2.00, respectively. Also from Table (4.22), it found that $C_{Ra}^{s,ac}$ were

ranged from 0.13 to 2.82 Bq/L, with an average value of 0.70±0.12 Bq/L. The results of $C_U^{s,ac}$ in unit ppm as shown in Table (4.22) were ranged from 0.17 to 3.72, with an average value of 0.92±0.16.

Table (4.22): Radon, radium and uranium results in tap water samples.

No.	Sample code	^{222}Rn			^{226}Ra	^{238}U
		C_{Rn}^{a} (Bq/m^3)	C_{Rn}^{s} (kBq/m^3)	$C_{Rn}^{s,ac}$ (Bq/L)	$C_{Ra}^{s,ac}$ (Bq/L)	$C_U^{s,ac}$ (ppm)
1	T1	603.01	29.53	15.67	0.96	1.26
2	T2	1709.72	83.74	44.44	2.72	3.59
3	T3	546.26	26.75	14.20	0.87	1.15
4	T4	312.15	15.29	8.11	0.50	0.65
5	T5	177.36	8.69	4.61	0.28	0.37
6	T6	81.58	4.00	2.12	0.13	0.17
7	T7	184.45	9.03	4.79	0.29	0.39
8	T8	883.24	43.26	22.96	1.41	1.85
9	T9	645.58	31.62	16.78	1.03	1.35
10	T10	319.24	15.64	8.30	0.51	0.67
11	T11	290.86	14.25	7.56	0.46	0.61
12	T12	113.51	5.56	2.95	0.18	0.24
13	T13	539.16	26.41	14.01	0.86	1.13
14	T14	255.39	12.51	6.64	0.41	0.54
15	T15	390.18	19.11	10.14	0.62	0.82
16	T16	1773.57	86.87	46.10	2.82	3.72
17	T17	216.37	10.60	5.62	0.34	0.45
18	T18	145.43	7.12	3.78	0.23	0.30
19	T19	542.71	26.58	14.11	0.86	1.14
20	T20	230.56	11.29	5.99	0.37	0.48
21	T21	134.79	6.60	3.50	0.21	0.28
22	T22	439.84	21.54	11.43	0.70	0.92
23	T23	1135.08	55.59	29.50	1.81	2.38
24	T24	177.36	8.69	4.61	0.28	0.37
25	T25	241.20	11.81	6.27	0.38	0.51
26	T26	106.41	5.21	2.77	0.17	0.22
27	T27	301.51	14.77	7.84	0.48	0.63
28	T28	102.87	5.04	2.67	0.16	0.22

⟶Next

29	T29	156.07	7.64	4.06	0.25	0.33
30	T30	493.05	24.15	12.81	0.78	1.03
Minimum		**81.58**	**4.00**	**2.12**	**0.13**	**0.17**
Maximum		**1773.57**	**86.87**	**46.10**	**2.82**	**3.72**
Average±S.E		**441.61±77.02**	**21.62±3.77**	**11.47±2.00**	**0.70±0.12**	**0.92±0.16**

The map illustrated in the Figure (4.8) represent the concentrations of radon in the samples of tap water samples. The technique which used to drew is GIS with ArcGIS 10.7.1. The color gradation in the map indicates the different concentrations of radon in the tap water samples.

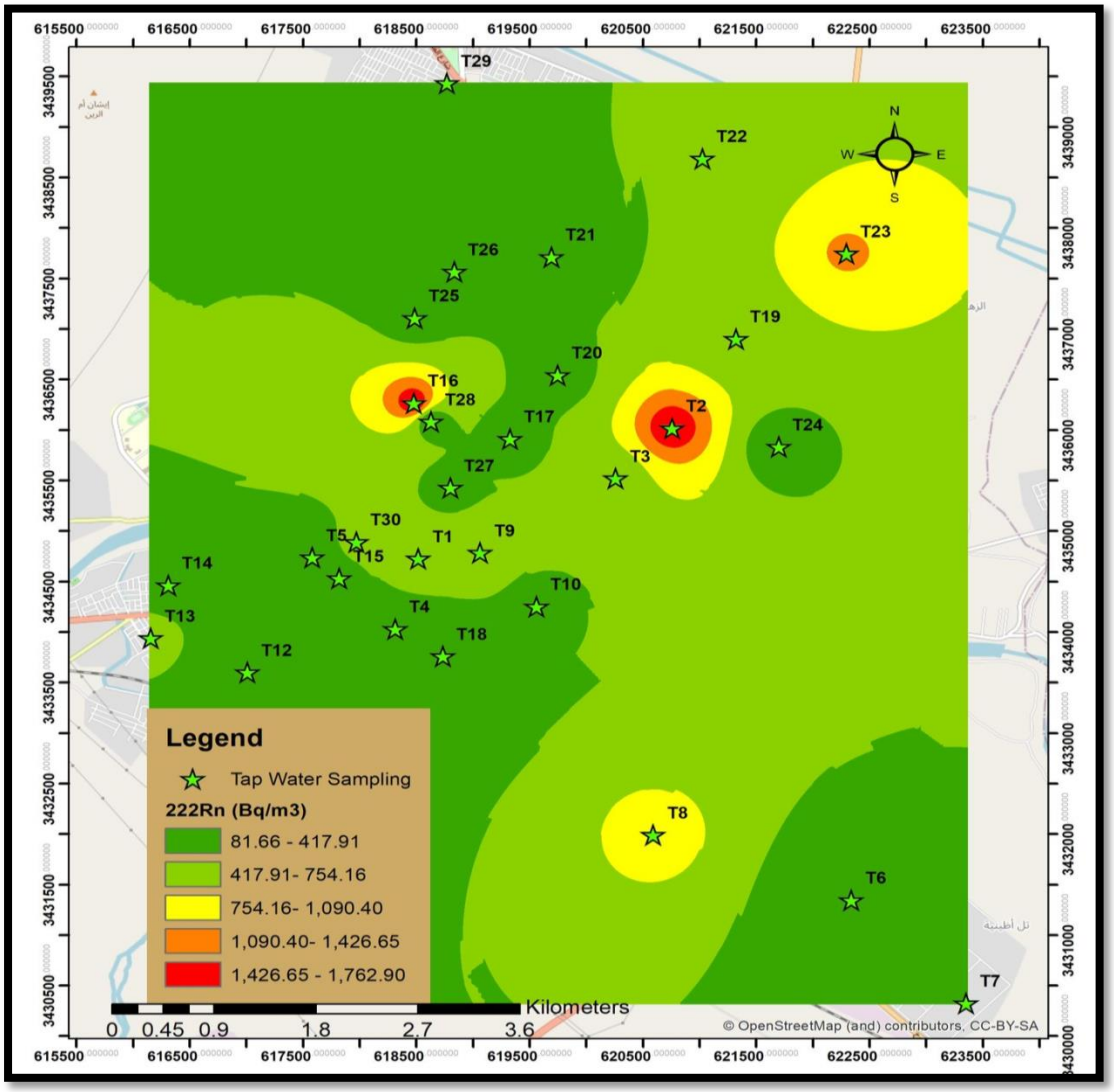

Figure (4.8): The map of the radon concentrations of tap water.

AED due to activity of ^{222}Rn, ^{226}Ra, and the total of AED in tap water samples are shown in Table (4.23). It is found that the AED in mSv/y for ^{222}Rn, ^{226}Ra, and total of AED were ranged from 0.006 to 0.118, with an average value of 0.029±0.005, from 0.028 to 0.577, with an average value of 0.143±0.02 and from 0.03 to 0.69, with an average value of 0.17±0.03, respectively. The lifetime risk in accordance with taken water was also evaluated. The sample T16 had the highest lifetime risk as a consequence of water consumption, whereas the sample T6 had the lowest lifetime risk. Ingestion of ^{222}Rn and ^{226}Ra in tap water samples resulted in lifetime risks ranging from 1.28×10^{-4} to 26.75×10^{-4}, with an average value of $(6.66\pm1.61)\times10^{-4}$.

Table (4.23): The AED and lifetime cancer risk results of tap water.

No.	Sample code	AED (mSv/y)		Total AED (mSv/y)	Lifetime cancer risk$\times10^{-4}$
		^{222}Rn	^{226}Ra		
1	T1	0.040	0.196	0.24	9.10
2	T2	0.114	0.556	0.67	25.79
3	T3	0.036	0.178	0.21	8.24
4	T4	0.021	0.102	0.12	4.71
5	T5	0.012	0.058	0.07	2.68
6	T6	0.006	0.028	0.03	1.28
7	T7	0.012	0.060	0.07	2.78
8	T8	0.059	0.287	0.35	13.32
9	T9	0.043	0.210	0.25	9.74
10	T10	0.021	0.104	0.13	4.82
11	T11	0.019	0.095	0.11	4.39
12	T12	0.008	0.037	0.04	1.71
13	T13	0.036	0.175	0.21	8.13
14	T14	0.017	0.083	0.10	3.85
15	T15	0.026	0.127	0.15	5.89
16	T16	0.118	0.577	0.69	26.75
17	T17	0.014	0.070	0.08	3.26
18	T18	0.010	0.047	0.06	2.19
19	T19	0.036	0.177	0.21	8.19
20	T20	0.015	0.075	0.09	3.48

⟶Next

21	T21	0.009	0.044	0.05	2.03
22	T22	0.029	0.143	0.17	6.63
23	T23	0.075	0.369	0.44	17.12
24	T24	0.012	0.058	0.07	2.68
25	T25	0.016	0.078	0.09	3.64
26	T26	0.007	0.035	0.04	1.61
27	T27	0.020	0.098	0.12	4.55
28	T28	0.007	0.033	0.04	1.55
29	T29	0.010	0.051	0.06	2.35
30	T30	0.033	0.160	0.19	7.44
Minimum		**0.006**	**0.028**	**0.03**	**1.28**
Maximum		**0.118**	**0.577**	**069**	**26.75**
Average± S.E		**0.029±0.005**	**0.143±0.02**	**0.17±0.03**	**6.66±1.61**

4.3.2 Marshes Water

The (^{222}Rn, ^{226}Ra, and ^{238}U) concentrations in marshes water samples were determined. The results of ^{222}Rn (C_{Rn}^{a}, C_{Rn}^{s}, and $C_{Rn}^{s,ac}$), ^{226}Ra, and ^{238}U concentrations in the water samples for selected marshes are shown in Table (4.24). The values of C_{Rn}^{a} ranged between 88.68 Bq/m^3 in sample M15 to 709.43 Bq/m^3 in the sample M6 with an average value of 288.92±34.10 Bq/m^3, while the values of C_{Rn}^{s} in unit kBq/m^3 and $C_{Rn}^{s,ac}$ in unit Bq/L, were ranged from 4.34 to 34.75 in the with an average value of 14.15±1.67 and from 2.30 to 34.718.44 in the with an average value of 7.51±0.88, respectively. Also from Table (4.24), it found that $C_{Ra}^{s,ac}$ were ranged from 0.14 to 1.13 Bq/L, with an average value of 0.46±0.05 Bq/L. The results of $C_{U}^{s,ac}$ in unit ppm as shown in Table (4.24) were ranged from 0.19 to 1.49, with an average value of 0.61±0.07.

Table (4.24): The Radon, radium and uranium results in marshes water samples.

No.	Sample code	^{222}Rn			^{226}Ra	^{238}U
		C_{Rn}^{a} (Bq/m^3)	C_{Rn}^{s} (kBq/m^3)	$C_{Rn}^{s,ac}$ (Bq/L)	$C_{Ra}^{s,ac}$ (Bq/L)	$C_{U}^{s,ac}$ (ppm)
1	M1	319.24	15.64	8.30	0.51	0.67
2	M2	212.83	10.42	5.53	0.34	0.45
3	M3	301.51	14.77	7.84	0.48	0.63
4	M4	195.09	9.56	5.07	0.31	0.41
5	M5	212.83	10.42	5.53	0.34	0.45
6	M6	709.43	34.75	18.44	1.13	1.49
7	M7	173.81	8.51	4.52	0.28	0.36
8	M8	230.56	11.29	5.99	0.37	0.48
9	M9	496.60	24.32	12.91	0.79	1.04
10	M10	532.07	26.06	13.83	0.85	1.12
11	M11	372.45	18.24	9.68	0.59	0.78
12	M12	301.51	14.77	7.84	0.48	0.63
13	M13	141.89	6.95	3.69	0.23	0.30
14	M14	248.30	12.16	6.45	0.40	0.52
15	M15	88.68	4.34	2.30	0.14	0.19
16	M16	177.36	8.69	4.61	0.28	0.37
17	M17	407.92	19.98	10.60	0.65	0.86
18	M18	124.15	6.08	3.23	0.20	0.26
19	M19	159.62	7.82	4.15	0.25	0.33
20	M20	372.45	18.24	9.68	0.59	0.78
Minimum		**88.68**	**4.34**	**2.30**	**0.14**	**0.19**
Maximum		**709.43**	**34.75**	**18.44**	**1.13**	**1.49**
Average±S.E		**288.92±34.10**	**14.15±1.67**	**7.51±0.88**	**0.46±0.05**	**0.61±0.07**

The map illustrated in the Figure (4.9) represent the radon concentrations in the samples of marshes water. The technique which used to drew is GIS with ArcGIS 10.7.1. The color gradation in the map indicates the different concentrations of radon in the marshes water samples.

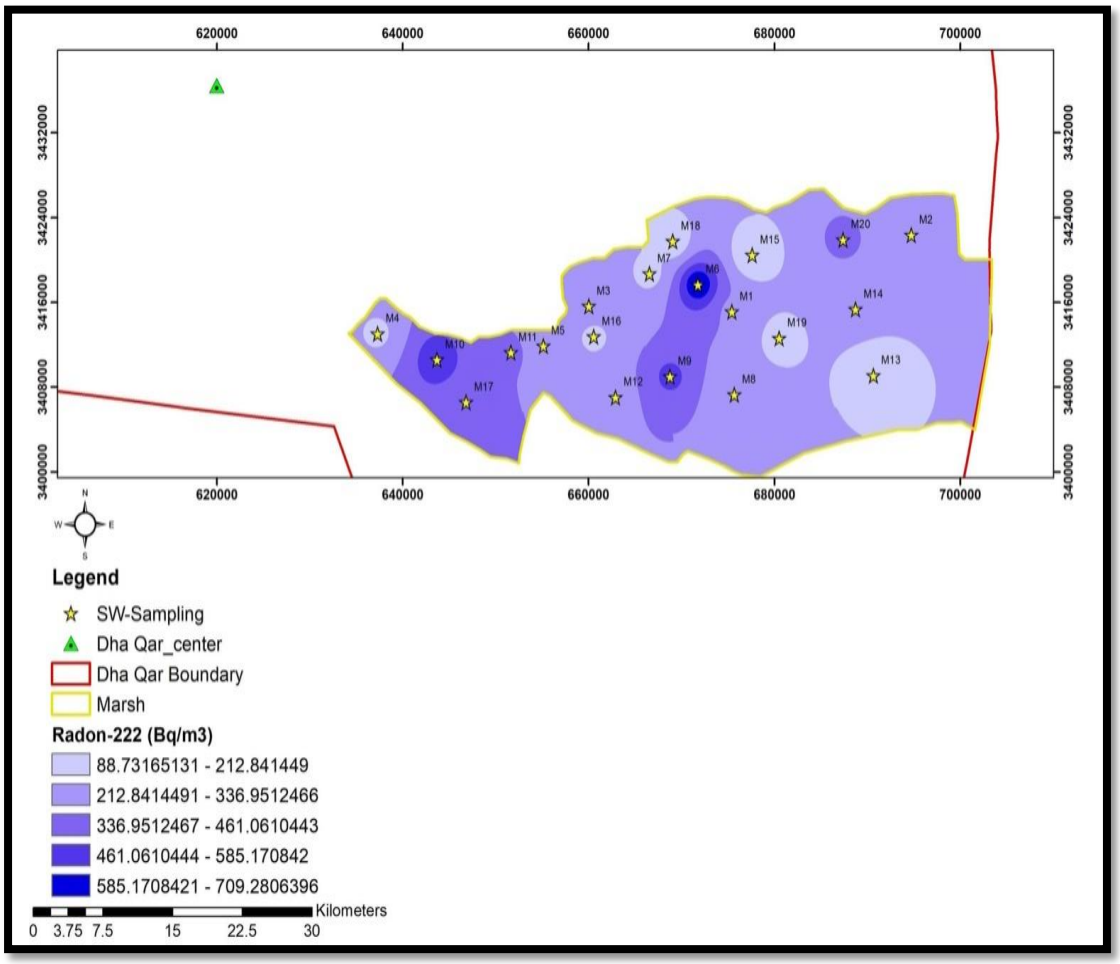

Figure (4.9): The map of the radon concentrations of marshes water.

AED due to activity of ^{222}Rn, ^{226}Ra, and the total of AED in water samples are shown in Table (4.25). It is found that the AED in mSv/y for ^{222}Rn, ^{226}Ra, and total of AED were ranged from 0.006 to 0.047, with an average value of 0.019±0.002, from 0.029 to 0.231, with an average value of 0.094±0.01 and from 0.03 to 0.28, with an average value of 0.11±0.01, respectively. The risk of a lifetime cancer risk was also assessed. The sample M6 had the highest lifetime risk as a consequence of water consumption, whereas the sample M15 had the lowest lifetime risk. The lifetime risk of ^{222}Rn and ^{226}Ra intake in water samples from certain marshes in Iraq's Dhi-Qar governorate ranged from 1.33×10^{-4} to 10.71×10^{-4}, with an average of $(4.3\pm0.05)\times10^{-4}$.

Table (4.25): The AED and lifetime cancer risk results of marshes water.

No.	Sample code	AED (mSv/y)		Total AED (mSv/y)	Lifetime cancer risk×10^{-4}
		^{222}Rn	^{226}Ra		
1	M1	0.021	0.104	0.13	4.83
2	M2	0.014	0.069	0.08	3.22
3	M3	0.020	0.098	0.12	4.55
4	M4	0.013	0.063	0.08	2.94
5	M5	0.014	0.069	0.08	3.22
6	M6	0.047	0.231	0.28	10.71
7	M7	0.012	0.057	0.07	2.65
8	M8	0.015	0.076	0.09	3.50
9	M9	0.033	0.161	0.19	7.49
10	M10	0.035	0.174	0.21	8.05
11	M11	0.025	0.121	0.15	5.60
12	M12	0.020	0.098	0.12	4.55
13	M13	0.009	0.047	0.06	2.17
14	M14	0.016	0.082	0.10	3.78
15	M15	0.006	0.029	0.03	1.33
16	M16	0.012	0.057	0.07	2.66
17	M17	0.027	0.133	0.16	6.16
18	M18	0.008	0.041	0.05	1.89
19	M19	0.011	0.051	0.06	2.38
20	M20	0.025	0.121	0.15	5.60
Minimum		**0.006**	**0.029**	**0.03**	**1.33**
Maximum		**0.047**	**0.231**	**0.28**	**10.71**
Average± S.E		**0.019±0.002**	**0.094±0.01**	**0.11±0.01**	**4.3±0.05**

4.3.3 Stations Water

Alpha emitters (^{222}Rn, ^{226}Ra, and ^{238}U) concentrations in samples of stations water. The results of ^{222}Rn (C_{Rn}^{a}, C_{Rn}^{s}, and $C_{Rn}^{s,ac}$), ^{226}Ra, and ^{238}U concentrations in the station water samples are shown in Table (4.26) where symbol (A) means before water treatment and symbol (B) means water after treatment. The values of C_{Rn}^{a} ranged between 70.94 Bq/m^3 in sample ST9 to 954.18 Bq/m^3 in the sample ST7 with an average value of 285.54±56.87 Bq/m^3, while the values of C_{Rn}^{s} in unit

kBq/m^3 and $C_{Rn}^{s,ac}$ in unit Bq/L, were ranged from 3.47 to 46.73 in the with an average value of 13.98±2.78 and from 1.84 to 24.80 in the with an average value of 7.42±1.47, respectively. Also from Table (4.26), it found that $C_{Ra}^{s,ac}$ were ranged from 0.11 to 1.52 Bq/L, with an average value of 0.45±0.09 Bq/L. The results of $C_{U}^{s,ac}$ in unit ppm as shown in Table (4.26) were ranged from 0.15 to 2.00, with an average value of 0.60±0.11.

Table (4.26): Radon, radium and uranium results in stations water samples.

No.	Sample code	^{222}Rn			^{226}Ra	^{238}U
		C_{Rn}^{a} (Bq/m^3)	C_{Rn}^{s} (kBq/m^3)	$C_{Rn}^{s,ac}$ (Bq/L)	$C_{Ra}^{s,ac}$ (Bq/L)	$C_{U}^{s,ac}$ (ppm)
1	ST1 (A)	141.89	6.95	3.69	0.23	0.30
2	ST2 (B)	106.41	5.21	2.77	0.17	0.22
3	ST3 (A)	255.39	12.51	6.64	0.41	0.54
4	ST4 (B)	195.09	9.56	5.07	0.31	0.41
5	ST5 (A)	131.24	6.43	3.41	0.21	0.28
6	ST6 (B)	85.13	4.17	2.21	0.14	0.18
7	ST7 (A)	954.18	46.73	24.80	1.52	2.00
8	ST8 (B)	163.17	7.99	4.24	0.26	0.34
9	ST9 (A)	70.94	3.47	1.84	0.11	0.15
10	ST10 (B)	177.36	8.69	4.61	0.28	0.37
11	ST11 (A)	716.52	35.09	18.62	1.14	1.50
12	ST12 (B)	890.33	43.61	23.14	1.42	1.87
13	ST13 (A)	329.88	16.16	8.57	0.53	0.69
14	ST14 (B)	283.77	13.90	7.38	0.45	0.60
15	ST15 (A)	117.06	5.73	3.04	0.19	0.25
16	ST16 (B)	124.15	6.08	3.23	0.20	0.26
17	ST17 (A)	102.87	5.04	2.67	0.16	0.22
18	ST18 (B)	223.47	10.95	5.81	0.36	0.47
19	ST19 (A)	336.98	16.50	8.76	0.54	0.71
20	ST20 (B)	305.05	14.94	7.93	0.49	0.64
Minimum		**70.94**	**3.47**	**1.84**	**0.11**	**0.15**
Maximum		**954.18**	**46.73**	**24.80**	**1.52**	**2.00**
Average±S.E		**285.54±56.87**	**13.98±2.78**	**7.42±1.47**	**0.45±0.09**	**0.60±0.11**

The map illustrated in the Figure (4.10) represent the radon concentrations water samples. The technique which used to drew is GIS with ArcGIS 10.7.1. The color gradation in the map indicates the different concentrations of radon in the stations (before treatment) water samples.

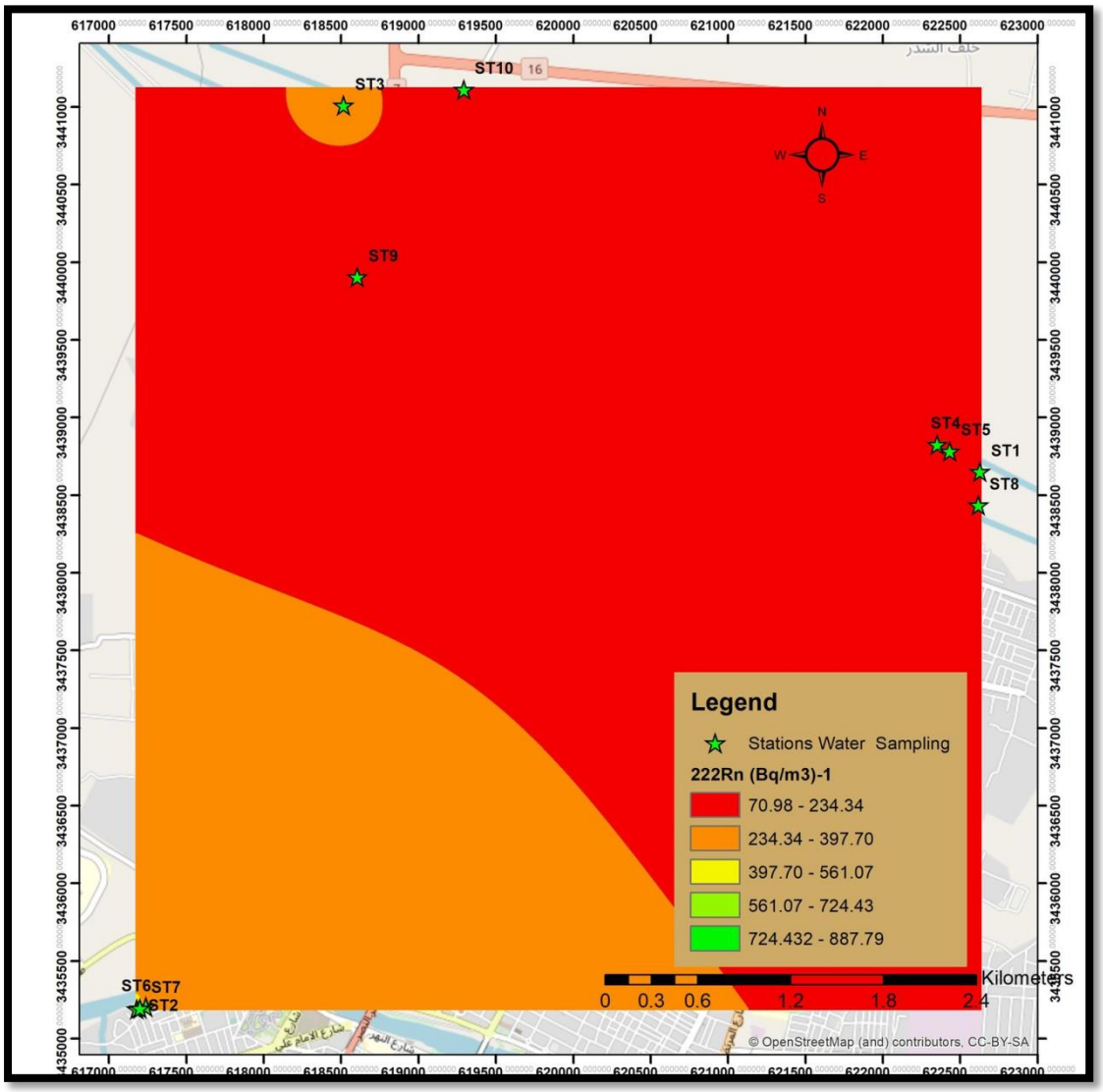

Figure (4.10): The map of the radon concentrations of stations water (before treatment).

The map illustrated in the Figure (4.11) represent the radon concentrations in the samples of stations water. The technique which used to drew is GIS with ArcGIS 10.7.1. The color gradation in the map

indicates the different concentrations of radon in the stations (after treatment) water samples.

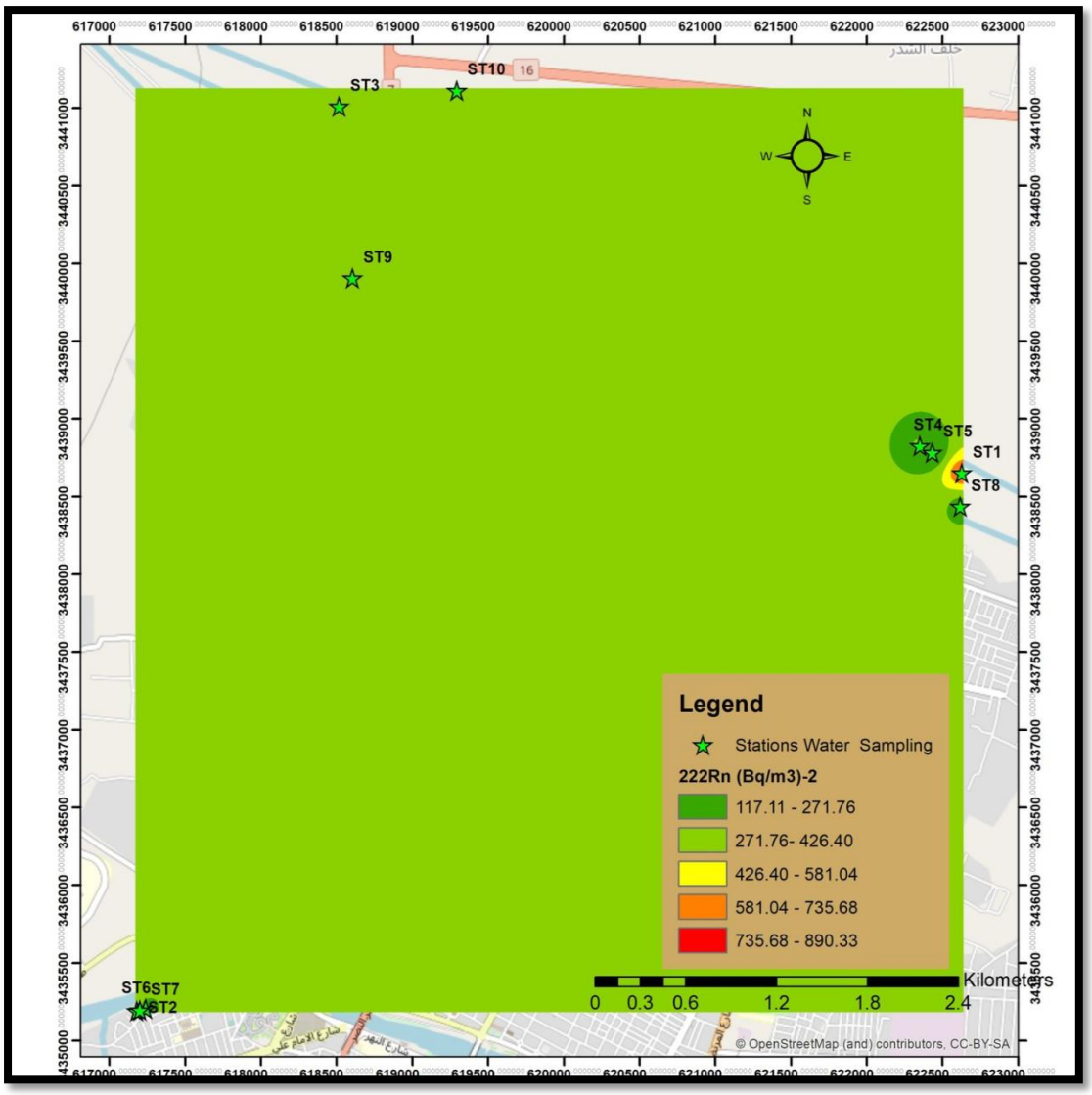

Figure (4.11): The map of the radon concentrations of stations water (after treatment).

AED due to activity of ^{222}Rn, ^{226}Ra, and the total of AED in stations water samples are shown in Table (4.27). It is found that the AED in mSv/y for ^{222}Rn, ^{226}Ra, and total of AED were ranged from 0.005 to 0.063, with an average value of 0.019±0.003, from 0.023 to 0.310, with an average value of 0.092±0.01 and from 0.03 to 0.37, with an average value of 0.11±0.02, respectively. The danger of a lifetime cancer risk was also assessed. The sample ST7 had the highest lifetime

risk as a consequence of water consumption, whereas the sample ST9 had the lowest lifetime risk. Ingestion of ^{222}Rn and ^{226}Ra in stations water samples resulted in lifetime risks ranging from 1.07×10^{-4} to 14.39×10^{-4}, with an average value of $(4.30\pm0.85)\times10^{-4}$.

Table (4.27): The AED and lifetime cancer risk results of stations water.

No.	Sample code	AED (mSv/y)		Total AED (mSv/y)	Lifetime cancer risk×10^{-4}
		^{222}Rn	^{226}Ra		
1	ST1(A)	0.009	0.046	0.06	2.14
2	ST2(B)	0.007	0.035	0.04	1.61
3	ST3(A)	0.017	0.083	0.10	3.85
4	ST4(B)	0.013	0.063	0.08	2.94
5	ST5(A)	0.009	0.043	0.05	1.98
6	ST6(B)	0.006	0.028	0.03	1.28
7	ST7(A)	0.063	0.310	0.37	14.39
8	ST8(B)	0.011	0.053	0.06	2.46
9	ST9(A)	0.005	0.023	0.03	1.07
10	ST10(B)	0.012	0.058	0.07	2.68
11	ST11(A)	0.048	0.233	0.28	10.81
12	ST12(B)	0.059	0.290	0.35	13.43
13	ST13(A)	0.022	0.107	0.13	4.98
14	ST14(B)	0.019	0.092	0.11	4.28
15	ST15(A)	0.008	0.038	0.05	1.77
16	ST16(B)	0.008	0.040	0.05	1.87
17	ST17(A)	0.007	0.033	0.04	1.55
18	ST18(B)	0.015	0.073	0.09	3.37
19	ST19(A)	0.022	0.110	0.13	5.08
20	ST20(B)	0.020	0.099	0.12	4.60
Minimum		**0.005**	**0.023**	**0.03**	**1.07**
Maximum		**0.063**	**0.310**	**0.37**	**14.39**
Average± S.E		**0.019±0.003**	**0.092±0.01**	**0.11±0.02**	**4.30±0.85**

4.3.4 Surface Water

Alpha emitters (^{222}Rn, ^{226}Ra, and ^{238}U) concentrations in samples of surface water. The results of ^{222}Rn (C_{Rn}^{a}, C_{Rn}^{s}, and $C_{Rn}^{s,ac}$), ^{226}Ra, and ^{238}U concentrations in the samples of surface water are shown in Table

(4.28). The values of C_{Rn}^{a} ranged between 102.87 Bq/m^3 in sample S12 to 922.25 Bq/m^3 in the sample S7 with an average value of 324.91±71.19 Bq/m^3, while the values of C_{Rn}^{s} in unit kBq/m^3 and $C_{Rn}^{s,ac}$ in unit Bq/L, were ranged from 5.04 to 45.17 in the with an average value of 15.91±3.48 and from 2.67 to 23.97 in the with an average value of 8.44±1.85, respectively. Also from Table (4.28), it found that $C_{Ra}^{s,ac}$ were ranged from 0.16 to 1.47 Bq/L, with an average value of 0.51±0.11 Bq/L. The results of $C_{U}^{s,ac}$ in unit ppm as shown in Table (4.28) were ranged from 0.22 to 1.93, with an average value of 0.68±0.14.

Table (4.28): Radon, radium and uranium results in surface water samples.

No.	Sample code	^{222}Rn			^{226}Ra	^{238}U
		C_{Rn}^{a} (Bq/m^3)	C_{Rn}^{s} (kBq/m^3)	$C_{Rn}^{s,ac}$ (Bq/L)	$C_{Ra}^{s,ac}$ (Bq/L)	$C_{U}^{s,ac}$ (ppm)
1	S1	897.42	43.95	23.32	1.43	1.88
2	S2	141.89	6.95	3.69	0.23	0.30
3	S3	198.64	9.73	5.16	0.32	0.42
4	S4	109.96	5.39	2.86	0.18	0.23
5	S5	248.30	12.16	6.45	0.40	0.52
6	S6	127.70	6.25	3.32	0.20	0.27
7	S7	922.25	45.17	23.97	1.47	1.93
8	S8	216.37	10.60	5.62	0.34	0.45
9	S9	138.34	6.78	3.60	0.22	0.29
10	S10	170.26	8.34	4.43	0.27	0.36
11	S11	638.48	31.27	16.59	1.02	1.34
12	S12	102.87	5.04	2.67	0.16	0.22
13	S13	156.07	7.64	4.06	0.25	0.33
14	S14	234.11	11.47	6.08	0.37	0.49
15	S15	571.09	27.97	14.84	0.91	1.20
Minimum		**102.87**	**5.04**	**2.67**	**0.16**	**0.22**
Maximum		**922.25**	**45.17**	**23.97**	**1.47**	**1.93**
Average± S.E		**324.91±71.19**	**15.91±3.48**	**8.44±1.85**	**0.51±0.11**	**0.682±0.14**

The map illustrated in the Figure (4.12) represent the radon concentrations in the surface water samples. The technique which used to drew is GIS with ArcGIS 10.7.1. The color gradation in the map indicates the different concentrations of radon in the surface water samples.

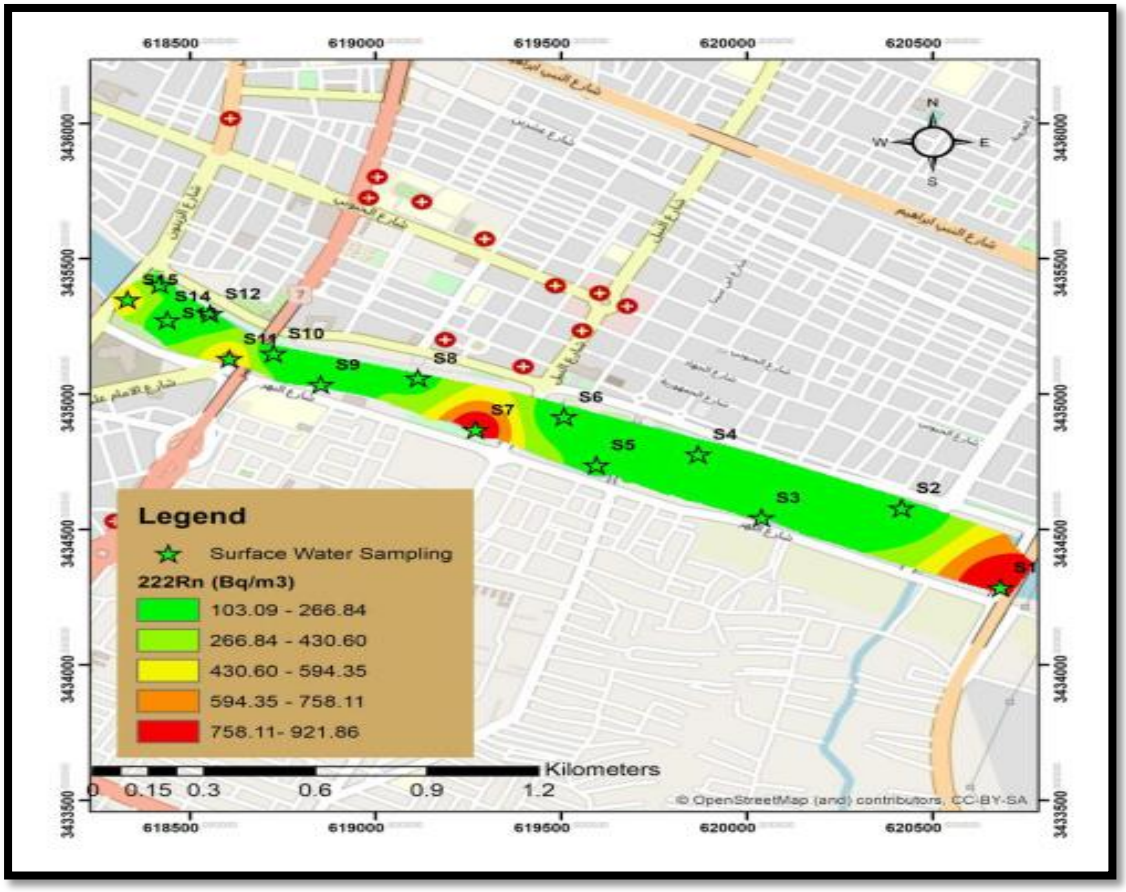

Figure (4.12): The map of the radon concentrations of surface water.

AED due to activity of ^{222}Rn, ^{226}Ra, and the total of AED in surface water samples are shown in Table (4.29). It is found that the AED in mSv/y for ^{222}Rn, ^{226}Ra, and total of AED were ranged from 0.007 to 0.061, with an average value of 0.021±0.004, from 0.033 to 0.300, with an average value of 0.105±0.02 and from 0.04 to 0.36, with an average value of 0.12±0.02, respectively. The danger of a lifetime cancer risk was also assessed. The sample S7 had the highest lifetime risk as a consequence of water consumption, whereas the sample S12 had the lowest lifetime risk. In surface water samples, the lifetime risk from

consumption of ^{222}Rn and ^{226}Ra ranged from 1.55×10^{-4} to 13.91×10^{-4}, with an average value of $(4.90\pm1.07)\times10^{-4}$.

Table (4.29): The AED and lifetime cancer risk results of surface water.

No.	Sample code	AED (mSv/y)		Total AED (mSv/y)	Lifetime cancer risk×10^{-4}
		^{222}Rn	^{226}Ra		
1	S1	0.060	0.292	0.35	13.54
2	S2	0.009	0.046	0.06	2.14
3	S3	0.013	0.065	0.08	3.00
4	S4	0.007	0.036	0.04	1.66
5	S5	0.016	0.081	0.10	3.75
6	S6	0.008	0.042	0.05	1.93
7	S7	0.061	0.300	0.36	13.91
8	S8	0.014	0.070	0.08	3.26
9	S9	0.009	0.045	0.05	2.09
10	S10	0.011	0.055	0.07	2.57
11	S11	0.042	0.208	0.25	9.63
12	S12	0.007	0.033	0.04	1.55
13	S13	0.010	0.051	0.06	2.35
14	S14	0.016	0.076	0.09	3.53
15	S15	0.038	0.186	0.22	8.61
Minimum		**0.007**	**0.033**	**0.04**	**1.55**
Maximum		**0.061**	**0.300**	**0.36**	**13.91**
Average± S.E		**0.021±0.004**	**0.105±0.02**	**0.12±0.02**	**4.90±1.07**

4.3.5 Groundwater

Alpha emitters (^{222}Rn, ^{226}Ra, and ^{238}U) concentrations in groundwater samples. The results of ^{222}Rn (C_{Rn}^{a}, C_{Rn}^{s}, and $C_{Rn}^{s,ac}$), ^{226}Ra, and ^{238}U concentrations in the groundwater samples are shown in Table (4.30). The values of C_{Rn}^{a} ranged between 106.41 Bq/m^3 in sample G12 to 532.07 Bq/m^3 in the sample G17 with an average value of 224.35±23.85 Bq/m^3, while the values of C_{Rn}^{s} in unit kBq/m^3 and $C_{Rn}^{s,ac}$ in unit Bq/L, were ranged from 5.21 to 26.06 in the with an average value

of 10.98±1.16 and from 2.77 to 13.83 in the with an average value of 5.83±0.61, respectively. Also from Table (4.30), it found that $C_{Ra}^{s,ac}$ were ranged from 0.17 to 0.85 Bq/L, with an average value of 0.35±0.03 Bq/L. The findings of $C_U^{s,ac}$ in unit ppm as shown in Table (4.30) were ranged from 0.22 to 1.12, with an average value of 0.47±0.05.

Table (4.30): Radon, radium and uranium results in groundwater samples.

No.	Sample code	^{222}Rn			^{226}Ra	^{238}U
		C_{Rn}^{a} (Bq/m^3)	C_{Rn}^{s} (kBq/m^3)	$C_{Rn}^{s,ac}$ (Bq/L)	$C_{Ra}^{s,ac}$ (Bq/L)	$C_U^{s,ac}$ (ppm)
1	G1	191.55	9.38	4.98	0.30	0.40
2	G2	283.77	13.90	7.38	0.45	0.60
3	G3	251.85	12.33	6.55	0.40	0.53
4	G4	234.11	11.47	6.08	0.37	0.49
5	G5	173.81	8.51	4.52	0.28	0.36
6	G6	124.15	6.08	3.23	0.20	0.26
7	G7	202.19	9.90	5.25	0.32	0.42
8	G8	177.36	8.69	4.61	0.28	0.37
9	G9	216.37	10.60	5.62	0.34	0.45
10	G10	113.51	5.56	2.95	0.18	0.24
11	G11	248.30	12.16	6.45	0.40	0.52
12	G12	106.41	5.21	2.77	0.17	0.22
13	G13	297.96	14.59	7.74	0.47	0.62
14	G14	266.03	13.03	6.91	0.42	0.56
15	G15	159.62	7.82	4.15	0.25	0.33
16	G16	141.89	6.95	3.69	0.23	0.30
17	G17	532.07	26.06	13.83	0.85	1.12
18	G18	173.81	8.51	4.52	0.28	0.36
19	G19	461.13	22.59	11.98	0.73	0.97
20	G20	131.24	6.43	3.41	0.21	0.28
Minimum		**106.41**	**5.21**	**2.77**	**0.17**	**0.22**
Maximum		**532.07**	**26.06**	**13.83**	**0.85**	**1.12**
Average± S.E		**224.35±23.85**	**10.98±1.16**	**5.83±0.61**	**0.35±0.03**	**0.47±0.05**

The map illustrated in the Figure (4.13) represent the radon concentrations in the groundwater samples. The technique which used to drew is GIS with ArcGIS 10.7.1. The color gradation in the map indicates the different concentrations of radon in the groundwater samples.

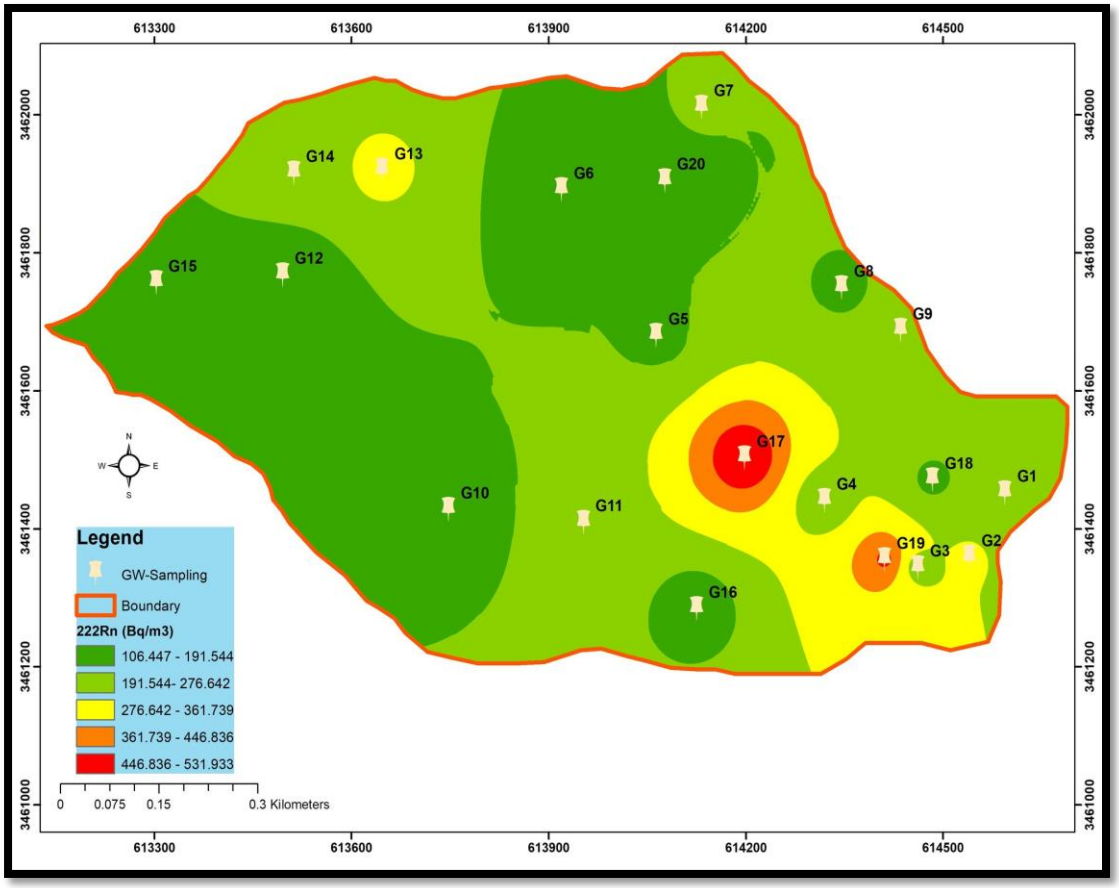

Figure (4.13): The map of the radon concentrations of groundwater.

AED due to activity of ^{222}Rn, ^{226}Ra, and the total of AED in groundwater samples are shown in Table (4.31). It is found that the AED in mSv/y for ^{222}Rn, ^{226}Ra, and total of AED were ranged from 0.007 to 0.035, with an average value of 0.015±0.001, from 0.035 to 0.173, with an average value of 0.073±0.007 and from 0.04 to 0.21, with an average value of 0.08±0.009, respectively. The danger of a lifetime cancer risk was also assessed. The sample G17 had the highest lifetime risk as a consequence of water consumption, whereas the sample G12 had the lowest lifetime risk. Ingestion of ^{222}Rn and ^{226}Ra in groundwater samples

resulted in lifetime risks ranging from 1.61 $\times 10^{-4}$ to 8.03 $\times 10^{-4}$, with an average value of (3.38±0.36) $\times 10^{-4}$.

Table (4.31): The AED and lifetime cancer risk results of groundwater.

No.	Sample code	AED (mSv/y)		Total AED (mSv/y)	Lifetime cancer risk$\times 10^{-4}$
		^{222}Rn	^{226}Ra		
1	G1	0.013	0.062	0.08	2.89
2	G2	0.019	0.092	0.11	4.28
3	G3	0.017	0.082	0.10	3.80
4	G4	0.016	0.076	0.09	3.53
5	G5	0.012	0.057	0.07	2.62
6	G6	0.008	0.040	0.05	1.87
7	G7	0.013	0.066	0.08	3.05
8	G8	0.012	0.058	0.07	2.68
9	G9	0.014	0.070	0.08	3.26
10	G10	0.008	0.037	0.04	1.71
11	G11	0.016	0.081	0.10	3.75
12	G12	0.007	0.035	0.04	1.61
13	G13	0.020	0.097	0.12	4.49
14	G14	0.018	0.087	0.10	4.01
15	G15	0.011	0.052	0.06	2.41
16	G16	0.009	0.046	0.06	2.14
17	G17	0.035	0.173	0.21	8.03
18	G18	0.012	0.057	0.07	2.62
19	G19	0.031	0.150	0.18	6.96
20	G20	0.009	0.043	0.05	1.98
Minimum		**0.007**	**0.035**	**0.04**	**1.61**
Maximum		**0.035**	**0.173**	**0.21**	**8.03**
Average± S.E		**0.015±0.001**	**0.073±0.007**	**0.088±0.009**	**3.38±0.36**

4.3.6 RO Water

Alpha emitters (^{222}Rn, ^{226}Ra, and ^{238}U) concentrations in RO samples. The results of ^{222}Rn (C_{Rn}^{a}, C_{Rn}^{s}, and $C_{Rn}^{s,ac}$), ^{226}Ra, and ^{238}U concentrations in the RO samples are shown in Table (4.32). The values of C_{Rn}^{a} ranged between 124.15 Bq/m^3 in sample RO20 to 1209.57 Bq/m^3

in the sample RO19 with an average value of 389.47±68.60 Bq/m^3, while the values of C_{Rn}^{s} in unit kBq/m^3 and $C_{Rn}^{s,ac}$ in unit Bq/L, were ranged from 6.08 to 59.24 in the with an average value of 19.07±3.36 and from 3.23 to 31.44 in the with an average value of 10.12±1.78, respectively. Also from Table (4.32), it found that $C_{Ra}^{s,ac}$ were ranged from 0.20 to 1.93 Bq/L, with an average value of 0.62±0.10 Bq/L. The results of $C_{U}^{s,ac}$ in unit ppm as shown in Table (4.32) were ranged from 0.26 to 2.54, with an average value of 0.81±0.14.

Table (4.32): Radon, radium and uranium results in RO water samples.

No.	Sample code	^{222}Rn			^{226}Ra	^{238}U
		C_{Rn}^{a} (Bq/m^3)	C_{Rn}^{s} (kBq/m^3)	$C_{Rn}^{s,ac}$ (Bq/L)	$C_{Ra}^{s,ac}$ (Bq/L)	$C_{U}^{s,ac}$ (ppm)
1	RO1	588.82	28.84	15.30	0.94	1.23
2	RO2	418.56	20.50	10.88	0.67	0.88
3	RO3	443.39	21.72	11.52	0.71	0.93
4	RO4	383.09	18.76	9.96	0.61	0.80
5	RO5	156.07	7.64	4.06	0.25	0.33
6	RO6	255.39	12.51	6.64	0.41	0.54
7	RO7	280.22	13.72	7.28	0.45	0.59
8	RO8	195.09	9.56	5.07	0.31	0.41
9	RO9	170.26	8.34	4.43	0.27	0.36
10	RO10	234.11	11.47	6.08	0.37	0.49
11	RO11	131.24	6.43	3.41	0.21	0.28
12	RO12	219.92	10.77	5.72	0.35	0.46
13	RO13	365.35	17.89	9.50	0.58	0.77
14	RO14	184.45	9.03	4.79	0.29	0.39
15	RO15	1184.74	58.03	30.79	1.89	2.48
16	RO16	457.58	22.41	11.89	0.73	0.96
17	RO17	645.58	31.62	16.78	1.03	1.35
18	RO18	141.89	6.95	3.69	0.23	0.30
19	RO19	1209.57	59.24	31.44	1.93	2.54
20	RO20	124.15	6.08	3.23	0.20	0.26
Minimum		**124.15**	**6.08**	**3.23**	**0.20**	**0.26**

⟶ Next

Maximum	**1209.57**	**59.24**	**31.44**	**1.93**	**2.54**
Average± S.E	**389.47±68.60**	**19.07±3.36**	**10.123±1.78**	**0.62±0.10**	**0.81±0.14**

The map illustrated in the Figure (4.14) represent the radon concentrations in the RO water samples. The technique which used to drew is GIS with ArcGIS 10.7.1. The color gradation in the map indicates the different concentrations of radon in the RO water samples.

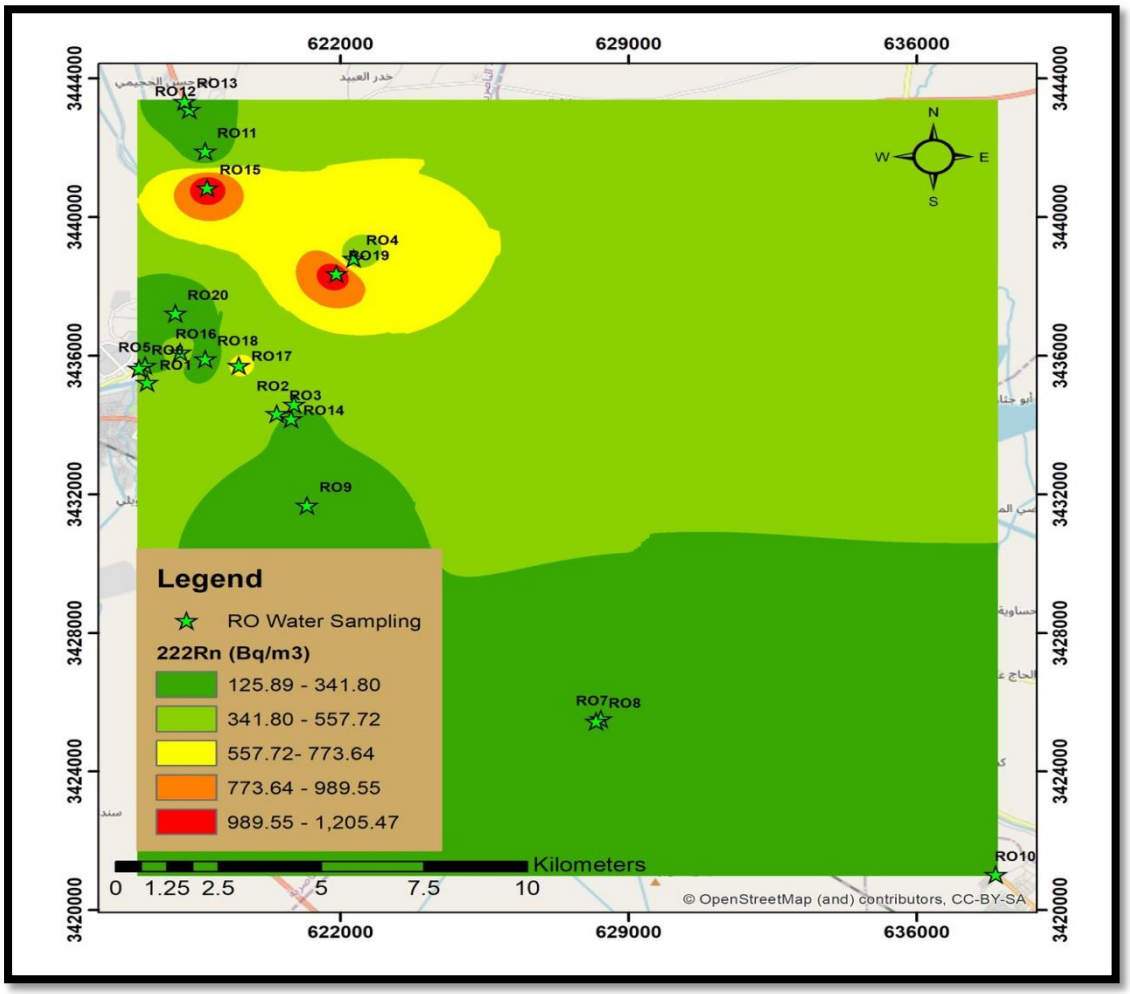

Figure (4.14): The map of the radon concentrations of RO water.

AED due to activity of ^{222}Rn, ^{226}Ra, and the total of AED in RO water samples are shown in Table (4.33). It is found that the AED in mSv/y for ^{222}Rn, ^{226}Ra, and total of AED were ranged from 0.008 to 0.080, with an average value of 0.025±0.004, from 0.040 to 0.394, with

an average value of 0.126±0.02 and from 0.05 to 0.47, with an average value of 0.15±0.02, respectively. The danger of a lifetime cancer risk was also assessed. The sample RO19 had the highest lifetime risk as a consequence of water consumption, whereas the sample RO20 had the lowest lifetime risk. Ingestion of ^{222}Rn and ^{226}Ra in RO water samples resulted in a lifetime risk ranging from 1.87×10^{-4} to 18.25×10^{-4}, with an average value of $(5.87\pm1.03)\times10^{-4}$.

Table (4.33): The AED and lifetime cancer risk results of RO water.

No.	Sample code	AED (mSv/y)		Total AED (mSv/y)	Lifetime cancer risk×10^{-4}
		^{222}Rn	^{226}Ra		
1	RO1	0.039	0.192	0.23	8.88
2	RO2	0.028	0.136	0.16	6.31
3	RO3	0.029	0.144	0.17	6.69
4	RO4	0.025	0.125	0.15	5.78
5	RO5	0.010	0.051	0.06	2.35
6	RO6	0.017	0.083	0.10	3.85
7	RO7	0.019	0.091	0.11	4.23
8	RO8	0.013	0.063	0.08	2.94
9	RO9	0.011	0.055	0.07	2.57
10	RO10	0.016	0.076	0.09	3.53
11	RO11	0.009	0.043	0.05	1.98
12	RO12	0.015	0.072	0.09	3.32
13	RO13	0.024	0.119	0.14	5.51
14	RO14	0.012	0.060	0.07	2.78
15	RO15	0.079	0.386	0.46	17.87
16	RO16	0.030	0.149	0.18	6.90
17	RO17	0.043	0.210	0.25	9.74
18	RO18	0.009	0.046	0.06	2.14
19	RO19	0.080	0.394	0.47	18.25
20	RO20	0.008	0.040	0.05	1.87
Minimum		**0.008**	**0.040**	**0.05**	**1.87**
Maximum		**0.080**	**0.394**	**0.47**	**18.25**
Average± S.E		**0.025±0.004**	**0.126±0.02**	**0.152±0.02**	**5.87±1.03**

4.3.7 Discussion of Radon and Radiological Risks

The results of ^{222}Rn (C_{Rn}^{a}, C_{Rn}^{s}, and $C_{Rn}^{s,ac}$), ^{226}Ra, and ^{238}U concentrations in the water samples for selected water samples are shown in Tables (4.22), (4.24), (4.26), (4.28), (4.30) and (4.32). The values of C_{Rn}^{a} ranged between 70.94 Bq/m^3 in station water sample ST9 to 1773.57 Bq/m^3 in tap water sample T16 and average values varying from 224.35±23.85 Bq/m^3 in groundwater sample to 441.61±77.02 in the tap water samples, while the values of C_{Rn}^{s} in unit kBq/m^3 and $C_{Rn}^{s,ac}$ in unit Bq/L, were ranged from 3.47 to 86.87 average values varying from of 10.98±1.16 to 21.62±3.77 and from 1.84 to 46.10 the average values between 5.83±0.61 recorded in groundwater to 11.47±2.00 in tap water, respectively. Also from the same tables, it found that $C_{Ra}^{s,ac}$ were ranged from 0.11 Bq/L in stations water sample ST9 to 2.82 Bq/L in tap water sample T16, and the average values ranged from 0.35±0.03 Bq/L in groundwater samples to 0.70±0.12 in tap water samples. The results of $C_{U}^{s,ac}$ in unit ppm were ranged from 0.15 in station water sample to 3.72 in tap water sample, and the average values ranged from 0.47±0.05 to 0.92±0.16.

The results of ^{222}Rn concentration in water samples turn out to be lower than the acceptable limit as reported in WHO 2008 [125],[142]: 0.4Bq/L (400 Bq/m^3), except twenty five water samples in different regions were higher the worldwide limit. Variation was given, in values concentrations of radon in the water samples in the present study, because several factors such as the geology and their geochemistry and its components, which may vary from one area to another, as well as the difference in the concentrations of uranium and radium, because they are the main source of radon. It should be noted that the pollution that resulted from the radiation may be directly caused by the absorption of radionuclides of the atmosphere. By the way of comparing the values of

(C_{Rn}^{a}) and (C_{Rn}^{s}) of the investigated metrics, it is clear that the radon concentration of the samples itself is much higher than that of the airspace of the tube. The known fact that most of the radon atoms in the sample were destroyed before entering the tube space due to their short decay period of 3.82 day may be ascribed to the obvious discrepancy between the two readings [133]. In addition to this, the existence of the radium (i.e. radon parent) is inside the sample, and not in the airspace of the tube. As can be seen from pervious tables, the activities of alpha due to radium in water samples were found to be lower than those caused by radon. This can be explained by that the radon has less half-life (3.82 d) than that of the radium (1600 y) [129],[136]. The results of $C_{Ra}^{s,ac}$ for collected samples of water in the were within the global average limitations (1 Bq/L) that recommended by WHO 2011[21], except fourteen water Samples was larger than global average limitations.

The values of $C_{U}^{s,ac}$ for most collected water samples are higher than the global average limitations (0.566 ppm) in healthy drinking water according to EPA organization [143].

AED due to activity of ^{222}Rn, ^{226}Ra, and the total of AED in water collected water samples are shown in Tables (4.23), (4.25), (4.27), (4.29), (4.31) and (4.33). It is found that the AED in mSv/y for ^{222}Rn, ^{226}Ra, and total of AED were ranged from 0.005 in stations water sample ST9 to 0.118 in tap water sample T16, and the average values varying from 0.015±0.001 in groundwater samples to 0.029±0.005 in tap water samples, from 0.023 to 0.577, and the average values varying from 0.073±0.007 to 0.143±0.02 respectively. While the values of the total AED were ranged from 0.03mSv/y in stations water sample ST9 to 0.69 mSv/y in the tap water sample T16, the average values varying from 0.088±0.009 to 0.17±0.03mSv/y. The typical radiation display to people from normal sources is approximately 0.3 mSv/y due to ingestion of food

and drink via normal routes. The overall suggested radiation dosage is kept to less than 0.1 mSv/y by ingesting radionuclides via drinking water [21].

If these radionuclides produced more than one limit, the resultant AED is the total of the AED equivalents from each of the radioelements present. The total AED for two radionuclides (^{222}Rn and ^{226}Ra) is less than the action limit of 1.0 mSv/y on average (excluding ^{222}Rn). The average AED from drinking water containing ^{222}Rn was estimated to be as low as 0.002 mSv/y [144]. The lifetime cancer risk in accordance with gathered water was also estimated.

The lowest lifetime cancer risk resulted from water intake was 1.07×10^{-4} seen in station water sample ST9, while the biggest lifetime cancer risk was 26.75×10^{-4} found in tap the sample T16. The average values varying from $(3.38\pm0.36)\times10^{-4}$ to $(6.66\pm1.61)\times10^{-4}$ "exceeding the admissible limit of 10^{-4}"[145]. The results of alpha emissions differed across all water samples examined, owing to radioactivity in the source or natural components that make up the samples contents, such as chemical material, as well as another significant component, geology. The concentration of radon in majority of the samples under investigation was determined to be low and insignificant in terms of health risk.

4.3.8 Summary of Mean Radon Concentrations

Table (4.34): Summary of radon, radium and uranium for all water samples.

Water Type		^{222}Rn			^{226}Ra	^{238}U
		C^{a}_{Rn} (Bq/m^3)	C^{s}_{Rn} (KBq/m^3)	$C^{s,ac}_{Rn}$ (Bq/L)	$C^{s,ac}_{Ra}$ (Bq/L)	$C^{s,ac}_{U}$ (ppm)
Tap	Minimum	81.58	4.00	2.12	0.13	0.17
	Maximum	1773.57	86.87	46.10	2.82	3.72
	Average± S.E	441.61±77.02	21.62±3.77	11.47±2.00	0.70±0.12	0.92±0.16
Marshes	Minimum	88.68	4.34	2.30	0.14	0.19
	Maximum	709.43	34.75	18.44	1.13	1.49

⟶ Next

	Average± S.E	**288.92±34.10**	**14.15±1.67**	**7.51±0.88**	**0.46±0.05**	**0.61±0.07**
Station	**Minimum**	**70.94**	**3.47**	**1.84**	**0.11**	**0.15**
	Maximum	**954.18**	**46.73**	**24.80**	**1.52**	**2.00**
	Average± S.E	**285.54±56.87**	**13.98±2.78**	**7.42±1.47**	**0.45±0.09**	**0.60±0.11**
Surface	**Minimum**	**102.87**	**5.04**	**2.67**	**0.16**	**0.22**
	Maximum	**922.25**	**45.17**	**23.97**	**1.47**	**1.93**
	Average± S.E	**324.91±71.19**	**15.91±3.48**	**8.44±1.85**	**0.51±0.11**	**0.68±0.14**
Ground	**Minimum**	**106.41**	**5.21**	**2.77**	**0.17**	**0.22**
	Maximum	**532.07**	**26.06**	**13.83**	**0.85**	**1.12**
	Average± S.E	**224.35±23.85**	**10.98±1.16**	**5.83±0.61**	**0.35±0.03**	**0.47±0.05**
RO	**Minimum**	**124.15**	**6.08**	**3.23**	**0.20**	**0.26**
	Maximum	**1209.57**	**59.24**	**31.44**	**1.93**	**2.54**
	Average± S.E	**389.47±68.60**	**19.07±3.36**	**10.12±1.78**	**0.62±0.10**	**0.81±0.14**

Table (4.35): Summary AED and lifetime cancer risk for all water samples.

Water Type		**AED (mSv/y)**		**Total AED (mSv/y)**	**Lifetime cancer risk $\times 10^{-4}$**
		^{222}Rn	**^{226}Ra**		
Tap	**Minimum**	**0.006**	**0.028**	**0.03**	**1.28**
	Maximum	**0.118**	**0.577**	**0.69**	**26.75**
	Average± S.E	**0.029±0.005**	**0.143±0.02**	**0.17±0.03**	**6.66±1.61**
Marshes	**Minimum**	**0.006**	**0.029**	**0.03**	**1.33**
	Maximum	**0.047**	**0.231**	**0.28**	**10.71**
	Average± S.E	**0.019±0.002**	**0.094±0.01**	**0.11±0.01**	**4.30±0.05**
Station	**Minimum**	**0.005**	**0.023**	**0.03**	**1.07**
	Maximum	**0.063**	**0.310**	**0.37**	**14.39**
	Average± S.E	**0.019±0.003**	**0.092±0.01**	**0.11±0.02**	**4.30±0.85**
Surface	**Minimum**	**0.007**	**0.033**	**0.04**	**1.55**
	Maximum	**0.061**	**0.300**	**0.36**	**13.91**

⟶Next

	Average± S.E	**0.021±0.004**	**0.105±0.02**	**0.12±0.02**	**4.90±1.07**
Ground	**Minimum**	**0.007**	**0.035**	**0.04**	**1.61**
	Maximum	**0.035**	**0.173**	**0.21**	**8.03**
	Average± S.E	**0.015±0.001**	**0.073±0.007**	**0.088±0.009**	**3.38±0.36**
RO	**Minimum**	**0.008**	**0.040**	**0.05**	**1.87**
	Maximum	**0.080**	**0.394**	**0.47**	**18.25**
	Average± S.E	**0.025±0.004**	**0.126±0.02**	**0.152±0.02**	**5.87±1.03**

4.4 Various Measurement Techniques

In this study the concentrations of uranium and radon were measured using three different measurement techniques, two of which are experimental and the other is a theoretical method using the (MATLAB) program. Each of these methods has advantages, for example the (TASL) method in which the track density is calculated automatically after entering all the required data, such as the radiation background and the duration of the irradiation, and it can deal with 64 track detectors, while the process of inspecting and calculating the nuclear tracks takes a long time using the manual method (microscopy), but this method is characterized by accuracy in calculating the number of nuclear tracks .While the process of calculating nuclear tracks using the MATLAB program only takes a few seconds. The purpose of the diversity of measurement techniques is to ascertain the measured concentrations and to find the correlation between the different measurement techniques. The results of the concentrations of uranium and radon will be presented for each studied area with an indication of the correlation of all the techniques that were used.

4.4.1 Uranium Concentrations

Table (4.36) illustrates the concentrations of uranium obtained by using different detection techniques, using TASLIMAGE dosimetry system and microscopic, and by using the developed (CR-39-D2) program.

Table (4.36): Results of uranium concentrations for all detection techniques.

Water type		Concentration of Uranium (µg/L)		
		TASL	Manually	CR-39-D2
Tap	Minimum	0.77	0.75	0.76
	Maximum	1.20	1.10	1.26
	Average± S.E	0.89±0.02	0.90±0.01	0.94±0.02
Marshes	Minimum	0.81	0.76	0.78
	Maximum	1.41	1.30	1.17
	Average± S.E	0.97±0.03	0.93±0.03	0.95±0.02
Station	Minimum	0.75	0.76	0.76
	Maximum	1.03	0.95	1.02
	Average± S.E	0.84±0.01	0.82±0.01	0.85±0.01
Surface	Minimum	0.76	0.75	0.77
	Maximum	1.49	1.25	1.10
	Average± S.E	0.87±0.04	0.86±0.03	0.88±0.02
Ground	Minimum	0.77	0.75	0.75
	Maximum	1.18	1.08	1.34
	Average± S.E	0.87±0.02	0.83±0.01	0.86±0.03
RO	Minimum	0.76	0.76	0.77
	Maximum	1.46	1.37	1.29
	Average± S.E	0.93±0.04	0.91±0.03	0.92±0.03

4.4.1.1 Correlation Factor of Uranium

Table (4.37) illustrates the correlation factor to different techniques are used to obtained the concentrations of uranium in water samples.

Table (4.37): Correlation factor for all detection techniques.

Tap			
Correlation factor	TASL	Manually	CR-39-D2
TASL	1.00	0.91	0.87
Manually	0.91	1.00	0.82
CR-39-D2	0.87	0.82	1.00
Marshes			
Correlation factor	TASL	Manually	CR-39-D2
TASL	1.00	0.82	0.77
Manually	0.82	1.00	0.80
CR-39-D2	0.77	0.80	1.00
Station			
Correlation factor	TASL	Manually	CR-39-D2
TASL	1.00	0.90	0.74
Manually	0.90	1.00	0.76
CR-39-D2	0.74	0.76	1.00
Surface			
Correlation factor	TASL	Manually	CR-39-D2
TASL	1.00	0.92	0.79
Manually	0.92	1.00	0.89
CR-39-D2	0.79	0.89	1.00
Ground			
Correlation factor	TASL	Manually	CR-39-D2
TASL	1.00	0.79	0.90
Manually	0.79	1.00	0.77
CR-39-D2	0.90	0.77	1.00
RO			
Correlation factor	TASL	Manually	CR-39-D2
TASL	1.00	0.92	0.94
Manually	0.92	1.00	0.89
CR-39-D2	0.94	0.89	1.00

Table (4.38) illustrates the correlation factor of all water sample of different techniques are used to obtained the concentrations of uranium regardless of the quality of water samples .

Table (4.38): Correlation factor for detection techniques for all water samples.

Correlation factor	TASL	Manually	CR-39-D2
TASL	1.00	0.88	0.84
Manually	0.88	1.00	0.82
CR-39-D2	0.84	0.82	1.00

4.4.1.2 Correlation Uranium VS Physicochemical Properties

The pH, EC, and TDS values for the samples of water in the research are shown in Table (4.39). The pH values varied from 7.3 to 8.2, with an average of 7.84±0.22, as shown in Table (4.39). In addition, the data shows that the EC values varied from 1808 to 7802 µS/cm, with an average of 3999.95±294.45µS/cm. The values of TDS, in unit mg/L, varied from 1175 to 5119, with an average of 2601.35±197.77, according to the same table. The pH is a measurement that indicates whether or not a solution is alkaline or acidic in type and density. The WHO recommends a pH range of 6.5 to 9.2 as the highest acceptable level [37]. All of the water samples had pH values that were somewhat acidic, but within WHO's acceptable range. On reality, the geology of the sample locations may have a role in the pH of the surface water's ultimate pH. "The EC values for all of the examined samples were detected to be higher than the WHO2011(750 µS/cm) [21] and Iraq standards 2009 (1500 µS/cm) for water of drinking [146], as well as the WHO2011(2000 µS/cm) [147] and "Iraq standards 2009 (2500 µS/cm) for irrigation water"[148]. The existence of a large quantity of dissolved inorganic compounds (solutes) in an ionized state is indicated by high EC values.

TDS stands for total dissolved solids in a solution or water, and it shows how salty water. Water supply with a TDS of more than 500 mg/L is considered an unfit source of drinking water. WHO and Iraq standards allow for a TDS maximum of 1000 mg/L in groundwater [147]. As a result, all TDS levels for collected samples (see Table 6) exceed Iraqi regulations and the "WHO 2011 limit of 1000 mg/L"[146],[148].

Table (4.39): Results of pH, EC and TDS.

No.	Sample code	pH	EC (µS/cm)	TDS (mg/L)
1	M1	7.5	3600	1988
2	M2	7.8	4020	3012
3	M3	7.6	3074	1998
4	M4	8.1	7802	5119
5	M5	7.7	2733	1769
6	M6	7.3	1808	1175
7	M7	7.7	1912	1210
8	M8	7.9	4916	3095
9	M9	8.0	4816	3130
10	M10	8.2	5012	3400
11	M11	8.0	4675	3026
12	M12	8.2	4610	2995
13	M13	7.8	3950	2565
14	M14	7.9	3722	2419
15	M15	7.8	5000	3245
16	M16	7.8	3149	2045
17	M17	7.7	2710	1710
18	M18	7.7	3153	2050
19	M19	8.1	4643	3021
20	M20	8.0	4694	3055
Minimum		**7.3**	**1808**	**1175**
Maximum		**8.2**	**7802**	**5119**
Average±S.E		**7.84±0.22**	**3999.95±294.45**	**2601.35±197.77**

For the three parameters, the correlation coefficients are numerical values obtained from Table (4.40). There is a significant positive relationship between UC and pH (0.61), UC and EC (0.89), UC and TDS (0.90), pH and EC (0.74), pH and TDS (0.76), and TDS and EC (0.99). The positive connection among uranium concentrations and pH, EC, and TDS may be clarified by the existence of uranium in drinking water as dissolved salts containing these chemical properties [149],[150].

Table (4.40): Correlation factor of uranium concentrations with Physiochemical properties.

	UC	pH	EC	TDS
UC	1.00	0.61	0.89	0.90
pH	0.61	1.00	0.74	0.76
EC	0.89	0.74	1.00	0.99
TDS	0.90	0.76	0.99	1.00

4.4.2 Radon Concentrations

Different detection techniques are used to determine the radon concentrations in the present study the concentrations of radon detected by three techniques , TASLIMAGE dosimetry system, microscopic and by using the developed MATLAB (CR-39-D2) program. Table (4.41) illustrates the concentrations of radon of water samples.

Table (4.41): Results of radon concentrations for all detection techniques.

Water type		**Concentration of Radon (Bq/m^3)**		
		TASL	**Manually**	**CR-39-D2**
Tap	**Minimum**	81.58	92.23	88.68
	Maximum	1173.57	1560.74	1241.5
	Average± S.E	441.61±77.02	427.54±60.31	416.30±48.15
Marshes	**Minimum**	88.68	106.41	56.75
	Maximum	709.43	645.58	680.34

⟶ Next

	Average± S.E	288.91±34.10	288.01±31.21	282.45±39.81
Station	**Minimum**	70.94	78.04	78.04
	Maximum	954.18	922.25	1135.08
	Average± S.E	285.54±56.87	274.19±50.24	333.78±67.39
Surface	**Minimum**	102.87	106.41	70.94
	Maximum	922.25	709.43	989.65
	Average± S.E	324.91±71.19	274.78±45.00	368.92±66.53
Ground	**Minimum**	106.41	106.41	113.51
	Maximum	532.07	638.48	500.15
	Average± S.E	224.35±23.85	219.21±27.88	222.22±22.37
RO	**Minimum**	124.15	74.49	106.41
	Maximum	1209.57	1064.14	886.78
	Average± S.E	389.47±68.60	296.36±48.69	399.93±46.20

4.4.2.1 Correlation Factor of Radon

The correlation factor to different techniques are used to obtained the concentrations of radon in water samples. Table (4.42) illustrates the correlation factor of radon concentrations to the collected water samples.

Table(4.42): Correlation factor of radon for all detection techniques.

Tap			
Correlation factor	TASL	Manually	CR-39-D2
TASL	1.00	0.75	0.91
Manually	0.75	1.00	0.83
CR-39-D2	0.91	0.83	1.00
Marshes			
Correlation factor	TASL	Manually	CR-39-D2
TASL	1.00	0.85	0.77
Manually	0.85	1.00	0.81
CR-39-D2	0.77	0.81	1.00
Station			
Correlation factor	TASL	Manually	CR-39-D2
TASL	1.00	0.92	0.86
Manually	0.92	1.00	0.90

⟶ Next

CR-39-D2	0.86	0.90	1.00
Surface			
Correlation factor	TASL	Manually	CR-39-D2
TASL	1.00	0.84	0.89
Manually	0.84	1.00	0.77
CR-39-D2	0.89	0.77	1.00
Ground			
Correlation factor	TASL	Manually	CR-39-D2
TASL	1.00	0.80	0.82
Manually	0.80	1.00	0.75
CR-39-D2	0.82	0.75	1.00
RO			
Correlation factor	TASL	Manually	CR-39-D2
TASL	1.00	0.84	0.90
Manually	0.84	1.00	0.71
CR-39-D2	0.90	0.71	1.00

Table (4.43) illustrates the correlation factor of all water sample of different techniques are used to obtained the concentrations of radon regardless of the quality of water samples .

Table(4.43): Correlation factor for all detection techniques for all water samples.

Correlation factor	**TASL**	**Manually**	**CR-39-D2**
TASL	1.00	0.80	0.88
Manually	0.80	1.00	0.79
CR-39-D2	0.88	0.79	1.00

4.4.2.2 Radon Concentrations Using RAD-7

The concentration of ^{222}Rn in groundwater samples was measured. ^{222}Rn concentrations varied from 0.032±0.022 Bq/L in the sample (G9) to 0.780±0.110 Bq/L in the sample (G17), with an average

of 0.205±0.04 Bq/L, according to the findings of analyzing the samples in groundwater given in Table (4.44). The current study radon gas concentrations in groundwater were determined to be below the acceptable limit established by the "US Environmental Protection Agency (EPA)" based on the findings in Table (4.44). The maximum allowable radon concentration in water (11.1) Bq/L [151]. Furthermore, with the exception of samples G17 and G19, the ^{222}Rn content in groundwater samples utilized as drinking water was lower than the ICRP-recommended concentration limit (0.4Bq/L) [121]. Rainwater that enters the ground via its rock layers or geological water coming from rocks between fresh water or oceans that hold water between their rocks are the two main sources of groundwater in these regions.

The findings in Table (4.44) demonstrate that radon concentrations vary across all samples, which may be ascribed to differences in the geological character of each location, as well as the flow of water and its pace [34]. "Temperature, air pressure, humidity, and changes in the Earth's strata", on the other hand, influence radon gas concentration. Finally, the findings show that radioactive radon gas levels in the groundwater in the current research region have not surpassed the allowable limit and have had no detrimental effects on human or environmental health.

Table (4.44): Radon concentrations using RAD-7.

No.	Sample code	^{222}Rn concentrations (Bq/L)
1	G1	0.160±0.050
2	G2	0.192±0.055
3	G3	0.222±0.059
4	G4	0.188±0.054
5	G5	0.159±0.050
6	G6	0.118±0.043
7	G7	0.042±0.026
8	G8	0.199±0.056
9	G9	0.032±0.022
10	G10	0.170±0.052
11	G11	0.096±0.039
12	G12	0.112±0.042

⟶ Next

13	G13	0.264±0.064
14	G14	0.182±0.053
15	G15	0.170±0.052
16	G16	0.197±0.055
17	G17	0.780±0.110
18	G18	0.053±0.029
19	G19	0.669±0.102
20	G20	0.092±0.038
Minimum		**0.032±0.022**
Maximum		**0.780±0.110**
Average±S.E		**0.205±0.04**

The map illustrated in the Figure (4.15) represent the radon concentrations in groundwater samples. The technique which used to drew is GIS with ArcGIS 10.7.1. The color gradation in the map indicates the different concentrations of radon in the groundwater samples by using RAD-7.

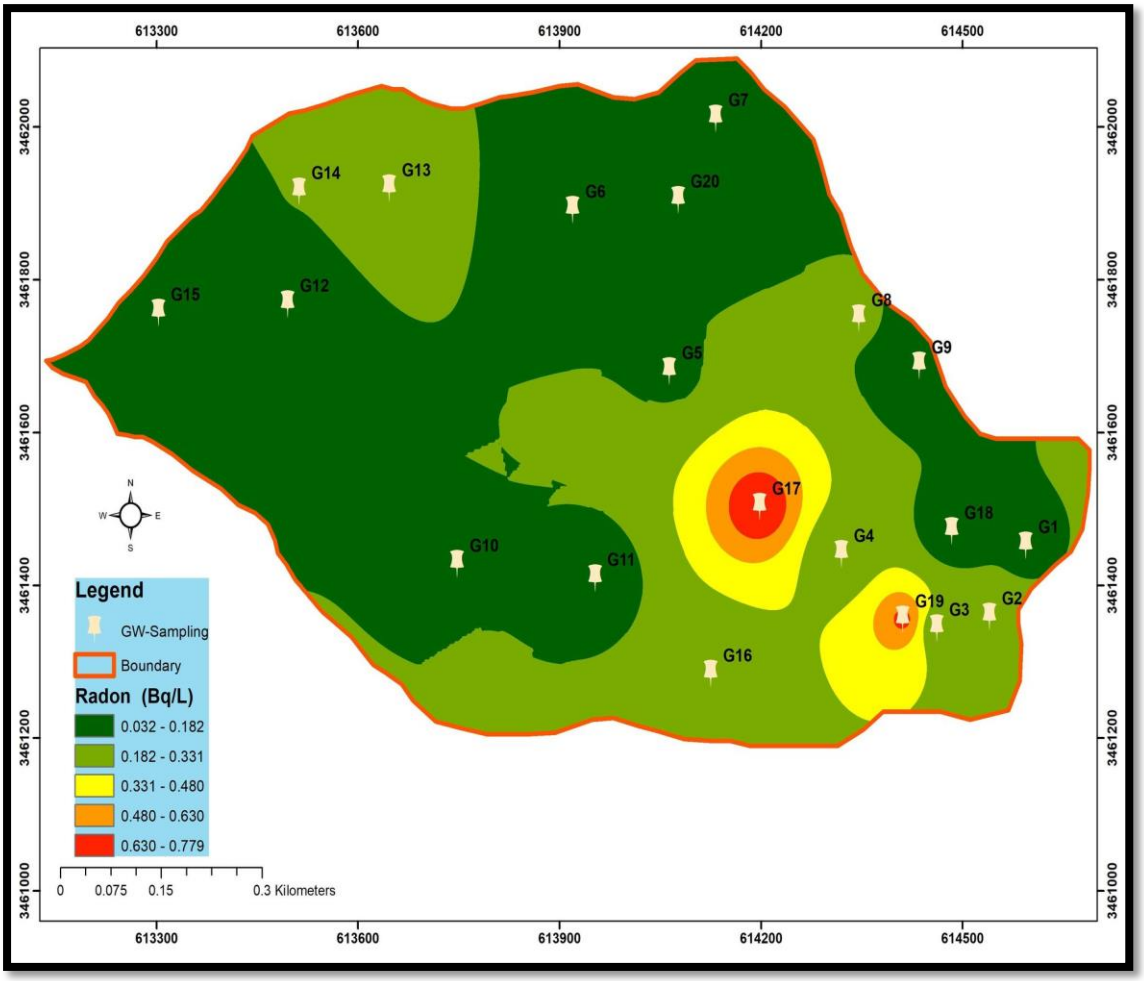

Figure(4.15): The map of the radon concentrations of groundwater using RAD-7.

4.4.2.3 Radon Results of RAD-7 VS CR-39

The correlation coefficients are numerical values for the radon concentrations to groundwater samples which measured by Rad-7 device with the radon concentrations that was measured by the technique of solid state nuclear track detectors. which are obtained from Table (4.45)**.** The above table show that there is highly positive correlation between values of radon concentrations of RAD-7 and CR-39 (0.88).

Table (4.45): Correlation factor RAD-7 VS CR-39.

Correlation factor	RAD -7	CR-39
CR-39	0.88	1
RAD-7	1	0.88

4.5 Comparing With Other Studies

4.5.1 Uranium Concentrations

The bounds of uranium in water fixed by several organizations and commissions, including the EPA, WHO, UNSCEAR, and ICRP, uranium concentration values of 30 µg/L, 15 µg/L, 9 µg/L, and 1.9 µg/L, respectively. In present investigation, the mean value of uranium concentrations of tap, marshes, station, surface, ground and RO water were 0.89 µg/L, 1.23 µg/L, 0.84 µg/L,0.87 µg/L,0.87 µg/L and 0.93 µg/L , respectively. Various uranium contents in various water samples from different nations are shown in Table (4.46). We can see from the depicted numbers in the Table (4.46) that the present findings of uranium concentrations vary somewhat from one nation to the next.

Table (4.46): Average of UC in some countries [37]**.**

No.	Country	UC (µg/L)
1	Canada	0.40
2	Argentina	1.3
3	Jordan	2.4
4	Turkey	8.9
5	Kuwait	1.5
6	Iraq (Baghdad)	3.3
7	Iraq (Najaf)	1.2
8	Present study (Tap)	0.89
	Present study (Marshes)	1.23
	Present study (Station)	0.84
	Present study (Surface)	0.87
	Present study (Ground)	0.87
	Present study (RO)	0.93
	Present study (Dhi-Qar)	0.94

4.5.2 Radon Concentrations

Radon concentrations in collected water samples from the studies sites was compared with those similar investigations in the other countries are shown in Table (4.47). The mean value of radon concentrations of current studies were for tap, marshes, station, surface, ground and RO water 0.441 Bq/L, 0.288 Bq/L,0.285 Bq/L, 0.324 Bq/L, 0.224 Bq/L and 0.389 Bq/L.

Table (4.47): Average of radon concentrations in some countries [152]**.**

No.	Country	Average radon concentration (Bq/L)
1	Jordan	3.9
2	Turkey	0.091
3	Kuwait	0.74
4	Algeria	7
5	Syria	13
6	Iraq (Nineveh)	1.13

⟶ Next

7	Iraq (Baghdad)	0.111
8	Present study (Tap)	0.448
	Present study (Marshes)	0.228
	Present study (Station)	0.285
	Present study (Surface)	0.324
	Present study (Ground)	0.224
	Present study (RO)	0.389
	Present study (Dhi-Qar)	0.316

4.6 Theoretical Study of Alpha Emitters

This study explored theoretical results of the optimization, geometrical, electronic structure, sensitivity and spectroscopy properties of the poly allyldiglycol carbonate (CR-39) detector of radon gas by using quantum chemical method. The calculations at ground state are performed theoretically employing density functional theory (DFT) at three parameters B3LYP (Becke's three parameter exchange with Lee, Yang and Parr correlation functional) with SDD (Stuttgart Dresden triple zeta ECPs (Effective-Core Potential)) basis sets in gas phase [153],[154]. Initially, the CR-39 detector structure and the CR-39-Rn irradiated system were developed using the Gauss View 5.0.8 software, which was later relaxed using the Gaussian 09 suite of tools [105],[155]. The excited states characteristics and the transference states of the relaxed compositions are investigation by employing the time dependent density functional theory "TD-DFT at B3LYP-SDD" level [153]. Recent developments in computer and software technology have enabled us to calculate many key chemical and physical characteristics of chemical systems using different computational methods in a predictive way. Furthermore, DFT simulations have high precision, making them ideal for establishing the relationship between a molecule's shape and the factors that influence the CR-39 detector's efficiency structure [156]. The

chemical structure of the monomer structure of the CR-39 polymer under investigation is shown in Figure (4.16) [157].

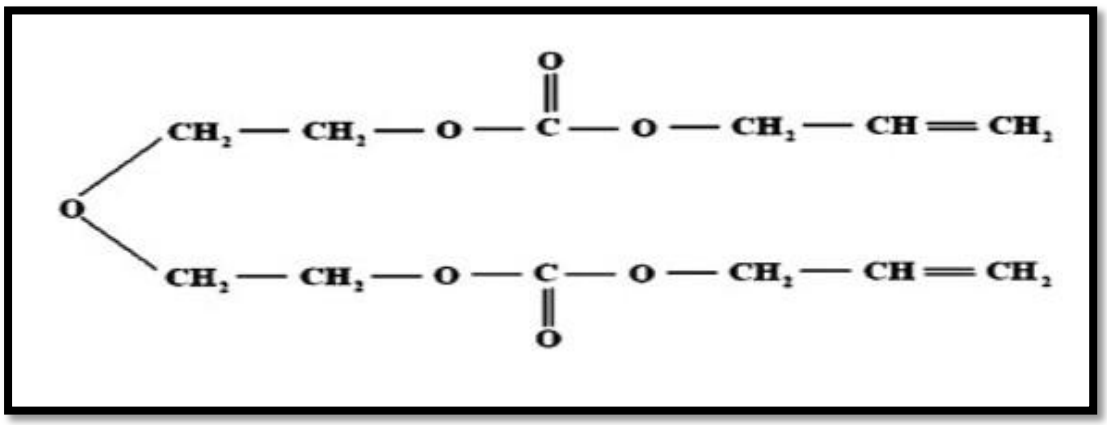

Figure (4.16): Chemical structure of the monomer structure of CR-39 polymer [157]**.**

4.6.1 Structural Properties

Figure (4.17) shows the geometric optimizations of CR-39 molecule and interaction between the detector and the α-radiation (radon gas) at the DFT under the B3LYP hybrid functional with SDD basis sets in ground state. The average geometric dimensions of the CR-39 molecule after relaxations were found to be as follows: C==C= 1.486, C—C= 1.52– 15812, C—H= 1.073–1.075, C—O= 1.4300–1.4879 and O==C= 1.4020–1.4379Å respectively. It was also found that the values of angles between atoms as follows; H–C–H=109.001–109.4712, H—C—C=90º, O—C—O=90º, C—C—C=180º and C—O—C=180º respectively. The angle of end all system: C2—O1—C5 was 111.4 – 109.5 ^{0}. Furthermore, the findings revealed that the successive units had similar dihedral angles (between 180^{o} and -180^{o}). The predicted bond and angle values for the CR-39 molecule in this study match well with experimental evidence [158].

As see in Figure (4.17) the CR-39 detector polymer irradiated using different number atoms of radon gas as source of alpha particles for investigated and reported the physical, structural, electronic and

spectroscopic properties. We note that the interactions between α-radiation and CR-39 molecular not affected on the bond lengths and angles after optimizations of the systems (detector + α-radiation (radon gas)).The distance between the center of detector and the ionizing radiation (radon atoms) were initially determined to 3.5Å, and performed using DFT/B3LYP-SDD level at ground state. The distance (D in Å) between the detector and the radioactive elements changed after optimizations that depending on the number and coordinates of radioactive element from the CR-39 molecule and their intensity as seen in Figure (4.17).

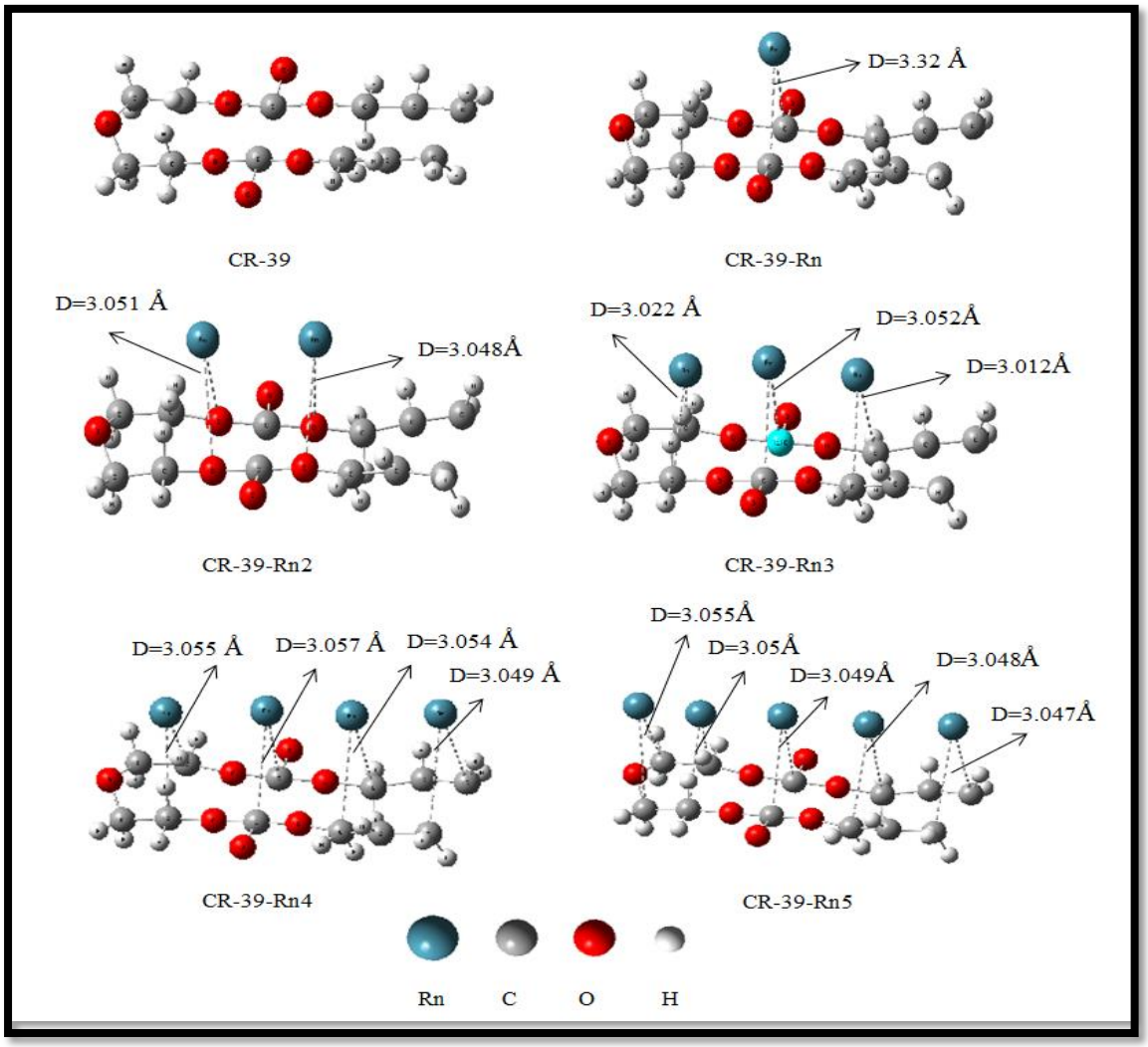

Figure (4.17): The geometric optimizations of the monomer structure of CR-39 polymer and the system (CR-39-Rn) using DFT/B3LYP with SDD basis sets.

4.6.2 Electronic Properties

It is crucial to investigate the structures of electronic for the investigated compounds in order to comprehend and comprehend the behavior of the absorption spectra of interactions with ionizing radiation (such as: α -ray). Table (4.48) shows the electronic properties of CR-39 molecule and the properties of the interaction the CR-39 molecule with radiation of radon gas obtained from the full minimization at DFT-B3LYP/SDD level of theory in ground state. This properties included the total energy ($E_{Tot.}$), high occupied molecular orbital energy (E_{HOMO}), lower unoccupied molecular orbital energy (E_{LUMO}), the energy gap ($\mathrm{E_{gap}}$) ($\mathrm{E_g = E_{LUMO} - E_{HOMO}}$) and the values of virial ratio($-V/T$) for the investigated systems according to Koopman's theorem [159],[160].

Table (4.48): The electronic properties of the monomer structure of CR-39 and systems (CR-39-Rn) at DFT-B3LYP/SDD level in ground state.

System	$E_{Tot.}$(a.u)	E_{HOMO} (eV)	E_{LUMO} (eV)	E_{gap} (eV)	$-V/T$
CR-39	-191. 281	-6.876	-2.727	4.150	2.0046
CR-39-Rn	-205.782	-6.502	-4.220	2.282	2.0021
CR-39-Rn2	-219.196	-6.447	-4.272	2.175	2.0036
CR-39-Rn3	-233.586	-6.114	-4.353	1.761	2.0044
CR-39-Rn4	-247.962	-5.823	-4.435	1.388	2.0052
CR-39-Rn5	-262.980	-5.633	-4.506	1.127	2.0056

As seen from mentioning Table (4.48), the $E_{Tot.}$ of the CR-39 structure has the largest value of total energy this meaning CR-39 stracture was more stable comparison with systems in this study because

of the effect of ionizing α-radiation emitted from radon gas on CR-39 structure. It is fundamental to examine the constructions electronic of the investigated compounds in order to comprehend and comprehend the behavior of the absorption spectra of interactions with ionizing radiation (such as: α -ray):

CR-39>CR-39-Rn> CR-39-Rn2> CR-39-Rn3> CR-39-Rn4> CR-39-Rn5

The findings displayed that the energies of HOMO and LUMO are changed meaningfully as in Table (4.48) and the E_{LUMO} energies of all systems are greater than the E_{HOMO}. All E_{LUMO} energies of system are less than E_{LUMO} CR-39 detector and all E_{HOMO} energies of system are larger than E_{HOMO} CR-39 detector. Furthermore, the CR-39 detector has large separation between the two molecular orbitals (E_{gap} =4.1495 eV). Such findings agree with experimental value [161]. This large energy gap indicates that the structure CR-39 detector is quite stable in ground state and needed high energy to exaction. As noticed, all systems have energy gab smaller than CR-39 structure. The findings revealed that the HOMO and LUMO energy gaps are slightly different, implying that the intensity of ionizing radiation emitted by radon gas has a significant impact on electronic characteristics, progressing electron acceptance ability, and the impact of symmetry and distribution of the CR-39 structure. As a result, the decrease in band gap energy is consistent with the structural alterations seen in CR-39 following exposure to alpha radiation. Table (4.48) shows that following irradiation, the band gap decreases from 4.150 eV (for pure CR-39) to 1.127 eV. The energy gaps estimated were reduced in the following order:

CR-39 >CR-39-Rn > CR-39-Rn2 > CR-39-Rn3 > CR-39-Rn4 > CR-39-Rn5

The value of virial ratio ($\frac{-V}{T}$) for all molecules under study ranged from 2.0021 to 2.0056 in "which the experimental value for hydrogen atom ($\frac{-V}{T}$ =2.0032)"[159], without any imaginary frequency, these results gave an idea the relaxed geometries are true energy minima and the suitable DFT/ B3LYP-SDD method in this study.

The molecular orbitals on the horizon FMOs are essential descriptors for the rationalization of different chemical processes and played a critical role in the study of chemical reactivity at the atomic level. The role of the border molecular orbitals in identifying the charge isolated states of the structures under investigation is crucial. Figure (4.18) illustrate the distribution of the HOMO and LUMO of the CR-39 structure and all systems when irradiation by α-radiation at ground state in gas phase. The red color represents the positive charge and the green is the negative charge.

As seen in Figure (4.18), the α-particle emitted from Radon atoms play significant role in distribution and contribution of FMOs. The shapes of the HOMO and LUMO and charge density are changed in accordance with the energy change (intensity of α-radiation) depended of position of atoms and number of alpha source and electronegativity of atoms. The distribution and energy of the highest occupied molecular orbital measures the predisposition towards the donation of electron by a molecule. Consequently, the distribution and energy of HOMO designate better propensity towards the donation of electron, increasing the adsorption of the inhibitor by Radon gas and then better interaction with α-radiation and inhibition efficiency. This meaning the α-radiation played an important role on the optical, electrical and structural properties of CR-39 SSNTD, also formation and tracks on polymeric materials of CR-39 structure.

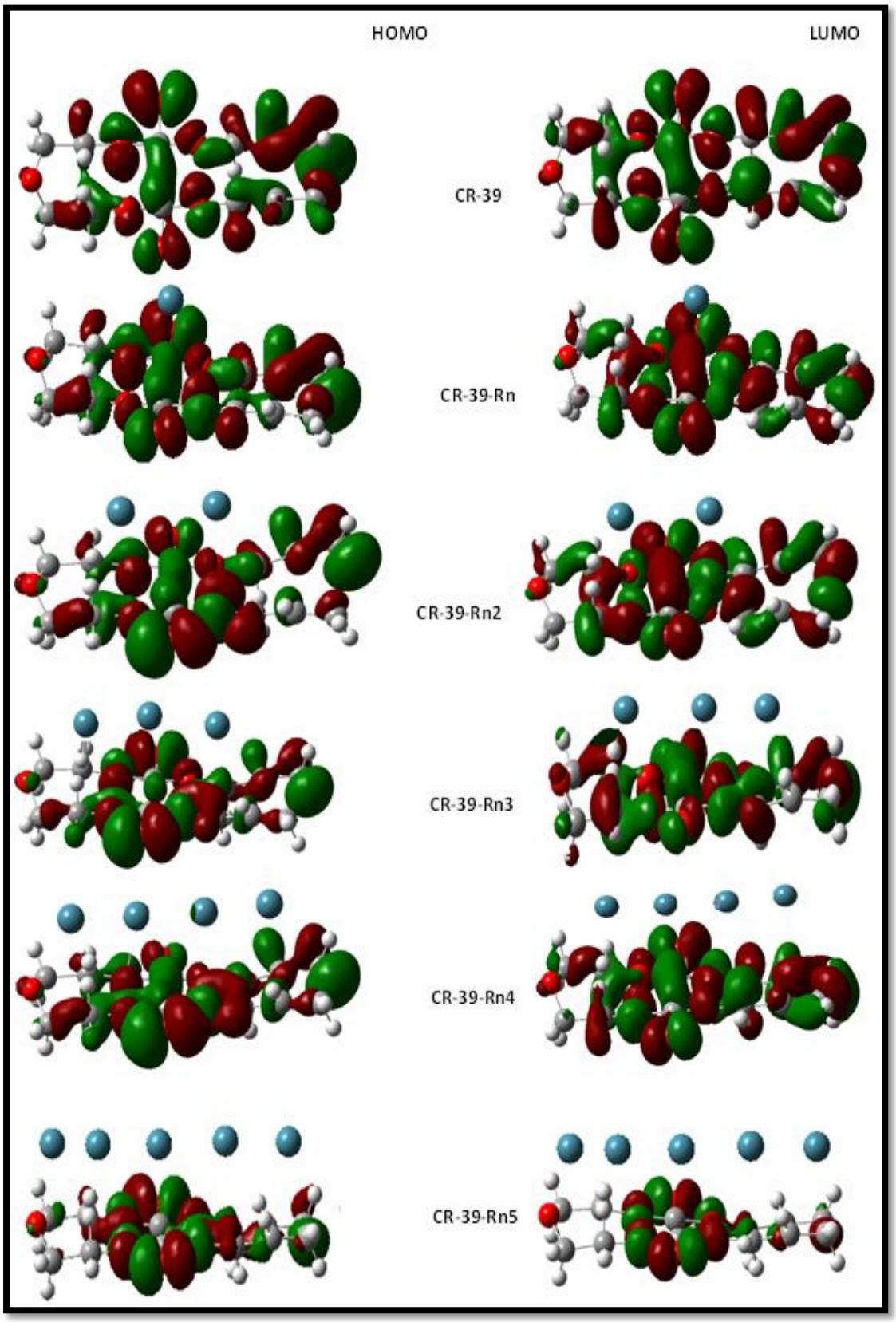

Figure (4.18): The distribution of HOMOs (left) and LUMOs (right) of the CR-39 and CR-39-Rn system computed at the DFT-B3LYP/SDD level at ground state.

4.6.3 Some Electronic Variables

The passage of alpha particles through the CR-39 structure causes ionization of almost all atoms in its path. This initial ionizing event sets in motion a cascade of additional chemical reactions that result in the formation of free radicals and other chemical entities. As a result, the polymer's physio-chemical characteristics, such as ionization potential, electron affinity, electrophilicity index, global hardness, and global softness, are altered. In this section the ionization potential ($I_E = -E_{HOMO}$), electron affinity ($E_A = -E_{LUMO}$), global hardness ($H = \frac{I_E - E_A}{2}$) global softness ($S = \frac{1}{2H}$) and electrophilicity index ($\omega = (-\frac{1}{2}(I_E + E_A))^2/2H$) are reported according to Koopman theorem. The values of I_E,E_A, H , S and ω of CR-39-Rn systems under investigation are mentioned in Table (4.49).

Table (4.49): Some electronic variables (I_E, E_A, H, ω in eV and S in eV^{-1}) of CR-39-Rn systems under study at the DFT-B3LYP/SDD level at ground state.

System	I_E (eV)	E_A (eV)	H (eV)	S (1/eV)	ω (eV)
CR-39	6.876	2.727	2.075	0.241	5.556
CR-39-Rn	6.502	4.220	1.141	0.438	12.591
CR-39-Rn2	6.447	4.272	1.087	0.460	13.207
CR-39-Rn3	6.114	4.353	0.880	0.568	15.556
CR-39-Rn4	5.823	4.435	0.694	0.720	18.953
CR-39-Rn5	5.633	4.506	0.563	0.887	22.808

The findings revealed that the CR-39-Rn5 system has a lower I_E than the other systems, implying that the CR-39-Rn5 system has a higher capacity to donate an electron to become action than the others. Above result can be discussed in terms of the low separation between the two edges of valence and conduction bands for the mentioned system. On the other hand and for the same reason, the large separation between the two edges in the CR-39 make from this compound to need high energy to donating an electron in comparison with the others. The large value of E_A is the factor for determining the high ability for the compound to accepting an electron, then these systems are in the following order:

CR-39 < CR-39-Rn < CR-39-Rn2 < CR-39-Rn3 < CR-39-Rn4 < CR-39-Rn5

Table (4.49) showed low values of electrochemical hardness (0.563 eV) for the CR-39-Rn5 in comparison with the other system. Low H implies that an electron movement from the valence to conduction band in the molecule is relatively easy. The above result indicates that the CR-39-Rn5 system has a narrow band gap see Figure (4.19a). The results of the electronic softness for the systems under study showed that the CR-39-Rn4 and CR-39-Rn5 have the highest value of electronic softness compared with the others, in which indicate to these systems needs to small excitation energy for an electron transfer. Soft system means small energy gap it has as Figure (4.19b). The values of net electrophilicity in Table (4.49) showed that the studied systems after irradiation by α-particle have high net electrophilicity and the contribution comes from the donating electrophilicity more than the accepting electrophilicity. As radiation is one of the important factors that change the structural and electronic characteristics of polymers. The passing of alpha particles within CR-39 structure and the number atom source of α-particle were

played significant role in electronic properties and tracks on CR-39 detector materials.

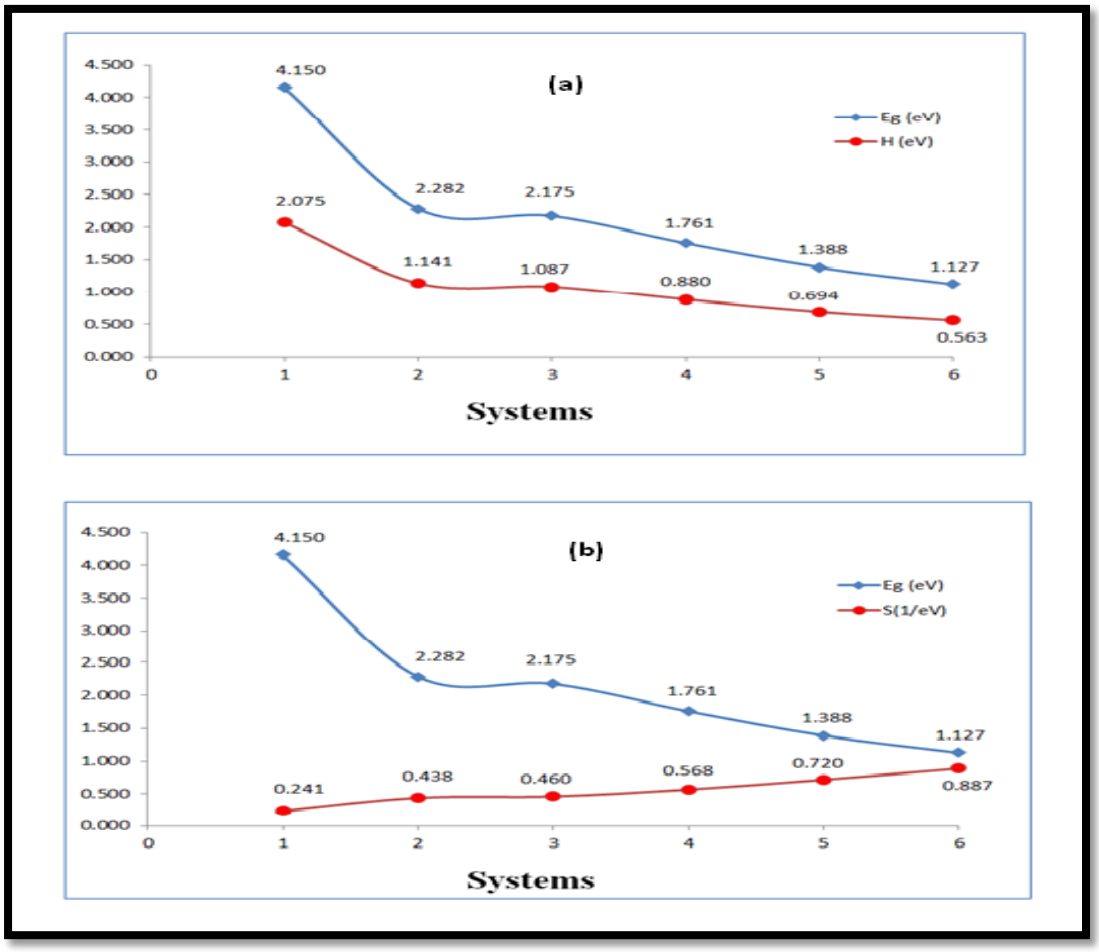

Figure (4.19 a, b): The relation hardness and softness with energy gab of all system under study.

4.6.4 Molecular Electrostatic Potential Surfaces

CR-39 detector has good sensitivity for radon gas, by recording particles radiated from these elements. At the point when CR-39 is presented to charged particles, it makes a series of hidden spoiling because of low straight vitality exchange (named inactive path) which can be made noticeable under microscope when scratched in a reasonable revealer under ideal circumstances. Radiation is one of the main parameters that changes the structural properties of polymers [157],[161]. The electrostatic potential ESP surfaces for the CR-39 molecule system

were displayed by DFT measurements across optimal geometries at the B3LYP/SDD level of theory in gas phase to explore reactive spots for electrophilic and nucleophilic assault. Figure (4.20) illustrates the 2-D counter distribution electrostatic potential of CR-39 structure and all system under radiation (α-source). A ESP surface is an electron density isosurface mapped with an electrostatic potential surface .

The sizes, shapes, charge concentrations, and reactive sites of the complexes may all be determined using the ESP surfaces. Various hues indicate different levels of electrostatic potential at the surfaces; red indicates areas with the lowest electrostatic potential, blue represents areas with the highest electrostatic potential, and green indicates areas with the lowest electrostatic potential. Electrophilic reactivity is associated with the negative areas of the ESP surfaces, whereas nucleophilic reactivity is associated with the positive (blue) areas [162]. The largest negative region of each compound's ESP surface is mostly centered around the oxygen atoms, reflecting that they are the ideal atomic targets for electrophilic attack. In general, the ESP was dragged towards the areas of high electronegativity due to presence of the oxygen atoms. Oxygen is more electronegative (3.44 eV) than carbon (2.55 eV) [159]. In this study the distribution of ESP changes due to adding the Radon atoms as α-source (positive charge). The α-source played significant role in distribution and contribution of electrostatic potential. The intensity of attraction or repulsion for the region around the molecule of the CR-39 structure produces the ESP maps.

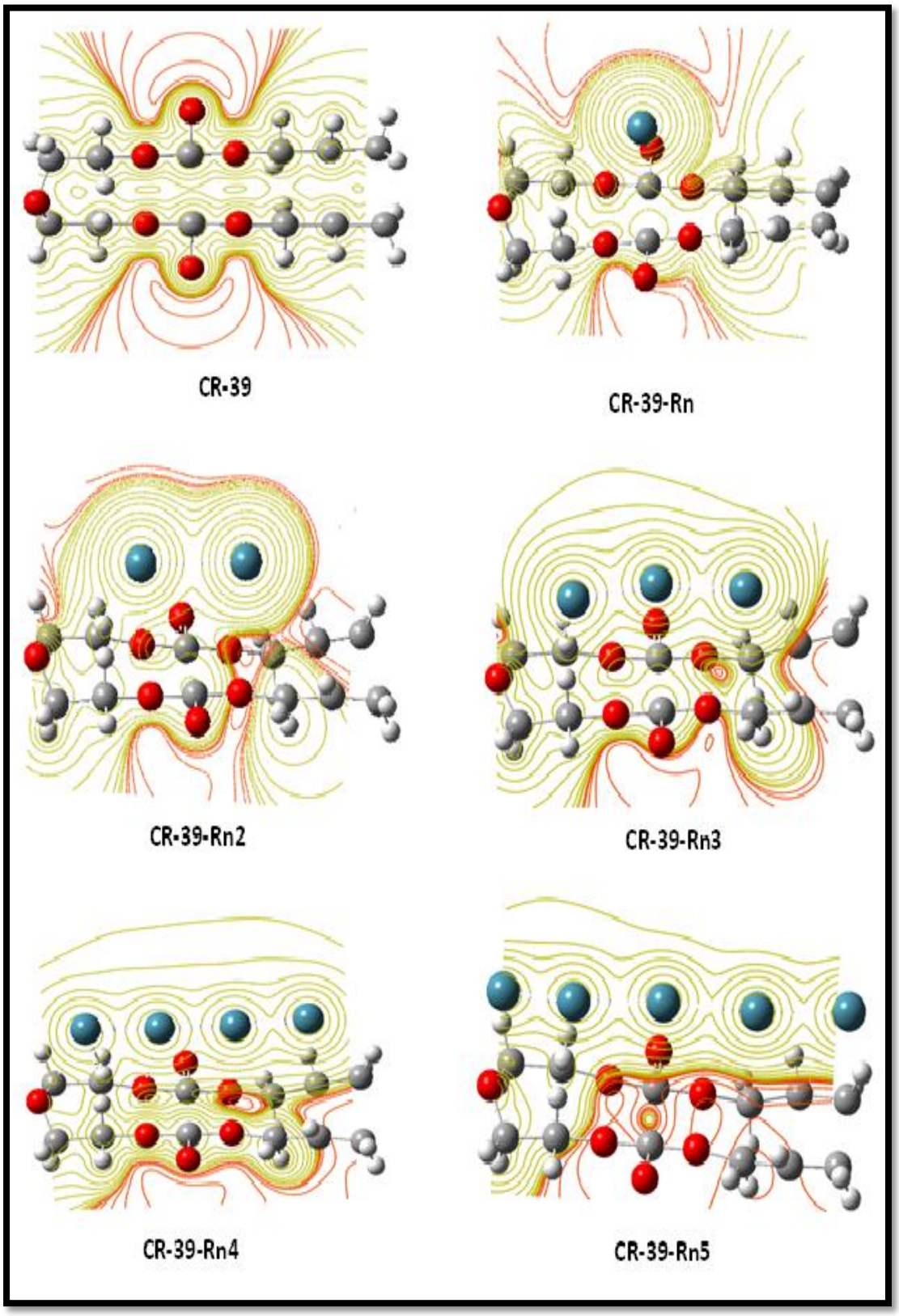

Figure (4.20): The 2-D counter of the ESP of the CR-39 structure and all systems under study at DFT-B3LYP/SDD level in gas phase.

4.6.5 The IR-Spectra

Figure (4.21) shows the infrared IR-spectra for pristine and irradiated CR-39 detectors with different fluencies of alpha particles by radon atom source analyzed from the DFT-B3LYP/SDD calculations. For CR-39 structure, the distinctive and sharp peaks are observed in CR-39 spectrum at 687, 1909, 2042, 2321, 2447, 2582, and 3261 cm^{-1}could be revealed, and supported the monomer texture agreement with experimental study [163]. Stretching C-H bonds were seen at (3028.73-3238.41) cm^{-1}, corresponding to low intensities of 49.89 km/mol and 0.111 Km/mol, respectively. Stretching C-C bonds were seen at (1548.71-1675.24) cm^{-1}, corresponding to a maximum intensity of 70.597 km/mol and a wavelength of 1617.63 cm^{-1}. The stretching C-O bond was detected at 1270.5cm^{-1}, whereas the bending C-H bonds were detected at (1412.08-1530.23) cm^{-1}. The stretching C-H bonds in the CR-39-Rn1 system are in the range (3037.62-3141.25) cm^{-1}, with a maximal intensity of 122.61 Km/mol. The bending C-H bonds were discovered at (1482.45-1527.35) cm^{-1}, while the stretching C-O bonds were discovered at 1281.77 cm^{-1}, leading to a high intensity of 490.167 Km/mol. There are increases in the intensity of the characteristic peaks with increasing the irradiation fluencies. One can observe that a number of the distinctive peaks at 686, 1908, 2043, 2320, 2582, 3261 and 3513 $cm^{-1}$are relevance with C–H stretching vibration, C=C phenyl ring stretching vibration, C=O stretching vibration, O=C=O vibration of carbonate group, CH3 stretching vibration , and C–H stretching vibration of aromatic compounds respectively. Predominately there are no new peaks created and there is no main variation in the CR-39 functional groups at alpha irradiation, but significant changes in the intensities are observed [164].

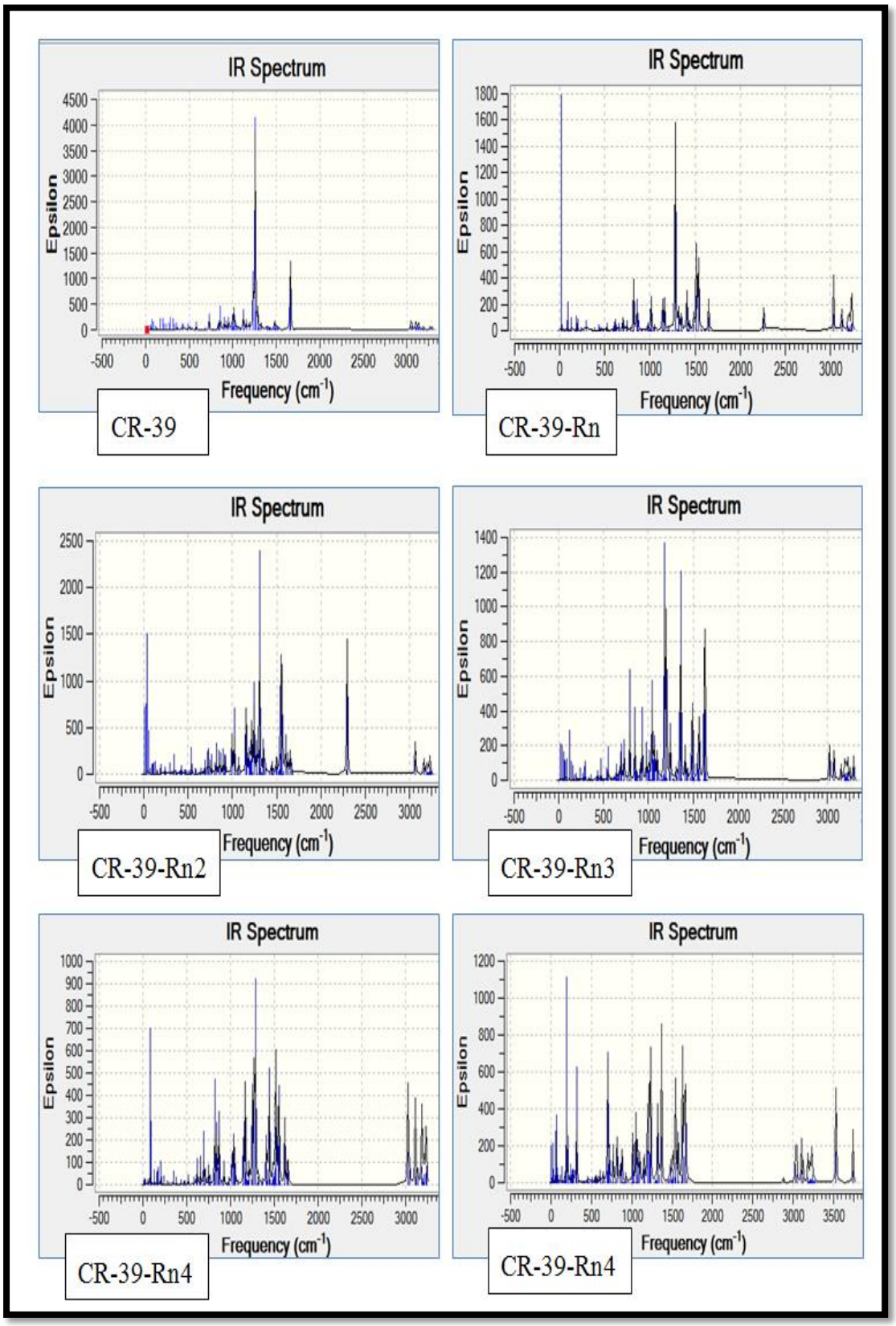

Figure (4.21): IR-Spectra of the Systems under study analyzed from the DFT-B3LYP/SDD calculations (Epsilon ≡ intensity in Km/mol.).

4.6.6 The UV-Vis. Spectra

From the founded relax molecular structures with the B3LYP/SDD-DFT method at ground state. All of the systems' UV-Vis spectra were examined and evaluated in gas phase using the time dependent density function theory (TD-DFT) technique using the identical hybrid functional and basis sets. The absorption spectra of the combinations that are comparable to the solar spectrum are the most important aspect in determining whether they can be used as detector materials. In interaction radiation with matter and electronic spectra, the frontier orbitals (HOMOs and LUMOs) are played a significant role such as interaction of alpha particles with CR-39 detector. Figure (4.22) illustrates that the CR-39 detector has one peak of excitation energy at 626.75nm wavelength and has direct transitions from the valence to conduction (full transition between the frontier orbitals HOMO→LUMO) with absorption wave length 358.187 nm, respectively. Table (4.50) declares the simulation energies of the major band, wavelength, oscillator strength and electronic transmissions HOMO-LUMO and molecular orbital character MOC % of all systems under study. It is evident from studying the results of the excited states using the TD-DFT method that increasing the number of radon gas atoms played an important role. This is due to the increase in the interaction between the alpha particles emitted from radon gas and this causes an increase in the number of transitions between HOMO and LUMO in addition to a decrease in the excitation energy with the increase in the emitted wavelengths as shown in Table (4.50). As a result, this leads to a distortion of the polymer material that the CR-39 detector is made of and to obtain the tracks that are related to the intensity of the radiation (alpha particles emitted).

Table (4.50): The absorption spectra calculations of the systems at TD-DFT with B3LYP/SDD level.

System	Excitation Energy (eV)	Wavelength (nm)	Oscillator Strength	Transitions HOMO→LUMO (%)
CR-39	3.4810	358.187	0.00456	HOMO→LUMO (100%)
CR-39-Rn	52.51	493.071	1.2979	HOMO→LUMO (78%) HOMO-1→LUMO (17%) HOMO→ LUMO +2 (6%)
CR-39-Rn2	2.198	566.372	1.0821	HOMO→LUMO (65%) H-2→LUMO (21%), H-1→ LUMO +1 (10%) HOMO→ LUMO +1 (4%)
CR-39-Rn3	1.978	626.752	0.0021	HOMO→L+1 (70%) H-2→LUMO (12%) H-1→LUMO (14%) HOMO→LUMO (4%)
CR-39-Rn4	1.852	669.202	0.0195	1%)6HOMO→LUMO (HOMO→LUMO+1 (10%) HOMO-1→LUMO (8%) H-2→LUMO (8%) H-2→L+1 (7%) H-1→LUMO (6%),
CR-39-Rn5	1.829	687.578	0.0288	HOMO→LUMO (44%) H-2→LUMO (18%), H-1→L+1 (10%) HOMO→L+1 (8%) H-2→LUMO+1 (6%), H-1→LUMO (5%) HOMO-1→L (4%) HOMO-2→L+1 (3%) HOMO-1→L+2 (3%)

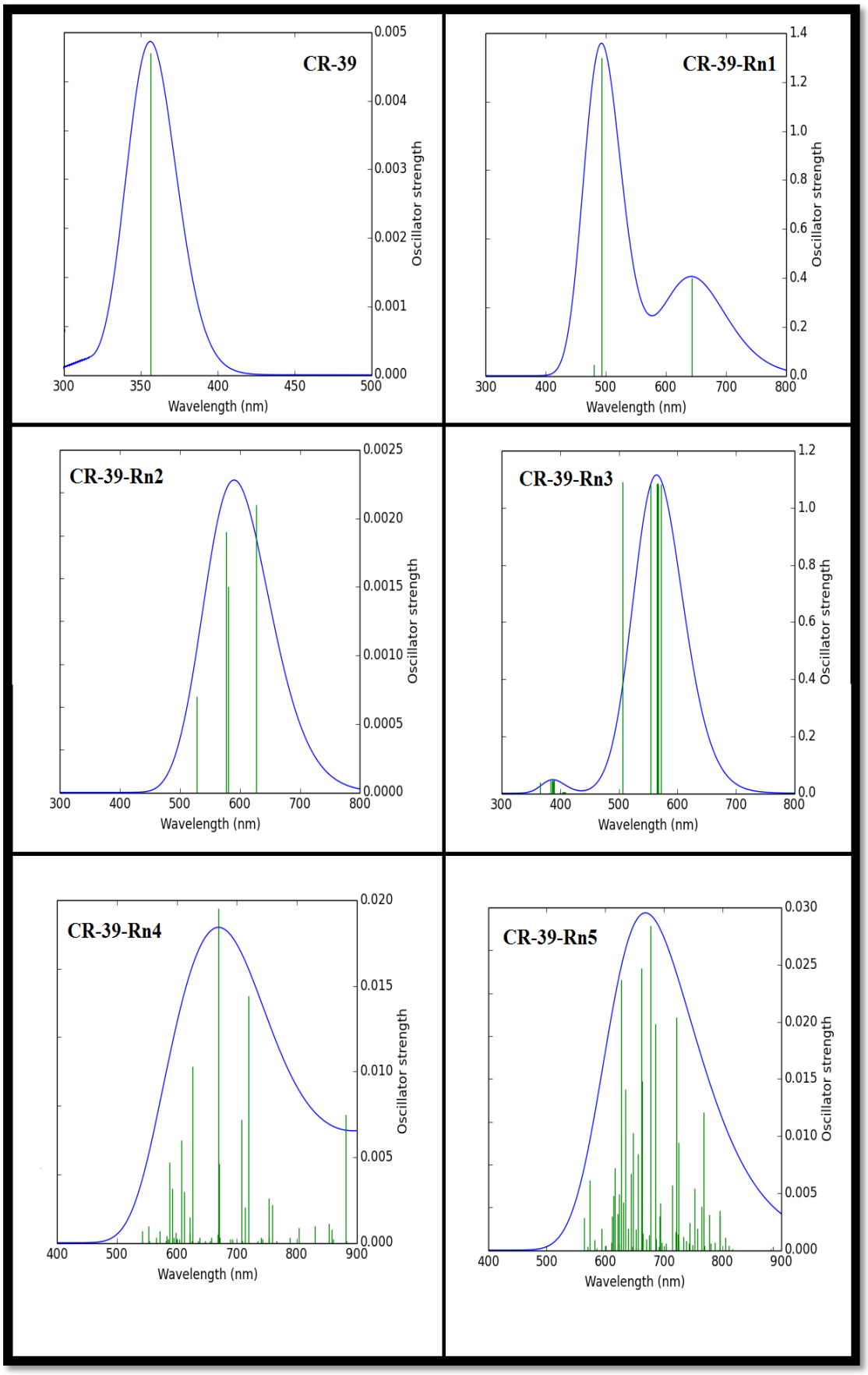

Figure (4.22): UV-Vis Spectra of the systems at TD-DFT with B3LYP/SDD level.

4.7 Conclusions

From the results, obtained the form alpha emitters (uranium concentrations and radon concentrations) for 125 water samples (tap water, marshes water, stations water, surface water, groundwater, and RO water) in Dhi-Qar governorate using CR-39 detectors as well as a theoretical properties (structural and optical) of CR-39 detector we can be concluded that:

1. CR-39 stracture was more stable comparison with systems in this study because of the effect of ionizing α-radiation emitted from radon gas on CR-39 structure. As noticed, all systems have energy gab smaller than CR-39 structure.
2. The results of uranium concentrations and its isotopes in all water samples were within the world average that recommended ICRP.
3. The results of radiological toxicity risk (AED and ELCR), and chemical toxicity risk (LADD and HQ based to uranium concentrations with uranium isotopes in all water samples under study within the acceptable level suggested by different the world organization such as ICRP and WHO.
4. The results of radon concentrations in most water samples were within the world average that recommended WHO. Also, radium-226 in all water samples were lower that the acceptable level that recommended by WHO, while uranium-238 in most samples were within the world average by EPA.
5. The results of annual effective dose (AED) based on radon-222 with radium-226 concentrations when used water in the present samples as drinking water in all samples lower than the worldwide by WHO, while cancer risk (ELCR) in all samples were higher than safety limit for the healthy drinking water.

6. The results value of pH in all marshes water samples were found to be slightly acidic and within desirable limits considered by WHO, while the values of EC and TDS for most water samples were found to be greater than the limit prescribed by WHO. Therefore, it is not safe to drink in terms of physiochemical properties because it has values higher than the permissible limit but suitable for irrigation and agricultural activities.
7. Also, it may be concluded to find good correlation between many parameters such as measuring uranium and radon concentrations using three counting track method (TASL, Manually, and CR-39-D2), uranium concentrations with pH, EC, and TDS for marshes water, and radon concentrations using CR-39 and RAD-7 detectors.
8. Geostatistical tools of ArcGIS software analyzed uranium and radon concentrations in water samples in Dhi-Qar governorate pollution by element mapping.
9. The α-source played significant role in distribution and contribution of electrostatic potential. The intensity of attraction or repulsion for the region around the molecule of the CR-39 structure produces the ESP maps. Also, the number atom source of α-particle were played significant role in electronic properties and tracks on CR-39 detector materials.
10. In areas of study, most water samples are safe, as long as they have alpha emitters (radon and uranium concentrations) and are not a danger to humans.

4.8 Recommendations

Through the present study and according to the obtained results and the conclusions, many ideas for the suggestion concerning the works and important recommendations can be outlined

1. Provide science and academic institutions and are modern enough conduct its own environmental tests of radioactivity programs and physiochemical parameter.
2. Forming a specialized work team to conduct a radiological survey for water in all governorates of the country, planning an integrated radiological map, increasing the number of samples studied, and to draw the radiation map.
3. The need to routinely monitor the concentration of uranium and radon in all type of water for Dhi-Qar and other governorates, by periodically.
4. Study the quality of drinking water before it hits the consumer's tap to ensure optimized drinking water pumping to suit the physical , chemical and bio-local and global.
5. Study properties of other types of solid state nuclear track detectors (LR-115 and CN-85) by using DFT and other quantum chemical methods.

REFERNCES

[1] Wetzel, R. G., and Limnology, G. (2001). Lake and river ecosystems. *Limnology*, *37*, 490-525.

[2] Koshal, R. K. (1976). Water pollution and human health. *Water, Air, and Soil Pollution*, *5*(3), 289-297.

[3] Tawfiq, N. F. (2013). Uranium and radon concentration in ground water in Aucashat city (Iraq) and the associated health effects. *Advances in Applied Science Research*, *4*(3), 167-171.

[4] El-Gamal, H., Sefelnasr, A., and Salaheldin, G. (2019). Determination of natural radionuclides for water resources on the west bank of the Nile River, Assiut Governorate, Egypt. *Water*, *11*(2), 311.

[5] Al-Bayati, A. T. (2019, July). Measurement of uranium concentration in the water samples collected from the areas surrounding in Al-Tuwaitha nuclear site using the CR-39 detector. In *Journal of Physics: Conference Series* (Vol. 1234, No. 1, p. 012007). IOP Publishing.

[6] Cember, H., Johnson, T. E., and Alaei, P. (2008). Introduction to health physics. *Medical Physics*, *35*(12), 5959.

[7] Martin, J. E. (2006). *Physics for radiation protection: a handbook*. John Wiley & Sons.

[8] Van der Steen, J., and Van Weers, A. W. (2004, May). Radiation protection in NORM industries. In *International Congress of the International Radiation Protection Association* (Vol. 11).

[9] Flores, O. B., Estrada, A. M., Suarez, R. R., Zerquera, J. T., and Pérez, A. H. (2008). Natural radionuclide content in building materials and gamma dose rate in dwellings in Cuba. *Journal of Environmental Radioactivity*, *99*(12), 1834-1837.

[10] United Nations. Scientific Committee on the Effects of Atomic Radiation. (2000). Sources and effects of ionizing radiation: sources (Vol. 1). United Nations Publications.

[11] Ojovan, M. I., Lee, W. E., and Kalmykov, S. N. (2019). *An introduction to nuclear waste immobilisation*. Elsevier.

[12] Ceccarello, S., Black, S., Read, D., and Hodson, M. E. (2004). Industrial radioactive barite scale: suppression of radium uptake by introduction of competing ions. *Minerals engineering*, *17*(2), 323-330.

[13] Ali, M. M., Zhao, H., Li, Z., and Maglas, N. N. (2019). Concentrations of TENORMs in the petroleum industry and their environmental and health effects. *RSC Advances*, *9*(67), 39201-39229.

[14] Grasty, R. L., and LaMarre, J. R. (2004). The annual effective dose from natural sources of ionising radiation in Canada. *Radiation protection dosimetry*, *108*(3), 215-226.

[15] Tufail, M., Akhtar, N., and Waqas, M. (2006). Radioactive rock phosphate: the feed stock of phosphate fertilizers used in Pakistan. *Health physics*, *90*(4), 361-370.

[16] Mahler, R. L., and Hamid, A. (1994). Evaluation of water potential, fertilizer placement and incubation time on volatilization losses of urea in two northern Idaho soils. *Communications in soil science and plant analysis*, *25*(11-12), 1991-2004.

[17] Taylor, D. M., and Taylor, S. K. (1997). Environmental uranium and human health. *Reviews on environmental health*, *12*(3), 147-158.

[18] Cothern, C. R. (Ed.). (2019). *Handbook for environmental risk decision making: Values, perceptions, and ethics*. CRC Press.

[19] Darby, S., Hill, D., and Doll, R. (2001). Radon: a likely carcinogen at all exposures. *Annals of Oncology*, *12*(10), 1341-1351.

[20] United Nations Scientific Committee on the Effects of Atomic Radiation. (2017). *Sources, Effects and Risks of Ionizing Radiation, United Nations Scientific Committee on the Effects of Atomic Radiation (UNSCEAR) 2016 Report: Report to the General Assembly, with Scientific Annexes*. United Nations.

[21] Herschy, R. W. (2012). Water quality for drinking: WHO guidelines. *Encyclopedia of Lakes and Reservoirs*, 876-883.

[22] Solanki, H. A. (2015). Physico-chemical parameters of water in Bibi Lake, Ahmedabad, Gujarat, India. *Journal of Pollution Effects & Control*, 1-5.

[23] Dirisu, C. G., Mafiana, M. O., Dirisu, G. B., and Amodu, R. (2016). Level of pH in drinking water of an oil and gas producing community and perceived biological and health implications. *European Journal of Basic and Applied Sciences Vol*, *3*(3).

[24] Nicolau, R., Galera-Cunha, A., and Lucas, Y. (2006). Transfer of nutrients and labile metals from the continent to the sea by a small Mediterranean river. *Chemosphere*, *63*(3), 469-476.

[25] Agbozu, I. E., Ekweozor, I. K. E., and Opuene, K. (2007). Survey of heavy metals in the catfish Synodontis clarias. *International Journal of Environmental Science & Technology*, *4*(1), 93-97.

[26] Klokpah, D. (2011). *Quality Evaluation of Domestic Water Sources within Ziope Community of the Volta Region* (Doctoral dissertation).

[27] Morrison, G., Fatoki, O. S., Persson, L., and Ekberg, A. (2001). Assessment of the impact of point source pollution from the Keiskammahoek Sewage Treatment Plant on the Keiskamma River-pH, electrical conductivity, oxygen-demanding substance (COD) and nutrients. *Water Sa*, *27*(4), 475-480.

[28] Rushton, K. R. (2004). *Groundwater hydrology: conceptual and computational models*. John Wiley & Sons.

[29] Ali, A. H., Mheemeed, A. K., and Hassan, H. I. (2015). Concentration measurements of uranium, thorium and their daughter products in water produced from and near oil fields in north of Iraq using SSNTRD's passive method. *Journal of Radioanalytical and Nuclear Chemistry*, *303*(1), 959-965.

[30] Liesch, T., Hinrichsen, S., and Goldscheider, N. (2015). Uranium in groundwater—fertilizers versus geogenic sources. *Science of the Total Environment*, *536*, 981-995.

[31] Virk, H. S. (2016). Measurement of concentration of natural uranium in ground waters of bathinda district (S. Punjab) for the assessment of annual effective dose. *Global J. of Human-Social Science*, *16*(5), 25-29.

[32] Amrane, M., and Oufni, L. (2017). Determination for levels of uranium and thorium in water along Oum Er-Rabia river using alpha track detectors. *Journal of radiation research and applied sciences*, *10*(3), 246-251.

[33] Rohit, M., Anamika, K. and Praveen, M. (2018). A Comparative Study of Uranium Concentration Using Two Different Analytical Techniques and Assessment of Physicochemical Parameters in Groundwater. *J. Radiat. Nucl. Appl*, 3(3), 149–156.

[34] Abojassim, A. A., Mohammed, H. A. U., Najam, L. A., and El-Taher, A. (2019). Uranium isotopes concentrations in surface water samples for Al-Manathera and Al-Heerra regions of An-Najaf, Iraq. *Environmental earth sciences*, *78*(5), 1-7.

[35] Sekudewicz, I., and Gąsiorowski, M. (2019). Determination of the activity and the average annual dose of absorbed uranium and polonium in drinking water from Warsaw. *Journal of Radioanalytical and Nuclear Chemistry*, *319*(3), 1351-1358.

[36] Sharma, T., Sharma, A., Kaur, I., Mahajan, R. K., Litoria, P. K., Sahoo, S. K., and Bajwa, B. S. (2019). Uranium distribution in groundwater and assessment of age dependent radiation dose in Amritsar, Gurdaspur and Pathankot districts of Punjab, India. *Chemosphere*, *219*, 607-616.

[37] Abojassim, A. A., and Neama, H. H. (2020). Radiological and chemical risk assessment from uranium concentrations in groundwater samples collected from Al-Kufa area, Iraq. *Water Supply*, *20*(8), 3194-3206.

[38] Al-Zaalimiu, T. H., and Al-Hamzawi, A. A. (2021). Measurement of uranium concentrations in tap water samples collected from Muthanna governorate, Iraq using nuclear track detector CR-39. In *IOP Conference Series: Earth and Environmental Science* (Vol. 722, No. 1, p. 012039). IOP Publishing.

[39] Abojassim, A. A., Gazaly, H. H. A., Al-Taweel, M. H., and Kadhim, S. H. (2015). Radon concentrations in selected samples of tap water in Baghdad Government/Iraq. *Research Journal of Applied Sciences, Engineering and Technology*, *11*(12), 1358-1364.

[40] Najam, L. A., Mansour, H. L., Tawfiq, N. F., and Karim, M. S. (2016). Measurement of radon gas concentrations in tap water samples for thi-qar governorate using nuclear track detector (CR-39). *Detection*, *4*(01), 1-8.

[41] Al-jnaby, M. K. M. (2016). Radon concentration in drinking water samples at Hilla city, Iraq. *World Scientific News*, (52), 130-142.

[42] Seoud, M. S. (2017). Measurement of radon-222 concentration in bottled natural mineral drinking water in Kuwait using the nuclear track detector (CR-39). *Int J Phys*, *5*, 201-7.

[43] Rasouli, J., and Khosravi, S. M. (2018). The role of radon in drinking water pollution in Bukan (North West Iran). *Material Sci & Eng*, *2*(6), 252-256.

[44] Opoku-Ntim, I., Gyampo, O., and Andam, A. B. (2019). Risk assessment of radon in some bottled water on the Ghanaian market. *Environmental Research Communications*, *1*(10), 105001.

[45] El-Araby, E. H., Soliman, H. A., and Abo-Elmagd, M. (2019). Measurement of radon levels in water and the associated health hazards in Jazan, Saudi Arabia. *Journal of Radiation Research and Applied Sciences*, *12*(1), 31-36.

[46] Al-Alawy, I. T., and Hasan, A. A. (2018). Measurement of radon gas concentrations and hazard effects in underground water samples in Karbala Governorate of Iraq. *Engineering and Technology Journal*, *36*(2), 118-122.

[47] Abojassim, A. A. (2020). Comparative study between active and passive techniques for measuring radon concentrations in groundwater of

Al-Najaf city, Iraq. *Groundwater for Sustainable Development*, *11*, 100476.

[48] Abojassim, A. A. (2021). Age-Dependent Health Risk Assessment for Radon Concentrations from Drinking Water Available in the Iraqi Markets. *Egyptian Journal of Chemistry*, *64*(4), 3-4.

[49] Amanial, H. R. (2015). Assessment of physicochemical quality of spring water in Arbaminch, Ethiopia. *J Environ Anal Chem*, *2*(157), 2380-2391.

[50] Singh, S., and Hussian, A. (2016). Water quality index development for groundwater quality assessment of Greater Noida sub-basin, Uttar Pradesh, India. *Cogent Engineering*, *3*(1), 1177155.

[51] Abd El-Aziz, S. H. (2017). Evaluation of groundwater quality for drinking and irrigation purposes in the north-western area of Libya (Aligeelat). *Environmental Earth Sciences*, *76*(4), 1-17.

[52] Qaseem, N. M. A., and Al-Barwary, M. R. A. (2018). Evaluation of physical and chemical quality of well water in Zakho District, Kurdistan region, Iraq Evaluation of physical and chemical quality of well water in Zakho District, Kurdistan region. In *Iraq. Vol. 454, No. 1, IOP Conf*.

[53] Abdullah, S. A., Abdullah, A. H. J., Hammadi, N. S., and Al-Rubiai, O.A.(2019). Evaluation of physiochemical properties in Al-Sweib river,Basrah provence, Iraq. *Journal of Basrah Researches Sciences*, *45*(1).

[54] Hussein, A. K., Kadhim, N. A., Jaber, A. S., & Abojassim, A. A. (2020, November). Water Quality Index for Surface Water Assessment by Using Gis Techniques, Alnajaf, Kufa, Iraq. In *IOP Conference Series:*

Materials Science and Engineering (Vol. 928, No. 7, p. 072023). IOP Publishing.

[55] Soceanu, A., Dobrinas, S., Dumitrescu, C. I., Manea, N., Sirbu, A., Popescu, V., and Vizitiu, G. (2021). Physico-Chemical Parameters and Health Risk Analysis of Groundwater Quality. *Applied Sciences*, *11*(11), 4775.

[56] Hameed, A. S., Hashim, A. K., and Mohammed, E. J. (2020). The effective radium content and radon concentrations in coffee samples. *International Journal of Radiation Research*, *18*(3), 461-466.

[57] Magill, J., and Galy, J. (2005). *Radioactivity-Radionuclides-Radiation: Including the Universal Nuclide Chart on CD-ROM*. Springer.

[58] Maged, A. F. (2017). Alpha Particles Induced Modification on SSNTDs Stored for Long Time. *Egyptian Journal of Radiation Sciences and Applications*, *30*(2), 109-115.

[59] Nouh, S. A., El-Mahdy, N. A., Morsy, A. A., and Morsy, M. (2005). Modification of thermal, optical and structural properties of Bayfol nuclear track detector by alpha particles irradiation. *Radiation measurements*, *39*(5), 471-477.

[60] AL-Temimei, F. A., and Mhaimeed, M. S. (2020). Electronic structure, photovoltaic and absorption properties of designed photo-efficient new organic dyes with D-π-A framework. *International Journal of Nuclear Energy Science and Technology*, *14*(1), 61-70.

[61] Obotowo, I. N., Obot, I. B., and Ekpe, U. J. (2016). Organic sensitizers for dye-sensitized solar cell (DSSC): Properties from computation, progress and future perspectives. *Journal of Molecular Structure*, *1122*, 80-87.

[62] Qaim, S. M., Spahn, I., Scholten, B., and Neumaier, B. (2016). Uses of alpha particles, especially in nuclear reaction studies and medical radionuclide production. *Radiochimica acta*, *104*(9), 601-624.

[63]. Todd, M., Wohlers D., and Citra. (2003). Agency for toxic substances and disease registry. *Agency toxic Subst. Dis. Regist*.

[64] Saha, G. B., and Saha, G. B. (2004). *Fundamentals of nuclear pharmacy* (Vol. 6, pp. 96-100). New York: Springer.

[65] Todorov, P. T., and Ilieva, E. N. (2006). Contamination with uranium from natural and antropological sources. *Romanian Journal of Physics*, *51*(1/2), 27.

[66] Gavrilescu, M., Pavel, L. V., and Cretescu, I. (2009). Characterization and remediation of soils contaminated with uranium. *Journal of hazardous materials*, *163*(2-3), 475-510.

[67] Makhijani, A., Chalmers, L., and Smith, B. (2004). Uranium enrichment: Just plain facts to fuel an informed debate on nuclear proliferation and nuclear power. *Institute for Energy and Environmental Research, 15*.

[68] Miaullis, A. P. (2012). *Uranium contamination values and limits* (Doctoral dissertation, Colorado State University).

[69] Bem, H., and Bou-Rabee, F. (2004). Environmental and health consequences of depleted uranium use in the 1991 Gulf War. *Environment international*, *30*(1), 123-134.

[70] Squibb, K. S., and McDiarmid, M. A. (2006). Depleted uranium exposure and health effects in Gulf War veterans. *Philosophical*

Transactions of the Royal Society B: Biological Sciences, *361*(1468), 639-648.

[71] Ali, K. K., and Ajina, A. R. (2015). Use of radium in studying water resources in Shanafiya-Samawa area-south Iraq. *Iraqi Journal of Science*, *56*(2), 1719-1727.

[72] Thompson, M. A. (2012). *Determination of ^{226}Ra In Fish Using Liquid Scintillation Analysis* (Doctoral dissertation).

[73] Gott, M., Steinbach, J., and Mamat, C. (2016). The radiochemical and radiopharmaceutical applications of radium. *Open Chemistry*, *14*(1), 118-129.

[74] Carvalho, F., Chambers, D., Fernandes, S., Fesenko, S., Goulet, R., Howard, B., and Yankovich, T. (2014). The environmental behaviour of radium: revised edition.

[75] Charette, M. A., Gonneea, M. E., Morris, P. J., Statham, P., Fones, G., Planquette, H., and Garabato, A. N. (2007). Radium isotopes as tracers of iron sources fueling a Southern Ocean phytoplankton bloom. *Deep Sea Research Part II: Topical Studies in Oceanography*, *54*(18-20), 1989-1998.

[76] Brugge, D., and Buchner, V. (2012). Radium in the environment: exposure pathways and health effects. *Rev. Environ. Health*, 27(1), 1–17.

[77] Rowland, R. E. (1994). Radium in humans: a review of US studies. Argonne National Laboratory, Chicago.

[78] Lee, J. M., and Kim, G. (2006). A simple and rapid method for analyzing radon in coastal and ground waters using a radon-in-air monitor. *Journal of environmental radioactivity*, *89*(3), 219-228.

[79] Duenas, C., Fernandez, M. C., Carretero, J., Liger, E., and Canete, S. (1999). 226Ra and 222Rn concentrations and doses in bottled waters in Spain. *Journal of environmental radioactivity*, *45*(3), 283-290.

[80] Ezzulddin S. K. (2014). Radon-222 and Radium-226 Activity Concentration Measurement in Erbil Governorate Drinking Water Resources Using Active and Passive Detection Methods. *Ms.c thesis, Salahaddin University.*

[81] Virk, H. S., and Singh, B. (1993). Radon anomalies in soil-gas and groundwater as earthquake precursor phenomena. *Tectonophysics*, *227*(1-4), 215-224.

[82] Nelson, P. H., Rachiele, R., and Smith, A. (1983). Transport of radon in flowing boreholes at Stripa, Sweden. *Journal of Geophysical Research: Solid Earth*, *88*(B3), 2395-2405.

[83] Hashim, A. K., Awad, E. I., and Mezher, H. A. (2017). Measurement of annual effective dose for Radon in Kerbala University Campus, Freiha, Iraq. *Iraqi Journal of Public Health*, *1*(1), 20-25.

[84] Kang, J. K., Seo, S., and Jin, Y. W. (2019). Health effects of radon exposure. *Yonsei medical journal*, *60*(7), 597-603.

[85] Abumurad, K. M., and Al-Omari, R. A. (2008). Indoor radon levels in irbid and health risk from internal doses. *Radiation Measurements*, *43*, S389-S391.

[86] Nayif, S. S. (2019). Measurement of Radon Concentrations in the Air Buildings for some Schools at Karbala City Using CN - 85 and LR - 115 Type II Detectors. *Ms. c thesis, University of Kerbala*.

[87] Al-Tememy, L. T. (2007). Uranium Concentration Measurements of Human Blood Samples Using CR-39. *Al-Nahrain University, Ms. c thesis*.

[88] Mohammed, A. A. (2013). Concentration Measurements of Radon, Uranium and Background of Gamma Rays in Air at the University of Baghdad-Al-Jadiriyah Site. *Ms.c thesis, University of Baghdad*.

[89] Awad, E. M., Hassan, S., Bebers, E., and Rammah, Y. S. (2020). Bulk etch rate for PADC CR-39 at extended concentration range of NaOH mixed with ethanol and etchant viscosity study. *Nuclear Instruments and Methods in Physics Research Section B: Beam Interactions with Materials and Atoms*, *464*, 45-55.

[90] Ibrahim, A. A., and Yousif, W. H. (2018). Effect of etching solution on nuclear track detector CR-39. *IJAER*, *13*, 8659-8663.

[91] Al-Uboode, S. T. (2009). Determination of alpha emitters concentration in human urine via PM-355 SSNT Detector," Al-Nahrain University, *Ms.c thesis*.

[92] Salmon, P. L., Henshaw, D. L., Keitch, P. A., Allen, J. E., and Fews, A. P. (1994). TASTRAK spectroscopy of Polonium-210 alpha-particle activity at bone surfaces: evidence for a concentrated surface deposit less than 3 μm deep. *Radiation research*, *140*(1), 63-71.

[93] Ali, N., Khan, E. U., Akhter, P., Khan, F., and Waheed, A. (2010). Estimation of mean annual effective dose through radon concentration in the water and indoor air of Islamabad and Murree. *Radiation protection dosimetry*, *141*(2), 183-191.

[94] Lipkowitz, K. B., Cundari, T. R., and Boyd, D. B. (Eds.). (2008). *Reviews in computational chemistry* (Vol. 51). John Wiley & Sons.

[95] Hehre, W. J. (2003). *A guide to molecular mechanics and quantum chemical calculations* (Vol. 2). Irvine, CA: Wavefunction.

[96] Perdew, J. P., Ruzsinszky, A., Constantin, L. A., Sun, J., and Csonka, G. I. (2009). Some fundamental issues in ground-state density functional theory: A guide for the perplexed. *Journal of chemical theory and computation*, *5*(4), 902-908.

[97] Oliveira, A. F., Seifert, G., Heine, T., and Duarte, H. A. (2009). Density-functional based tight-binding: an approximate DFT method. *Journal of the Brazilian Chemical Society*, *20*, 1193-1205.

[98] Stanton, J. F. (2001). A Chemist's Guide to Density Functional Theory By Wolfram Koch (German Chemical Society, Frankfurt am Main) and Max C. Holthausen (Humbolt University Berlin). Wiley-VCH: Weinheim.

[99] Capelle, K. (2006). A bird's-eye view of density-functional theory. *Brazilian journal of physics*, *36*, 1318-1343.

[100] Bichinho, K. M., Pires, G. P., dos Santos, J. H. Z., de Camargo Forte, M. M., and Wolf, C. R. (2004). Determination of Mg, Ti and Cl in Ziegler-Natta catalysts by WDXRF. *Analytica chimica acta*, *512*(2), 359-367.

[101] Petersilka, M. G. U. J., Gossmann, U. J., and Gross, E. K. U. (1996). Excitation energies from time-dependent density-functional theory. *Physical review letters*, *76*(8), 1212.

[102] Gerber, I. C., and Angyán, J. G. (2005). Hybrid functional with separated range. *Chemical physics letters*, *415*(1-3), 100-105.

[103] Stephens, P. J., Devlin, F. J., Chabalowski, C. F., and Frisch, M. J. (1994). Ab initio calculation of vibrational absorption and circular dichroism spectra using density functional force fields. *The Journal of physical chemistry*, *98*(45), 11623-11627.

[104] Silver, D. M. (1971). Energy integrals involving both Slater-type and Gaussian atomic orbitals. *Journal de Physique*, *32*(2-3), 129-133.

[105] Frisch, M. J. E. A., Trucks, G. W., Schlegel, H. B., Scuseria, G. E., Robb, M. A., Cheeseman, J. R., and Fox, D. J. (2009). gaussian 09, Revision d. 01, Gaussian. *Inc., Wallingford CT*, *201*.

[106] Ewaid, S. H., Abed, S. A., and Al-Ansari, N. (2019). Crop water requirements and irrigation schedules for some major crops in Southern Iraq. *Water*, *11*(4), 756.

[107] Bedair, H. M., Al-Saad, H. T., and Salman, N. A. (2006). Iraq's southern marshes something special to be conserved; A case study. *Marsh Bulletin*, *2*(1), 99-126.

[108] Al-Furaiji, M. H. O., Karim, U. F., Augustijn, D. C., Waisi, B. I. H., and Hulscher, S. J. (2016). Evaluation of water demand and supply in the south of Iraq. *Journal of water reuse and desalination*, *6*(1), 214-226.

[109] Al-Gburi, H. F. A., Al-Tawash, B. S., and Al-Lafta, H. S. (2017). Environmental assessment of Al-Hammar Marsh, Southern Iraq. *Heliyon*, *3*(2), e00256.

[110] Attiyah, M. M. (2013). Determination of uranium concentration and annual effective dose in drinking water of Baghdad and Nineveh

Governorates using kinetic phosphorescence analyzer (KPA) and CR-39 nuclear track detector. *Ms.c thesis*, *Baghdad University*.

[111] Abojassima, A. A., Shltake, A. R., Najam, L. A., and Merzaa, I. R. (2017). Radiological parameters due to radon-222 in soil samples at Baghdad Governorate (Karakh), Iraq. *Pak. j. sci. ind. res. Ser. A: phys. sci*, *60*(2), 72-8.

[112] Zbalh, M. A., Ali Bakir, H. A., Abojassim, A. A., and Hassan, A. B. (2019). Monte Carlo Simulation to Estimate the Male and Female Effective Dose due to Radon Exposure in Al-Najaf. *Indian Journal of Public Health Research & Development*, *10*(7).

[113] Durridge Company Inc. (2009). RAD7 RAD H_2O radon in water accessory owner's manual.

[114] Qasim, A. M. S., Hussain, H. H., and Abojassim, A. A. (2018). Radon concentrations and annual effective dose in cigarette samples (domestic and importer) at the Iraqi markets. *Journal of Radiation and Nuclear Applications*, *3*(2), 83.

[115] Stabilini, A., Meier, K., and Yukihara, E. G. (2018). High dose fast neutron dosimetry using PADC plastic nuclear track detectors and grey level analysis. *Radiation protection dosimetry*, *180*(1-4), 220-224.

[116] Liu, C., Ma, H., Zeng, Z., Cheng, J., Li, J., and Zhang, H. (2018). Measurements of radon concentrations using CR-39 detectors in China JinPing Underground Laboratory (2015-2016). *arXiv preprint arXiv:1806.06567*.

[117] Al-Jubbori, M., and Al-Shumaisy, S. (2015). Computer Algorithm for Counting and Measuring Alpha Particles Track Diameters in CR-39 Detectors. *Jordan Journal of Physics*, *8*(1), 57-65.

[118] Abojassim, A. A., and Mohammed, H. A. U. (2017). Comparing of the uranium concentration in tap water samples at Al-Manathera and Al-Herra Regions of Al-Najaf, Iraq. *Karbala International Journal of Modern Science*, *3*(3), 111-118.

[119] Mohammed, H. A-U. (2017). Assessment of Annual Effective Dose due to the Exposure to Uranium is Isotopes in Water Samples at Al-Manathira and Al-Herra Regions. *Ms.c thesis, University of Kufa*.

[120] Nada, F. T., Laith, A. N., and Enas, M. Y. (2014). Uranium concentration and its associated health hazards in drinking water of Nineveh Province (Iraq). *World Applied Sciences Journal*, *31*(11), 1938-1944.

[121] ICRP (International Commission on Radiological Protection). (1993). Protection against radon-222 at home and at work. *ICRP Publication 65. Ann. ICRP*, *23*(2), 1-45.

[122] ICRP (International Commission on Radiological Protection). (1991). Recommendations of the International Commission on Radiological Protection. *ICRP Publication.*

[123] Mathews, G., Nagaiah, N., Kumar, M. K., and Ambika, M. R. (2015). Radiological and chemical toxicity due to ingestion of uranium through drinking water in the environment of Bangalore, India. *Journal of Radiological Protection*, *35*(2), 447.

[124] Kim, Y. S., Park, H. S., Kim, J. Y., Park, S. K., Cho, B. W., Sung, I. H., and Shin, D. C. (2004). Health risk assessment for uranium in Korean groundwater. *Journal of environmental radioactivity*, *77*(1), 77-85.

[125] Edition, F. (2011). Guidelines for drinking water quality. *WHO chronicle*, *38*(4), 104-108.

[126] Mayya, Y. S., Eappen, K. P., and Nambi, K. S. V. (1998). Methodology for mixed field inhalation dosimetry in monazite areas using a twin-cup dosemeter with three track detectors. *Radiation protection dosimetry*, *77*(3), 177-184.

[127] Mohammed, E. J. (2016). Radon concentrations in some soil and air samples of dwellings in Karbala City and influencing factors on lung cancer risks using CR-39. *Ms.c thesis, University of Kerbala.*

[128] Subber, A. R., Al-Hashmi, N. H., Nader, A. F., Jebur, J. H., and Khodier, M. K. (2015). Constructasa simple radon chamber for measurement of radon detectors calibration factors. *Pelagia research library, Advances in applied Science research*, *6*(2), 128-131.

[129] Elzain, A. E. A. (2014). Measurement of Radon-222 concentration levels in water samples in Sudan. *Advances in Applied Science Research*, *5*(2), 229-234.

[130] Abojassim, A. A., and Lawi, D. J. (2018). Alpha particles emissions in some samples of medical drugs (capsule) derived from medical plants in Iraq. *Plant arches*, *18*(1), 1137-7.

[131] Azam, A., Naqvi, A. H., and Srivastava, D. S. (1995). Radium concentration and radon exhalation measurements using LR-115 type II plastic track detectors. *Nuclear geophysics*, *9*(6), 653-657.

[132] Abojassim, A. (2018). Alpha particles concentrations from soil samples of Al-Najaf/Iraq. *Polish Journal of Soil Science*, *50*(2), 249.

[133] Sajo-Bohus, L., Gomez, J., Capote, T., Greaves, E. D., Herrera, O., Salazar, V., and Smith, A. (1997). Gross alpha radioactivity of drinking water in Venezuela. *Journal of environmental radioactivity*, *35*(3), 305-312.

[134] El-Taher, A. M., Abojassim, A. A., Najam, L. A., and Mraity, H. (2020). Assessment of annual effective dose for different age groups based on radon concentrations in the groundwater of Qassim, Saudi Arabia. *Iranian Journal of Medical Physics*, *17*(1), 15-20.

[135] Clement, C. H., Tirmarche, M., Harrison, J. D., Laurier, D., Paquet, F., Blanchardon, E., and Marsh, J. W. (2010). Lung cancer risk from radon and progeny and statement on radon. *Annals of the ICRP*, *40*(1), 1-64.

[136] Abid, A. A., Mraity Hussien, A. A., Husain, A. A., and Wood, M. (2017). Estimation of the excess lifetime cancer risk from radon exposure in some buildings of Kufa Technical Institute, Iraq. *Nucl. Phys. At. Energy*, 18(3), 276-286.

[137] Saliha, N. F., and Jaafarb, M. S. (2013). Estimation the dose on radiosensitive tissue for women in dwelling and health risks caused to reduce the fertility women and cancer in gonads in Iraqi Kurdistan regions. *J. Environ and Earth Sciences*, *3*(2), 125-133.

[138] YSI Incorporated. (2009). Multiparameter Water Quality Sondes User Manual, 374.

[139] Smith, H. (1993). Radon-222 at Home and at Work, International Commission on Radiological Protection (ICRP), Publication 65.

[140] Kim, Y. S., Park, H. S., Kim, J. Y., Park, S. K., Cho, B. W., Sung, I. H., and Shin, D. C. (2004). Health risk assessment for uranium in

Korean groundwater. *Journal of environmental radioactivity*, *77*(1), 77-85.

[141] WHO. (2004). Guidelines for drinking-water quality, 4th edn. World Health Organization.

[142] WHO. (2008). *WHO report on the global tobacco epidemic, 2008: the MPOWER package*. World Health Organization.

[143] Raymond-Whish, S., Mayer, L. P., O'Neal, T., Martinez, A., Sellers, M. A., Christian, P. J and Dyer, C. A. (2007). Drinking water with uranium below the US EPA water standard causes estrogen receptor–dependent responses in female mice. *Environmental health perspectives*, *115*(12), 1711-1716.

[144] Somlai, K., Tokonami, S., Ishikawa, T., Vancsura, P., Gáspár, M., Jobbágy, V, and Kovács, T. (2007). 222Rn concentrations of water in the Balaton Highland and in the southern part of Hungary, and the assessment of the resulting dose. *Radiation Measurements*, *42*(3), 491-495.

[145] Alomari, A. H., Saleh, M. A., Hashim, S., Alsayaheen, A., and Abdeldin, I. (2019). Activity concentrations of 226 Ra, 228 Ra, 222 Rn and their health impact in the groundwater of Jordan. *Journal of Radioanalytical and Nuclear Chemistry*, *322*(2), 305-318.

[146] Abbas, A. H. A., Dawood, A. S., and Al-Hasan, Z. M. (2017). Evaluation of groundwater quality for drinking purpose in basrahgovernorate by using application of water quality index. *Kufa Journal of Engineering*, *8*(1), 65-78.

[147] Shafik, S. S., Ahmed, B. A., and Mohammed, M. (2014). Determination uranium concentrations and effective dose of drinking

water for Nineveh Governorate Iraq, using Kinetic Phosphorescence Analyzer (KPA). *Journal of Environmental Protection*, *2014*.

[148] Chabuk, A., Hammood, Z. A., Al-Ansari, N., Abed, S. A., and Laue, J. (2021). Classification Maps for TDS Concentrations in the GIS Along Euphrates River, Iraq. *Water, Air, & Soil Pollution*, *232*(8), 1-15.

[149] Mittal, S., Rani, A., Mehra, R., Balaram, V., Satyanarayanan, M., and Sawant, S. S. (2017). Assessment of uranium in correlation with physico-chemical properties of drinking water of Northern Rajasthan. *Journal of the Geological Society of India*, *90*(2), 233-238.

[150] Singh, S., Rani, A., Mahajan, R. K., and Walia, T. P. S. (2003). Analysis of uranium and its correlation with some physico-chemical properties of drinking water samples from Amritsar, Punjab. *Journal of Environmental Monitoring*, *5*(6), 917-921.

[151] Al Zabadi, H., Musmar, S., Issa, S., Dwaikat, N., and Saffarini, G. (2012). Exposure assessment of radon in the drinking water supplies: a descriptive study in Palestine. *BMC research notes*, *5*(1), 1-8.

[152] Kadhim, I. H., Al-shimmary, I. H., and Al–Bodairy, O. H. (2016). Study the concentration of radon gas in groundwater in the selected samples of the province of Babel/Iraq. *Environmental Science: An Indian Journal*, *2*, 79-82.

[153] Heimel, G. (2013). *Modern Methods of Computational Electronic Structure Theory*. England: John Wiley & Sons Inc.

[154] Grotendorst, J. (2000). *Modern methods and algorithms of quantum chemistry*. NIC.

[155] Elenn, F., Hrant, P. H., and Roy, D. D. (2009). *GaussView 5 reference*, USA, Wallingford.

[156] Sen, F., and Goker, B. (2014). A theoretical investigation b monomer that is a plastic pol manufacture of eyeglass lens. *American Journal of Optics and Photon*, *2*(1), 7-11.

[157] Cassou, R. M., and Benton, E. V. (1978). Properties and applications of CR-39 polymeric nuclear track detector. *Nuclear Track Detection*, *2*(3), 173-179.

[158] Morrison, B. R.(2002). *Organic Chemistry*, 6th. edition, Prentice - Hall of India Private Limited.

[159] Peter, R. F. (2005). *Molecular Quantum Mechanics*, 4th edition. New York: Oxford University Press.

[160] Zarkadoula, E. N., Sharma, S., Dewhurst, J. K., Gross, E. K. U., and Lathiotakis, N. N. (2012). Ionization potentials and electron affinities from reduced-density-matrix functional theory. *Physical Review A*, *85*(3), 032504.

[161] Al-Saeedi, A. M. (2016). Optical Properties of CR-39 Plastic Detectors Irradiated by He : Ne Laser. *Int. J. Sci. Eng. Res*, 7(11), 1978–1993.

[162] Vitnik, V. D., Vitnik, Z. J., Banjac, N. R., Valentic, N. V., Uscumlic, G. S., and Juranic, I. O. (2014). Quantum mechanical and spectroscopic (FT-IR, 13C, 1H NMR and UV) investigations of potent antiepileptic drug 1-(4-chloro-phenyl)-3-phenyl-succinimide. *Spectrochimica Acta Part A: Molecular and Biomolecular Spectroscopy*, *117*, 42-53.

[163] Abdalla, A. M., Harraz, F. A., Al-Sayari, S. A., and Al-Hajry, A. (2015). Structural and optical investigation on alpha particle irradiated CR-39 surface coated by MEH-PPV conducting polymer. *Applied Surface Science*, *347*, 685-689.

[164] El Ghazaly, M., and Hassan, H. E. (2014). Spectroscopic studies on alpha particle-irradiated PADC (CR-39 detector). *Results in Physics*, *4*, 40-43.

الخلاصة

المياه لا غنى عنها للحياة لذلك فإن مراقبة جودة المياه لها أهمية كبيرة. يركز هذا البحث على قياس باعثات ألفا مثل تراكيز الرادون واليورانيوم في 125 عينة مياه من ستة أنواع (30 عينة من مياه الصنبور ، 20 عينة من مياه الأهوار ، 20 عينة من مياه المحطات ، 15 عينة من المياه السطحية ، 20 عينة من المياه الجوفية ، و 20 عينة من مياه التناضح العكسي) تم جمعها من مواقع مختلفة من محافظة ذي قار. تم إجراء الدراسة العملية بواسطة كاشف CR-39 المنتج من قبل (TASTRAK Analysis System). كما تم حساب بعض المخاطر الإشعاعية مع خطر السمية الكيميائية بسبب تراكيز اليورانيوم ونظائره , بالإضافة الى تراكيز ^{226}Ra وتراكيز^{238}U والمعاملات الإشعاعية الناتجة عن تراكيز الرادون باستخدام معادلات نظرية مختلفة. تم قياس تراكيز ^{222}Rn في المياه الجوفية باستخدام كاشف RAD-7. كما تم قياس تركيز ايون الهيدروجين والتوصيل الكهربائي والمواد الصلبة الذائبة الكلية في مياه الأهوار لنفس منطقة الدراسة باستخدام تقنيات مختلفة. بعد ذلك ، تم استخدام تقنية نظام المعلومات الجغرافية (GIS) لرسم خرائط لتراكيز اليورانيوم وتراكيز الرادون وبعض المخاطر الإشعاعية لجميع العينات قيد الدراسة.

كما يركز هذا البحث على دراسة الخصائص النظرية (التركيبية والبصرية) لكاشف الاثر النووي البوليمري (CR-39) باستخدام نظرية الكثافة الوظيفية (DFT). كان متوسط قيمة تراكيز اليورانيوم بوحدة ميكروغرام / لتر لستة أنواع من الماء على التوالي 0.89±0.021 ، 1.23±0.05، 0.84±0.016 ، 0.87±0.04، 0.87±0.02 ، 0.93±0.04، بينما نتائج متوسط قيمة الرادون كانت التراكيز بوحدة بيكريل / م^3 لنفس الأنواع الستة من الماء على التوالي 441.61±77.02، 288.92±34.10، 285.54±56.87، 324.91±71.19 ، 224.35±23.85، 389.47±68.60. كما وجد ارتباطا جيدا لقياس تراكيز اليورانيوم والرادون باستخدام ثلاث طرق عد مختلفة وهي نظام قياس الجرعات TASLIMAGE والنظام المجهري وبرنامج Matlab المطور (CR-39-D2).

تم العثور على ارتباط جيد بين تراكيز اليورانيوم والخصائص الفيزيائية والكيميائية لمياه الأهوار ، وكذلك ارتباط جيد لتراكيز غاز الرادون في المياه الجوفية باستخدام كاشف CR-39 و RAD-7. وكذلك زيادة عدد الانتقالات بين HOMO و LUMO بالإضافة إلى انخفاض طاقة الإثارة مع زيادة الأطوال الموجية المنبعثة بسبب زيادة التفاعل بين جسيمات ألفا المنبعثة من غاز الرادون. نتيجة لذلك ، يؤدي ذلك إلى تشويه مادة البوليمر التي يتكون منها كاشف CR-39

والحصول على المسارات المتعلقة بشدة الإشعاع (جسيمات ألفا المنبعثة). وفقًا لذلك ، كانت نتائج تراكيز اليورانيوم والرادون ، بالإضافة إلى مؤشر المخاطر الإشعاعية من المياه لستة أنواع من محافظة ذي قار ، ضمن حدود المستويات العالمية التي أوصت بها العديد من المنظمات والهيئات ، بما في ذلك وكالة حماية البيئة (EPA) ومنظمة الصحة العالمية (WHO) ولجنة الأمم المتحدة العلمية المعنية بآثار الإشعاع (UNSCEAR) و ICRP. أخيراً يمكن أن نستنتج أنه لا يوجد خطر من المخاطر الإشعاعية بسبب باعثات ألفا في معظم نماذج المياه في الدراسة الحالية حول صحة الإنسان.

جمهورية العراق
وزارة التعليم العالي والبحث العلمي
جامعة بابل – كلية العلوم
قسم الفيزياء

دراسة نظرية وعملية لتخمين باعثات الفا في نماذج الماء في محافظة ذي قار

اطروحة

مقدمة الى قسم الفيزياء - كلية العلوم - جامعة بابل
وهي جزء من متطلبات نيل درجة الدكتوراه في فلسفة العلوم / الفيزياء

من قبل
اوسام عبد الستار مرزه علي غلام

بكالوريوس علوم فيزياء / ٢٠١٠
ماجستير علوم فيزياء / ٢٠١٧

بإشراف

الأستاذ الدكتور
محمد عبد الامير الشريفي

الأستاذ الدكتور
علي عبد ابو جاسم

١٤٤٣هـ

٢٠٢١ م